Sede Amministrativa: Università degli Studi di Padova

Dipartimento di Medicina Molecolare

CORSO DI DOTTORATO DI RICERCA IN MEDICINA MOLECOLARE

CURRICOLO: MEDICINA RIGENERATIVA

CICLO XXX

Advanced cell therapy strategies to correct corneal disorders

Coordinatore: Ch.mo Prof. Stefano Piccolo

Supervisore: Ch.mo Prof. Giorgio Palù

Co-Supervisore: Dott. Enzo Di Iorio

Dottorando : Dott. Angelo Migliorati

Index

Index of figures and tables

Abbreviations

ABC	ATP Binding Cassette
ADULT	Acro-Dermato-Ungual-Lacrimal-Tooth Syndrome
AEC	Ankyloblepharon-Ectodermal defects and Clef lip/palate Syndrome
ALDH	Aldehyde Dehydrogenase
ALK	Anterior Lamellar Keratoplasty
ASCs	Adult Stem Cells
b-HLH	Basic Helix-Loop-Helix
CESCs	Conjunctival Epithelial Stem Cells
CFE	Colony Forming Efficiency
cK	Cytokeratin
DBD	DNA Binding Domain
EEC	Ectrodactyly-Ectodermal dysplasia and Clef lip/palate Syndrome
ESCs	Epithelial Stem Cells
GAPDH	Glyceraldehyde-3-Phosphate Dehydrogenase
HHs	Heterozygous Holoclones
HKLs	Human Keratoplasty Lenticules
IC	Impression Cytology
ID	Inhibitory Domain

IFE	Interfollicular Epidermis
Inv	Involucrine
iPSCs	Induced Pluripotent Stem Cells
Lam	Laminine
LESCs	Limbal Epithelial Stem Cells
LMS	Limb Mammary Syndrome
LSCD	Limbal Stem Cells Deficiency
MUC	Mucin
NICD	Notch Intracellular Domain
OD	Oligomerization Domain
OMESCs	Oral Mucosa Epithelial Stem Cells
PLK	Posterior Lamellar Keratoplasty
RBP	Recombining Binding Protein
RHS	Napp-Hodgkin Syndrome
SAM	Sterile Alpha Motif
SCs	Stem cells
SESCs	Skin Epithelial Stem Cells
SMA	Smooth Muscle Actin
SSCs	Somatic Stem Cells
TA (cells)	Transient Amplifying
TA (domain)	Transactivating
VSX	Visual System Homeobox

1 Abstract

Introduction

Epithelial homeostasis is guaranted by somatic stem cells wich, through different patways, such as p63 and Notch signaling, self-renew, differentiate and control tissue function and integrity. *In vivo* behavior of epithelial stem cells (ESCs) from different epithelia reflects differences in physiological role of the tissue.

Limbal stem cells deficiency (LSCD) is characterized by conjunctival epithelial ingrowth, neovascularization, recurrent corneal erosion and persistent ulcers, as well as corneal scarring and ultimately leads to visual impairment and blindness. When the cornea is entirely covered with a fibro-vascular tissue, the chances of success of a traditional penetrating keratoplasty are virtually absent. Transplantation of autologous limbal epithelial stem cells (LESCs) or oral mucosa epithelial stem cells (OMESCs) cultured on fibrin glue has shown to be successful for unilateral or bilateral LSCD treatment, respectively. Despite that, fibrin presented several limitations including inability to repair or replace damaged corneal stroma.

Aim

The purpose of this work is to better understand the potentiality of somatic epithelial stem cells in order to identify possible approaches to exploit this potentiality. In the light of this, my research group has been able to identify and set up a cell therapy approach for a unique homozygous-heterozygous mosaicism of EEC Syndrome, demonstrating that epithelial stem cells have an intrinsic potential for regenerative medicine that can be exploited with a deeper characterization. We, also, aimed to test human keratoplasty lenticules (HKLs): particularly attractive, full-thickness scaffolds for corneal epithelial and stromal reconstruction that provides an interesting organotypic culture system for evaluation of growth, proliferation, and differentiation processes of epithelial stem cells (ESCs).

Results

During the three years of PhD I had the opportunity to collect and review cellular biology data of four diverse types of primary epithelial cells, derived from four

different epithelia (skin, oral mucosa, limbus/cornea and conjunctiva) and, to better investigate the exhaustion of clonogenic potential and the self-renewal of epithelial stem cells we took in consideration also p63-defective oral mucosa primary cell lines obtained from three patients affected by EEC syndrome, already known to cause an acceleration in epithelial aging. Demonstrating that epithelial stem cells have an intrinsic potential for regenerative medicine that can be exploited with a deeper characterization, we have also been able to apply a cell therapy protocol to a patient affected by EEC syndrome in a rare form of mosaicism. We isolated the cell population with a mild phenotype from this patient, enriching these primary cells *in vitro* and producing well-organized and stratified epithelial sheets. The novelty and the importance of this case was related to the possibility to start a customized cell therapy approach for this unique case of EEC syndrome, based solely on epithelial stem cell manipulation.

Limbal stem cells (H-LESCs) expanded onto HKLs gave rise to a keratinized stratified squamous epithelium morphologically similar to that of normal corneas. To set up the cohort of animal patients, we proceded with the characterization of cell lines obtained from biopsies of the cornea (C-CESCs) and oral mucosa (C-OMESCs) of canine origin. Primary lines were serially propagated until exhaustion in order to get life span data to compare their behavior with human limbal stem cells. For each passage, we also performed colony forming efficiency assays (CFE) to estimate the proportion of clonogenic cells present in the culture. Results showed a trend of canine cell lines comparable to human limbal cells trend, with a similar decrease of clonogenic cells number, a similar percentage of aborted colonies during serial cultivation and a similar replicative senescence. Then, primary human and canine epithelial stem cells were seeded onto HKLs. The resulting epithelia was well organized and stratified into four to five cell layers with basal cuboidal cells differentiating upward to winged cells. The layer of basal cuboidal cells was firmly attached to the underlying ECM and to the basement membrane through integrinβ4. Maintenance of stemness potential and differentiation pathways were assessed checking the expression of the stem cells marker p63 and the terminally differentiated cells marker Involucrine. Importantly, expression of the different markers resembled that observed in normal epithelia, thus

suggesting that HKLs are able to support the growth and maintain the differentiation pathways of epithelial stem cells.

Discussion and conclusions

Our findings demonstrate that primary epithelial cells have unique characteristics with an inimitable potential that makes them a malleable tool, able to adapt to different necessities. And so on, although these data are intriguing, further investigation could provide more and more useful data for their clinical application in regenerative medicine. As a proof-of-principle that epithelial stem cells have an intrinsic potential for regenerative medicine that can be exploited with a deeper characterization, my group have been able to apply, *in vitro*, a cell therapy protocol to a patient affected by a rare mosaic form of EEC syndrome.

HKLs appear to be particularly attractive, animal-free (feeder-free) and full-thickness scaffolds for corneal reconstruction. We have already started with the the recruitment of canine patients to assess the transplantability and functionality of these organotypic structures and, through the collaboration with different veterinary departments, we are creating a small cohort on which to start with first transplantation trials.

2 Introduction and background

2.1 Mantainance of epithelial homeostasis: epithelial stem cells

Epithelia are tissues organized in sheets, consisting of regular-shaped cells clinging to each other and often residing at the interface between the external environment and the body's organs. The renewal and maintenance of tissues, under the name of homeostasis, are guaranteed by the presence of adult stem cells. Adult ASMs, also known as somatic SCs, are undifferentiated cells which are part of organs and tissues, including brain, bone marrow, peripheral blood, blood vessels, skeletal muscles, skin, teeth, heart, gut, liver, ovarian epithelium, testes and more. To respect the definition of stem cells they must guarantee two important characters: self-renewal and potency. The first one represents the capacity to undertake numerous cycles of cell division maintaining their undifferentiated state. Instead the second aspect indicates the ability to differentiate into mature cell type (multipotency or unipotency for somatic SCs). Multipotency implicates the possibility to produce only cells of a closely related family like the hematopoietic stem cells. Unipotent stem cells, instead, can produce only one cell type.

In vivo, recent evidence has shown that adult stem cells reside in specific and exclusive tissue regions (niches) where they remain quiescent without division until activation by a normal need of tissues mantainance, or during wound healing. The structure and the localization of these niches are tissue specific such as the tissue turnover and regenerative potential. However, they have in common the maintenance of microenvironment through fundamental factors, like *Wnt* and *Nocht* signalling, specific grow factors and communications with neighbouring cells (Bonthagarala 2013).

Although it is very exiguous, the number of SCs in each niche vary between tissue, and their behaviours differ according on the stimuli to which they are subjected.

The ability of stem cells to survive and retain their proliferative potential throughout the lifespan not necessarily imply that they have an endless capacity to divide, or that they undergo constant self-renewal. Rather, it means that the frequency and timing of actual stem cell self-renewal divisions are tightly regulated within the tissue to ensure

the lifelong maintenance of the stem cell population. If stem cells are exhausted too quickly, or if genetic defects or damage reduce their proliferative potential, tissue atrophy and premature ageing can arise. Conversely, mutations that promote more frequent stem cell divisions without appropriate differentiation balance can result in abnormal tissue development and even cancer (Fuchs and Chen 2013).

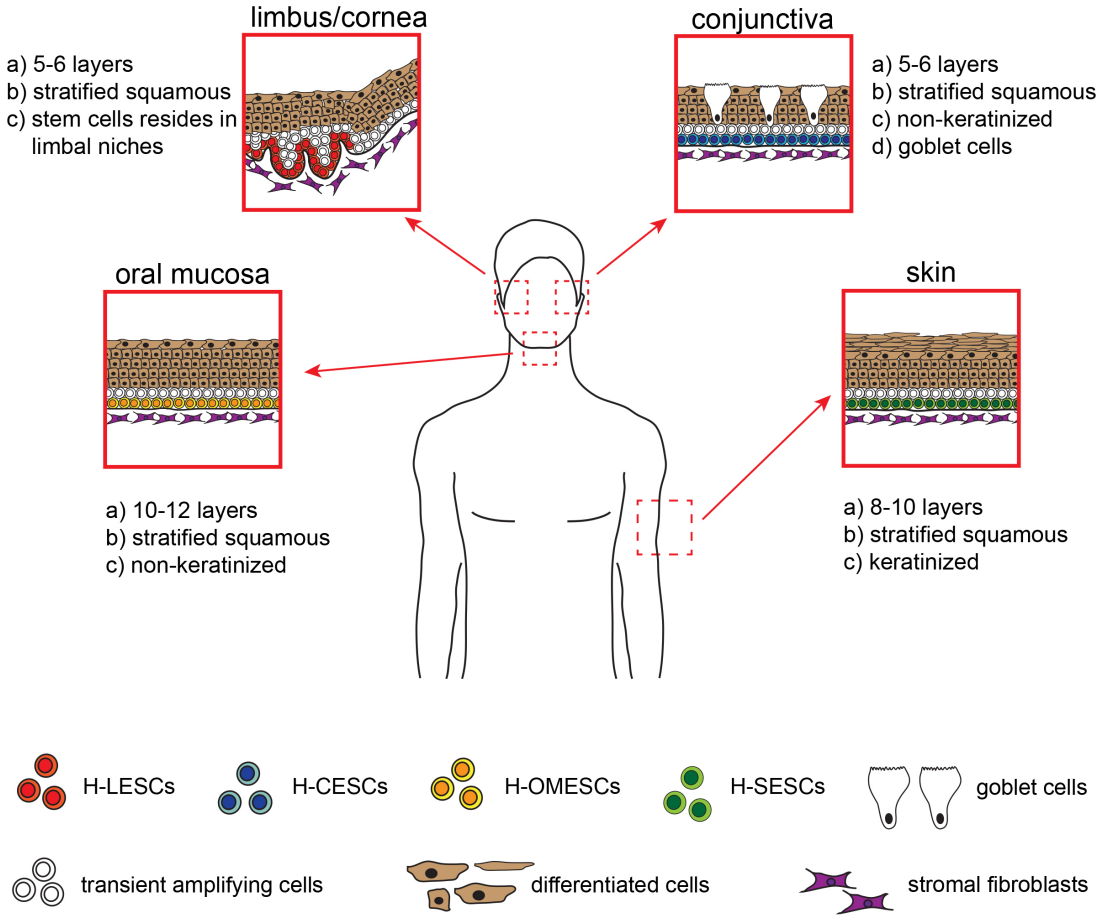

Figure 1. *Model of four epithelia: skin, oral mucosa, cornea and conjunctiva and their organization at tissue level.*
Abbreviations: SESCs, skin epithelia stem cells; OMESCs, oral mucosa epithelial stem cells; LESCs, limbal epithelia stem cells; CESCs, conjunctival epithelial stem cells.

Table 1. Tissue function, composition, stem cells niches and turnover times of the four different epithelium submitted to the analysis.

Tissue	Tissue function	Composition	SCs Niches	Turn-over time (days)
Skin	Protective, Thermoregulatory, Metabolic.	Corneus: 10 to 30 layers of polyhedral, anucleatedcorneocytes Translucent: found in the palms and soles Granular: Keratinocytes lose theirnucleiand theircytoplasmappears granular Spinous: Keratinocytes become connected throughdesmosomesand start produce lamellar bodies Basal: proliferating and non-proliferating keratinocytes	Spatially harboured in the throughout layer	28-30
Oral mucosa	Protection from external agents and mechanical stress	higher number of cell layers compared to skin basal spinous granular corneus: keratinized layer	Basal layer	14-24
Conjunctiva	Protection Lacrimal film maintenance	Variable number of layers varies among areas: marginal conj.: 5 layers of non-keratinised squamous epithelium; tarsal and orbital: 2 layers of stratified cuboidal epithelium; fornix and scleral: 3 layers of stratified squamous cells; limbal: 10 layers of stratified squamous cells.	Forniceal area	/
Cornea and Limbus	Protection Filtration of UV rays Refraction of light	5-7 layers of stratified squamous epithelial cells	Palisades of Vogt	/

2.2 Notch signalling and epithelial cells differentiation

Tissue homeostasis and wound repair require epithelial stem cells to perform different terminal differentiation programs. To achieve these results, stem cells must be instructed by their micro-environment to select a particular cell line.

Notch signaling controls selective cell-fate determination in variety of different tissues (Artavanis-Tsakonas, Rand, and Lake 1999). Conserved throughout eukaryotes, the canonical Notch pathway governs cell-fate decisions through close-range, cell-cell interactions (Cédric Blanpain, Horsley, and Fuchs 2007).

There are four Notch transmembrane receptors (Notch1-4) in mammals. Notch ligands are also transmembrane proteins and comprise three different subfamilies, each containing several members. In consequence to ligand binding, Notch receptors are sequentially cleaved by metalloproteinase and γ-secretase.

Once released, Notch's intracellular domain (NICD) is free to translocate to the nucleus, where it can associate with the DNA- binding protein RBP-J to convert it into a transcriptional activator (Cédric Blanpain, Horsley, and Fuchs 2007). The best characterized Notch target genes belong to the hairy enhancer of split (Hes) complex and consist of the b- HLH transcription factors Hes (1–7) and Hey (1–3) (Iso, Kedes, and Hamamori 2003). An example of the role of Notch signaling in promoting proliferation and differentiation can be also found in mammary epithelium. Overexpression of the active form of *Notch4* leads to mammary tumorigenesis (Hu et al. 2006), and although ablation of *RBP-J* does not disturb initial mammary gland morphogenesis, alveolar differentiation is severely impaired during pregnancy (Buono et al. 2006).

It is surprising that Notch is also implicated as a tumor suppressor in the cornea and epidermis, considering that loss of Notch1 in adult epidermis and cornea leads to epithelial hyperplasia followed by the expansion of basal layers (Rangarajan et al. 2001). Moreover, Additional support came from studies showing that Notch1-deficient skin displays a higher susceptibility of developing chemically induced cancer (Nicolas et al. 2003).

At first glance, it might appear as though Notch signaling promotes maintenance and self-renewal in some epithelial stem cells while inhibiting these processes in others.

However, multiple Notch receptors are expressed in the skin, and when all canonical Notch signaling is ablated in embryonic epidermis, proliferation is reduced and differentiation is impaired (Blanpain et al. 2004).

If the hyperproliferation observed on Notch1 ablation results from alterations in noncanonical Notch signaling or as an indirect consequence of epidermal barrier defects is still unclear. However, in the absence of RBP-J, follicle stem cells cannot be maintained, confirming multiple actions of canonical Notch signaling on epithelial stem cells (Blanpain and Fuchs 2006) (Yamamoto et al. 2003).

Like Wnt signaling, Notch signaling appears to exert its effects at multiple steps along lineage pathways. For example, in the hair follicle, NICD1 is also expressed in the matrix cells of both the hair shaft and its channel or inner root sheath (Pan et al. 2004), and conditional ablation of γ-*secretase*, or combined with the loss of either *Notch receptor genes* or *RBPJ*, results in defects in sebaceous gland development and terminal differentiation of the inner root sheath and hair shaft (Blanpain, Horsley, and Fuchs 2007) (Blanpain and Fuchs 2006) (Pan et al. 2004) (Vauclair et al. 2005) (Yamamoto et al. 2003). all these data confirm that Notch is a very complex signaling and has many roles not only in maintaining stem cells but also their lineages.

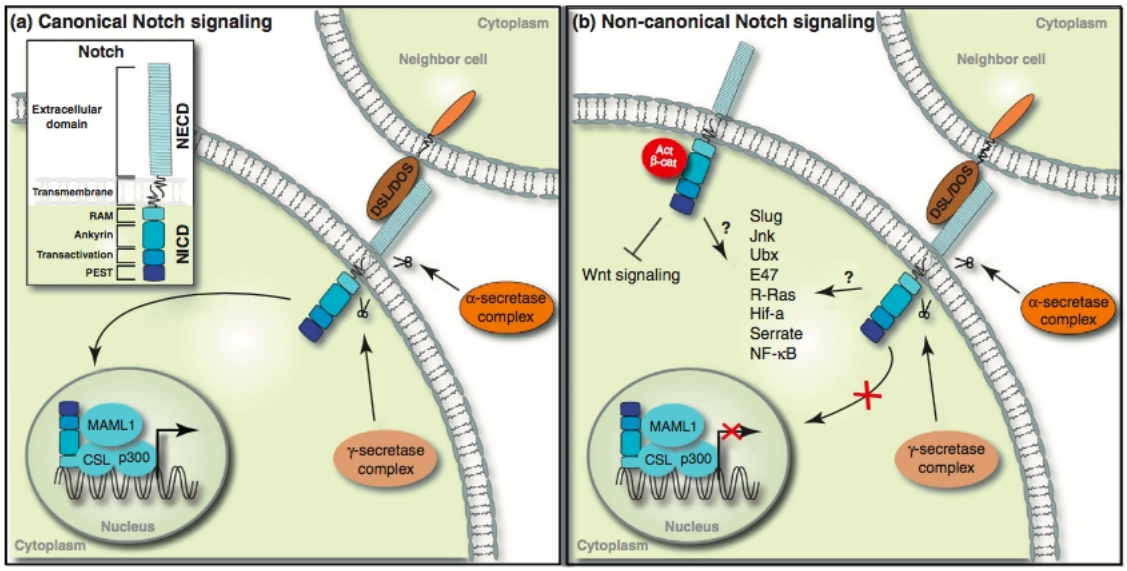

***Figure 2**. Canonical vs Non-canonical Notch signaling. Credit: (Andersen et al. 2012).*

2.3 The Ocular surface

The cornea is the tissue that covers most of the anterior ocula surface, comprising iris, pupil and anterior chamber. Since transparency is of primary importance, the cornea does not have blood vessels. Instead, oxygen dissolves in tears and then spreads throughout the cornea to keep it healthy (Brennan 2005). Similarly, nutrients are transported via diffusion from the tear fluid through the outside surface and the aqueous humour through the inside surface, and also from neurotrophins supplied by nerve fibres that innervate it. In humans, the cornea has a diameter of about 11,5 mm and a thickness of 0,5–0,6 mm in the center and 0,6–0,8 mm at the periphery. Transparency, avascularity, the presence of immature resident immune cells, and immunologic privilege makes the cornea a very unique tissue (Romer and Parsons 1977).

The human cornea borders with the sclera via the corneal limbus. In lampreys, the cornea is solely an extension of the sclera, and is separate from the skin above it, but in more advanced vertebrates it is always fused with the skin to form a single structure, albeit one composed of multiple layers. In fish, and aquatic vertebrates in general, the cornea plays no role in focusing light, since it has virtually the same refractive index as water (Romer and Parsons 1977).

The human cornea has five layers (possibly six, if the Dua's layer is included) (Romer and Parsons 1977). Corneas of other primates have five known layers. The corneas of cats, dogs, wolves, and other carnivores only have four (Merindano et al. 2002) (Hayashi, Osawa, and Tohyama 2002).

From the anterior to posterior the layers of the human cornea are:

Corneal epithelium: an exceedingly thin multicellular epithelial tissue layer (non-keratinized stratified squamous epithelium) of fast-growing and easily regenerated cells, kept moist with tears. Irregularity or edema of the corneal epithelium disrupts the smoothness of the air/tear-film interface, the most significant component of the total refractive power of the eye, thereby reducing visual acuity. It is continuous with the conjunctival epithelium, and is composed of about 6 layers of cells

which are shed constantly on the exposed layer and are regenerated by multiplication in the basal layer (Romer and Parsons 1977).

Bowman's layer (also known as the *anterior limiting membrane*): when discussed in lieu of a subepithelial basement membrane, Bowman's Layer is a tough layer composed of collagen (mainly type I collagen fibrils), laminin, nidogen, perlecan and other HSPGs that protects the corneal stroma. When discussed as a separate entity from the subepithelial basement membrane, Bowman's Layer can be described as an acellular, condensed region of the apical stroma, composed primarily of randomly organized yet tightly woven collagen fibrils. These fibrils interact with and attach onto each other. This layer is eight to 14 micrometres (μm) thick (Romer and Parsons 1977) and is absent or very thin in non-primates (Romer and Parsons 1977) (Hayashi, Osawa, and Tohyama 2002).

Corneal stroma (also *substantia propria*): a thick, transparent middle layer, consisting of regularly arranged collagen fibers along with sparsely distributed interconnected keratocytes, which are the cells for general repair and maintenance (Romer and Parsons 1977). They are parallel and are superimposed like book pages. The corneal stroma consists of approximately 200 layers of mainly type I collagen fibrils. Each layer is 1,5-2,5 μm. Up to 90% of the corneal thickness is composed of stroma (Romer and Parsons 1977). There are 2 theories of how transparency in the cornea comes about: (i) The lattice arrangements of the collagen fibrils in the stroma. The light scatter by individual fibrils is cancelled by destructive interference from the scattered light from other individual fibrils (Maurice 1957). (ii) The spacing of the neighboring collagen fibrils in the stroma must be < 200 nm to maintain transparency (Maurice 1957). Commercially available techniques, such as confocal reflectance microscopy or optical coherence tomography (OCT), enable three-dimensional (3D) cell-scale imaging of cornea. However, these techniques lack specificity or contrast when looking at the collagen organization of the corneal stroma. In the last decade, new microscopy techniques have allowed us to take a closer look at the organization of the collagen fibers composing the corneal stroma. For example, multiphoton microscopy and in particular second harmonic generation (SHG) microscopy is a powerful tool to explore the nonlinear properties of biological tissues containing

collagen, as is the particular case of the cornea. Because of the natural noncentrosymmetric organization with a triple helix complex structure, collagen type I generates large SHG signals, allowing the microscopic analysis of the corneal structure (Latour et al. 2011).

Bueno et al., in 2011 showed that the anterior corneal stroma was organized in interwoven short bands of collagen randomly distributed. The lamellae at the central and posterior stroma were densely packed and often presented longer bundles lying predominantly parallel to the corneal surface with characteristic spatial distributions for different species. Also Morishige et al., in 2006, through reconstruction of SHG signals, saw two patterns of lamellar organization: highly interwoven in the anterior stroma and orthogonally arranged in the posterior stroma. Unique to the human cornea was the presence of transverse, sutural lamellae that inserted into Bowman's layer, suggesting an anchoring function.

Descemet's membrane (also *posterior limiting membrane*): a thin acellular layer that serves as the modified basement membrane of the corneal endothelium, from which the cells are derived. This layer is composed mainly of collagen type IV fibrils, less rigid than collagen type I fibrils, and is around 5-20 µm thick, depending on the subject's age. Just anterior to Descemet's membare, a very thin and strong layer, Dua's layer, 15 microns thick and able to withstand 1.5 to 2 bars of pressure (Harminder S. Dua et al. 2013).

Corneal endothelium: a simple squamous or low cuboidal monolayer, approx 5 µm thick, of mitochondria-rich cells. These cells are responsible for regulating fluid and solute transport between the aqueous and corneal stromal compartments (Romer and Parsons 1977). The corneal endothelium is bathed by aqueous humor, not by blood or lymph, and has a very different origin, function, and appearance from vascular endothelia.) Unlike the corneal epithelium, the cells of the endothelium do not regenerate. Instead, they stretch to compensate for dead cells which reduces the overall cell density of the endothelium, which affects fluid regulation. If the endothelium can no longer maintain a proper fluid balance, stromal swelling due to excess fluids and subsequent loss of transparency will occur and this may cause corneal edema and interference with the transparency of the cornea and thus

impairing the image formed (Romer and Parsons 1977). Iris pigment cells deposited on the corneal endothelium can sometimes be washed into a distinct vertical pattern by the aqueous currents. This is known as Krukenberg's Spindle (Romer and Parsons 1977).

2.4 Limbal epithelial stem cells

They are located in the peripheral portion of the cornea (limbus), in particular niches defined palisades of Vogt. These adult stem cells are able to rapidly divide and rebuild a totally destroyed corneal surface. They are undifferentiated unipotent cells, capable to give rise to transient amplifying cells and, then, to differentiated cells of the corneal epithelium, periodically replaced with a rapid turnover. Limbal stem cells activity can be induced both in response to physiological need of renewal and in case of injurious insults that require a repair of the ocular surface (Pellegrini et al. 1997) (Pellegrini et al. 2001) (Di Iorio et al. 2005).

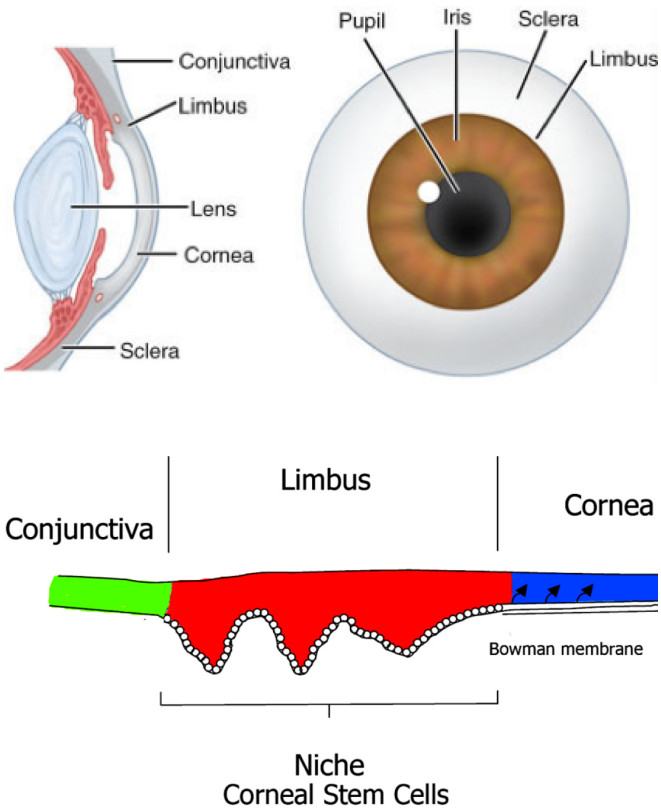

Figure 3. *Graphic representation of the ocular surface and corneal organization. Limbus separates corneal and conjunctival epithelium and represents the natural niche of corneal stem cells.*
Credit: http://www.louisvilleeyecenter.com/services/scleral-contact-lenses/

2.5 Corneal transplantation

In case of severe damages involving its transparency or its morphology (post-traumatic or post-inflammatory lesions, edema from endothelial decompensation, keratoconus, etc.) you can replace the injured tissue with sheets taken from donors (penetrating keratoplasty) (Ferrari et al. 2009). As known, the cornea is normally avascular so that immunological rejections are rare and systemic immunosuppressive therapy is generally not required. In the light of this, the intervention has a high success rate (up to 95%) when the tissue to be replaced is not vascularized and the peripheral ring (limbus, where corneal stem cells reside) is in good condition (keratoconus, corneal bullous keratopathy and leucomas) (Ferrari et al. 2009).

2.6 Limbal stem cells deficiency

Injury, genetic diseases and alterations of the limbal stem cell niche microenvironment can lead to LSCD (Kadar et al. 2011). Among these, chemical, heat or radiation burns and chronic inflammatory conditions are the most common sources of damage to LESCs in humans with LSCD (H. Dua 1998). Impaired repair mechanism of the corneal epithelial layer through Herpes simplex, neuroparalytic keratitis, drug toxicity, contact lens keratopathy and diseases such aspterygium, aniridia and Stevens Johnson syndrome are also associated to varying degrees of LSCD in humans (H. S. Dua et al. 2000).

When the cornea is entirely covered with a fibro-vascular tissue, the chances of success of a traditional penetrating keratoplasty are virtually null and in the past the only possible alternative was the installation of artificial keratoprosthesis (Aravena, Yu, and Aldave 2017) (Ang et al. 2017) or a complex surgery of osteo-odonto-keratoprosthesis (Plattner et al. 2017), in which a cylinder of transparent plastic was cemented within a tooth fragment taken from the patient and then implanted in place of the damaged cornea.

In these events of total disruption of the cornea, a complete replacement of the injured tissue has also been tried, using a sheet of larger diameter (12 mm sclero-corneal graft). Results, however, were unsatisfactory for the high incidence of

complications, most notably the rejection of the transplanted tissue. The frequency of this complication is directly proportional to the size of the sheet, because of the vessels present in the outer corneal ring (Salvalaio et al. 2003).

A rejection is actually rare in the current transplant techniques, because the corneal graft is usually performed through a "button" of tissue (diameter 8-8,5 mm), defined corneal lenticule (Salvalaio et al. 2003), lacking blood vessels and barely immunogenic.

2.7 Consequences of limbal stem cells deficiency

Pathological conditions associated with a limbal deficiency promote the propagation and migration of the conjunctival epithelium (the only source of epithelial repair) resulting in invasion and causing severe impairment of the corneal surface. The conjunctival pannus that is formed also involves neovascularization and inflammation, leading to clouding and subsequent weakening or loss of vision (H. S. Dua et al. 2000). Pain and photophobia are clinical consequences related to the loss of limbal stem cells, and these conditions, if untreated, can lead to chronic pain with persistent epithelial defects and high risk of bacterial keratitis, corneal perforation and blindness (H. S. Dua et al. 2000). A wide variety of chemical and toxic agents can cause extensive damage to the surface structures of the eye followed by alterations in the deeper stromal tissue.

2.8 Corneal lenticules

Until a few years ago, a full-thickness corneal transplantation (keratoplasty) was mainly carried out, including all the layers of the cornea: epithelium, stroma and endothelium. The anterior lamellar grafts were known but little practiced. In this type of transplant, the cornea was horizontally severed, replacing only the most anterior damaged part, (epithelium and anterior stroma). However, the surfaces obtained with these methods were extremely irregular and severely invalidated the visual results. The introduction of new technologies (excimer laser and microkeratome) able to get regular surfaces allowed the lamellar keratoplasty to be the elective indication in most of the cases. This is currently the procedure that provides the best results in terms of visual recovery and reduced incidence of complications, since the transplant is

performed obtaining a sheet of small size (corneal lenticule), with adequate thickness (300-350 microns) and diameter 8-8,5 mm. The lenticules can be prepared "fresh" or dehydrated in silica gel (Salvalaio et al. 2003).

2.9 Cell therapy and reconstruction of corneal epithelium and clinical application of autologous cultured corneal epithelial grafts

When the disease affects the function of the corneal epithelium, including stem cells, corneal transplantation must be preceded by a graft of autologous stem cells, from the contralateral healthy eye, amplified *in vitro* in order to obtain a sufficient amount to repopulate the limbus and guarantee the continuous self-renewal of the corneal surface. The identification of epithelial stem cells and the ability to amplify them *in vitro*, generating autologous epithelial sheets, opened a new horizon in regenerative medicine and represents a concrete step forward in the treatment of certain hardly treatable eye disorders up to a few years ago (Pellegrini et al. 2001) (Di Iorio et al. 2005).

The team for research and clinical production of the *Eye Bank Foundation of Veneto* has shown that is possible, from a small limbal biopsy (1 mm^2), to get cultured corneal epithelia, transferring limbal stem cells onto a fibrin matrix (Pellegrini et al. 1997) (Di Iorio et al. 2010). The fibrin-cultured epithelial sheet can, then, be transplanted onto the eye of the patient obtaining a correction of corneal impairment in over 70% of cases, allowing recovery of the visual acuity when the damage is limited to the corneal epithelium.

A valid alternative to LESCs are autologous OMESCs that may be used to reconstruct corneal surfaces and restore vision in patients with bilateral ocular surface (Nishida et al. 2004). In this work Nishida et al showed how during a mean follow-up period of 14 months, all corneal surfaces covered with OMESCs sheets remained transparent and there were no complications. Another particular circumstance concerns all the damage that extends even in the deeper stroma. the actual gold standard for the treatment of these lesions is a double surgery with a first application of fibrin cultured ESCs and then a penetrating keratoplasty for the replacement of the damaged stroma. With the second intervention most of stem cells previously transplanted that reside in the basal

layer of the entire corneal surface are removed, thus jeopardizing the transplant outcome. In the light of this, my group, in 2009, proposed the use of Human Keratoplasty Lenticules (HKLs) as a suitable scaffold for the cell terapy of LSCD (Barbaro et al. 2009). If plated on them, corneal epithelial stem cells were shown to proliferate, express differentiation markers, and bind to the underlying stroma with no alterations in clonogenic potential . HKLs have some advantages over currently used scaffolds, such as the possibility to allow cell growth with no feeder layers, to be freeze dried, and to preserve the integrity and viability of stromal keratocytes. The development of a tissue-engineered "hemicornea" might offer new therapeutic perspectives to patients affected by total limbal stem cell deficiency with stromal scarring (Barbaro et al. 2009).

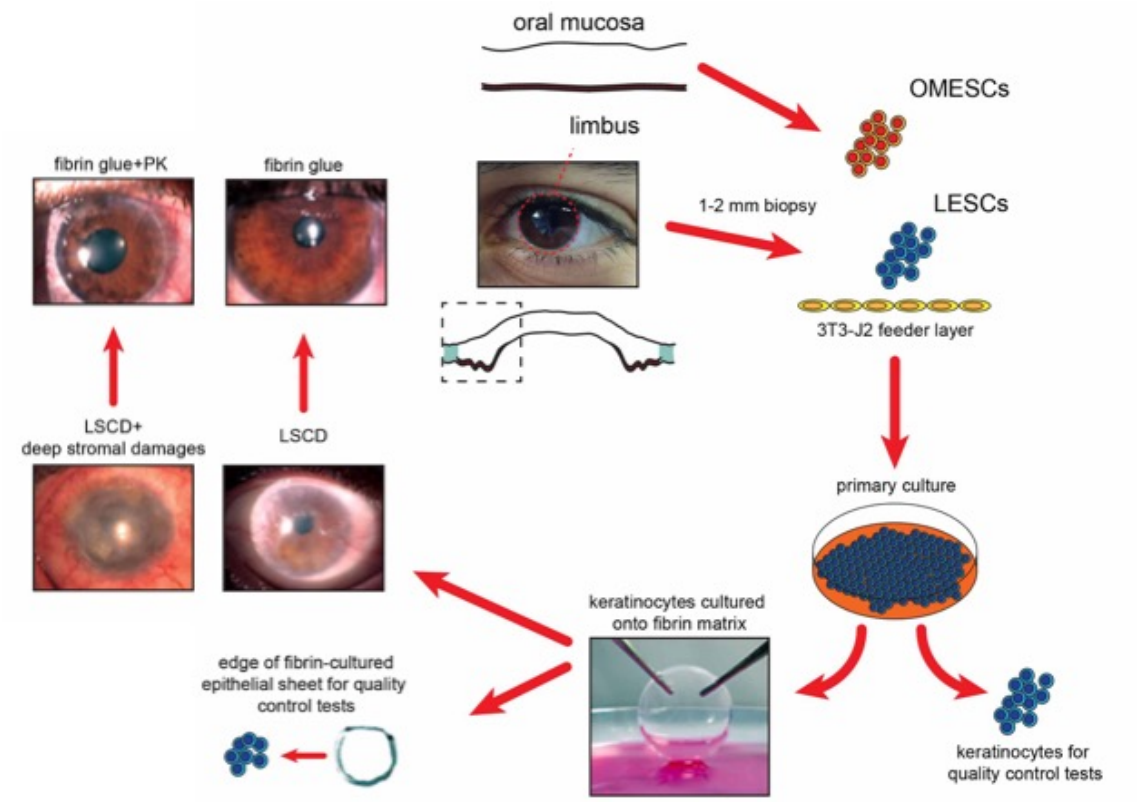

Figure 4. *model of the ex vivo cell therapy approach for corneal reconstruction in LSCD patients.*
Abbreviations: OMESCs, oral mucosa epithelial stem cells; LESCs, limbal epithelia stem cells; LSCD, limbal stem cells deficiency.

2.10 The EEC Syndrome

The Ectrodactyly-Ectodermal dysplasia-Clefting (EEC) syndrome (MIM#604292) is a rare autosomal dominantly inherited disease characterized by multi-organ dysfunctions including ectrodactyly (split-hand-foot malformation), ectodermal dysplasia, facial clefting (mostly in the form of cleft lip and palate) and urogenital abnormalities in 13 out of 25 cases (Nardi et al., 1992; Roelfsema and Cobben, 1996). It affects the skin, nails, hair, teeth, sweat glands and the ocular ectodermal derivatives. Hypohidrosis is variable, the hair is sparse, fair and dry and eyebrows and lashes are often absent. The teeth are small and may be partially formed, and hypodontia and anodontia occur. The nails are thin, brittle and ridged, and tear duct abnormalities are common. Developmental abnormalities of the meibomian glands and lacrimal glands are present at birth.

While in childhood clefting and hand deformities are the main clinical features, during early adulthood ocular problems become the predominant clinical aspect of EEC syndrome (Käsmann and Ruprecht, 1997). Patients often show ocular surface alterations such as recurrent blepharitis and conjunctivitis, superficial microlesions of the cornea, spontaneous corneal perforation and ulceration, defective regeneration and poor reepithelialization following trauma or penetrating keratoplasty (PK). They are characterized by dense vascularized corneal pannus, leading to progressive corneal clouding and eventually severe visual impairment (Willoughby et al. 2005).

Alterations leading to these symptoms are: (1) the atresia of the lacrimal duct system and the absence of meibomian glands causing tear film instability and (2) the epithelial defects of the cornea caused by mutations in the p63 gene. While tear film instability and dry eye symptoms can be overcome with tear supplements, despite all the knowledge accumulated no curative treatments are currently available for the epithelial defects; current ones are only palliative.

Figure 5. *EEC phenotype of a newborn patient.*

2.11 The genetic cause of the disease

The EEC syndrome is caused by mutations in the p63 gene, an important transcription factor during embryogenesis (it ensures the normal development of orofacial ectoderma and limbs) and for stem cell differentiation in stratified epithelia. Mutations in the p63 gene can cause at least 6 different syndromes: split-hand/split-foot malformation (SHFM), ectrodactyly-ectodermal dysplasia and cleft lip/palate (EEC) syndrome, ankyloblepharon-ectodermal defects-cleft lip/palate (AEC) syndrome, limb mammary syndrome (LMS), acro-dermato-ungual-lacrimal-tooth (ADULT) syndrome and Rapp-Hodgkin syndrome (RHS). The rare combination of ectrodactyly (lobster-claw deformity), ectodermal dysplasia and cleft lip with or without cleft palate has historically been described as EEC syndrome. The EEC syndrome is mainly caused by point mutations in the DNA binding domain of the p63 gene. Thirty-four different mutations have so far been reported, and at least 20 different amino acids are involved. Only 2 mutations are outside the DNA binding domain: one insertion (1572 InsA) and one point mutation (L563P) in the Sterile α-Motif (SAM) domain (Celli et al., 1999; Rinne et al., 2007). Five frequently mutated amino acids (R204, R227, R279, R280 and R304) were found in the EEC population, all located in the CpG islands (Rinne et al., 2007; Hamada et al., 2002). These 5 mutations account for almost 90% of all the EEC syndrome patients (Rinne et al., 2007; van Bokhoven and Brunner, 2002). Mutations found in the p63 gene of EEC patients appear therefore to impair p63 protein binding to DNA (Celli et al., 1999). Even if EEC mutations have dominant

negative effects, recent genotype-phenotype analyses for the five hot-spot mutations revealed significant differences between the corresponding phenotypes. For instance while cleft lip/palate is present in the R304 mutated population (80%), R227 patients seldom have cleft lip/palate. Syndactyly is completely absent in the R227 population, while 30−60% of the other hot-spot mutation population have syndactyly. Genito-urinary defects are frequently observed in R227 patients (40%), but less in other patients (Rinne et al., 2007). It thus seems that these hot-spot mutations might exert specific modifying effects as, for example, on promoters for p63 transcriptional target genes. All patients with R304Q, R279H, R279S, R311G, H208R, R280C, S272N and R311G show serious ocular problems and progressive loss of visual capacity (Willoughby et al., 2005). Most of cases are sporadic, related to de novo mutations arising during early-stage development. Familial cases show an autosomic dominant inheritance with variable penetrance. The incidence and prevalence of the EEC syndrome in the Italian and European populations are unknown. Males and females are equally affected.

2.12 p63 gene

p63 gene, a member of p53 superfamily, is located at 3q27-29. p63 encoded proteins with two different N-termini (TA and ΔN) and three different C termini (α, β and γ); so there are 6 isoforms, depending on specific alternative promoter usage and alternative splicing (Augustin et al., 1998; Yang et al., 1998).

Structure. p63 comprises up to five types of domains, depending on the isoform, and may contain transactivation (TA), DNA Binding (DBD), oligomerization (OD), C-terminal sterile α-motif (SAM), and/or C-terminal transcription inhibitory (ID) domains (Moll and Slade, 2004).

The DNA binding domains of p63 and p53 share over 60% identical primary aminoacid sequences, and they share 25% identity in TA domain. Some p53 target genes including Bax, MDM2 and p21 can be transactivated by TAp63 isoforms (Jost et al., 1997; Yang et al., 2002). The N-terminus may consist of a TA domain or a truncated version (ΔN) lacking the acidic TA domain, which is derived from an alternative promoter and initiation codon in intron 3 (Yang et al., 1998). Without the transactivation activity, ΔN

isoforms work in a dominant-negative manner, inhibiting TAp63 and other p53 family members. The C-termini of both TAp63 and ΔNp63 may be alternatively spliced to yield isoforms α, β and γ. TAp63α and ΔNp63α contain a protein-protein interaction SAM domain and a trans-inhibitory domain, resulting from the masking of N-terminal TA domain residues. (Mangiulli et al., 2009). p63 binds to DNA as either a homo- or heterotetramer, with isoform composition of the tetramer possibly determining transactivation activity. p63 may also form mixed dimers or tetramers with p73 at relatively higher affinity than with p53, suggesting functional cross talk to regulate transcriptional activity (Davison et al., 1999; Natan and Joerger, 2012). p63 appears to form a dimer of dimers, with monomers consisting of a β-strand followed by two helices (H1 and H2) that adopt a Z-shaped double-hairpin conformation with little intramolecular contact between structural elements.

Monomers dimerize via intermolecular antiparallel β-sheet interactions and antiparallel packing of the H1 helices, with important hydrophobic contacts made by key leucine, valine, tyrosine, methionine, and isoleucine residues. Tetramers are formed by hydrophobic H1-H1 interactions and H2-mediated contact where the H2 helices from the primary dimer clasps the adjacent dimer, packing the tetramer in an orthogonal fashion via H1 helices arrangement (Natan and Joerger, 2012). Analysis of the DBD of p63 shows higher similarity to that of p73 than p53, and appears to bind a 10 bp DNA sequence containing a "CATG" motif with A/T-rich flanking regions (Chen et al., 2011).

Expression. p63 is expressed in the surface ectoderm (in embryonic stem cells) during embryogenesis and in adult tissues it is restricted to the epithelial stem cells. Immunohistochemistry of p63 often shows strong nuclear-localized staining in basal epithelial cells. Additionally, TA and ΔN isoforms appear to be differentially expressed in particular tissue types. TAp63 variants are prevalent in the heart, testis, kidney, thymus, brain, and cerebellum. ΔNp63 transcripts are detected heavily in epithelial cells, kidney, spleen, cornea and thymus, but not in the heart, liver, testis, or brain (Yang et al., 1998; Dötsch et al., 2010).

Function. p63 acts as a motif-specific transcriptional activator or repressor, depending on the presence of TA or ID domains in the specific p63 isoform (Yang et al., 1998). It

plays a critical role in the maintenance of progenitor-cell populations that encourage epithelial development and morphogenesis (Romano et al., 2009), and it is the gene with the most striking effects on the development of stratified epithelia (Yang et al., 1998; Mills et al,. 1999; Yang et al., 1999; Koster et al., 2004). Ablation of the p63 gene in mice results in the absence of these epithelia (Mills et al., 1999; Yang et al., 1999). In particular, p63−/− mice show major defects in limb and craniofacial development, as well as a striking absence of stratified epithelia.

This could be explained either by the inability of p63−/− ectoderm to develop into epithelial lineages (Mills et al., 1999) or by the lack of stem cell features necessary to sustain epithelial morphogenesis and renewal (Yang et al., 1999). In humans, mutations of the p63 gene cause disorders of the epithelia and of nonepithelial structures whose development depends on the epithelial functions (Celli et al., 1999).

ΔNp63, once thought to serve as a dominant negative regulator due to its lack of a full TA domain, has recently been implicated in transcriptionally activating and repressing target genes such as keratin 5 and keratin 14 to dictate early epithelial development and determine keratinocyte cell fate and lineage choices (Yang et al., 1998; Romano et al., 2009). ΔNp63 sustains the keratinocyte proliferative potential (Parsa et al., 1999) that is characteristic of stem cells. Yet, the expression of p63 by the majority of basal cells and by suprabasal cells, as assessed by the 4A4 antibody recognizing all p63 isoforms, has been considered too broad to be stem cell specific (Sun and Lavker, 2004; Kaur et al., 2004). p53 tumor suppressor gene properties is due to its DNA binding and transactivation of target genes which specify cell cycle and apoptosis. TAp63 protein, when over-expressed in human cells, also binds to p53 target gene, and induces cell cycle arrest, differentiation and apoptosis in a p53-like manner. (Jacobs et al., 2005; Mills, 2006). ΔNp63 isoforms, unlike TAp63 isoforms which acts as tumor suppressors, act as oncogenes (Lee et al., 2006).

2.13 p63 expression in the cornea

Keratinocyte stem cells govern the renewal of squamous epithelia by generating transient amplifying cells (TA cells) that terminally differentiate after a limited number of cell divisions (Watt, 2001; Fuchs and Raghavan, 2002; Gambardella and Barrandon,

2003; Potten, 2004). Corneal stem cells (keratinocytes) are segregated in the basal layer of the limbus, which is the zone encircling the cornea and separating it from the bulbar conjunctiva. The limbus contains radially-oriented fibrovascular ridges known as the palisades of Vogt. TA cells that migrate from the limbus form the corneal epithelium (Sun and Lavker, 2004).

Clonal analysis of limbal epithelial cells show different types of cells, such as:

a. holoclones: putative stem cells with a diameter of 6-10µm. These cells have a high proliferating capability with ≤ 5% aborted colonies and ≥ 100 cell doublings;

b. meroclones: young transient amplifying cells with intermediate proliferating capacity having a diameter of 10-18 µm. These cells usually have 5-95% aborted colonies;

c. paraclones: terminally differentiated cells with 15-20 cell doublings and very low proliferative capability. These cells are 18-36 µm long in diameter.

Human keratinocyte stem and TA cells, when isolated in culture, generate holoclones and meroclones, respectively (Barrandon and Green, 1987; Rochat et al., 1994; Pellegrini et al., 1999).

That the limbus is the site of stem cell precursors of the corneal epithelium is clear for several reasons:

(1) the basal layer of the limbus lacks keratin 3 (a marker for corneal differentiation), whereas limbal suprabasal layers and all layers of the corneal epithelium express keratin 3 (Schermer et al., 1986);

(2) the limbus contains slow-cycling cells and holoclone-forming cells, but the corneal epithelium does not (Pellegrini et al., 1999; Cotsarelis et al., 1989);

(3) the corneal epithelial cells are not self-sustaining; they divide only a few times during their migration from the limbus to the central cornea (Lehrer et al., 1998);

(4) restoration of destroyed limbal/corneal epithelium requires limbal transplantation (Kenyon and Tseng, 1989) or grafts of autologous limbal cultures (Pellegrini et al., 1997; Tsai et al., 2000; Rama et al.2001).

Depending on the conditions, limbal and corneal keratinocytes may contain all three ΔN isoforms. In the uninjured surface of the eye, ΔNp63α is present in the limbus but absent from the corneal epithelium. ΔNp63β and ΔNp63γ appear upon wounding and correlate with limbal cell migration and corneal regeneration and differentiation (Di Iorio et al., 2005).

The finding that p63 is specifically expressed by stem cells of human epidermis and limbal epithelium strongly suggests that the phenotype of p63−/− mice should be ascribed to a failure to maintain stem cells rather than to the inability of p63−/− ectoderms to form epithelial lineages during development. p63 is essential for regenerative proliferation in epithelial development, distinguishes human keratinocyte stem cells from their TA progeny, is expressed by the basal cells of the limbal epithelium (but not by TA cells covering the corneal surface), and is abundantly expressed by epidermal and limbal holoclones, but undetectable in paraclones (Pellegrini et al., 2001; Nylander et al., 2002, Thurfjell et al., 2004, Di Iorio et al., 2005). In human corneal epithelia, ΔNp63α is the major p63 isoform expressed and it is necessary for the maintenance of the proliferative potential of limbal stem cells and essential for regenerative proliferation in the ocular surface (Di Iorio et al., 2005). Limbal-corneal keratinocytes express not only ΔNp63α but also the ΔNp63β and ΔNp63γ isoforms. However, while expression of ΔNp63α is restricted to the limbal stem cell compartment, the expression of ΔNp63β and ΔNp63γ correlates with limbal cell migration, corneal wound healing and corneal differentiation (Di Iorio et al., 2005; Di Iorio et al., 2006). ΔNp63α is expressed in a small amount of undifferentiated and small cells (stem cells). The percentage of these cells in primary cultures ranges between 3% and 8% and decreases progressively both during clonal conversion (the transition from holoclones to meroclones and paraclones) and serial propagation of stem cell in vitro (life-span).

2.14 Animal models of Limbal Stem Cells Deficiency (LSCD)

We can identify two main categories of LSCD models: animals with induced ocular surface damage and LSCD animal patients. In the first case, lesions to the cornea and the loss of stem cells reservoir are induced by the application of alkaline substances,

such as NaOH (Tananuvat et al, 2016) and Benzalkonium Chloride (Lin et al, 2016), of n-Heptanol (Pang et al, 2016) or through total limbal peritomy (Xu et al, 2012; Selver et al 2016).

Regarding LSCD animal patients, recent studies in veterinary have shown that in many animal species there is a corneal tissue organization like the human one, with stem cells segregated in the outer ring of the epithelium (Limbus), and there are also pathologies related to the loss of corneal stem cells pool comparable to LSCD (Nam et al, 2015; Sancak et al, 2014).

Several corneal diseases in small animals lead to vascularization, conjunctivalization and/or pigmentation of the corneal surface. Yet, despite a wealth of knowledge of conditions potentially associated with LSCD in domesticated animal species, and despite decades of scientific papers and textbooks dedicated to veterinary ophthalmology, LSCD is not commonly reported or discussed in the existing literature. (Nam et al, 2015; Sancak et al, 2014).

Corneal changes typically seen in LSCD include corneal conjunctivalization with vascularization, fibrosis and inflammatory infiltrate, and they give the cornea a dull, opaque and irregular appearance. (Dua et al, 2003; O'Callaghan et al, 2011). Similarly to humans with LSCD, there are corneal conditions in animals in which corneal disease is strongly suspected to result in LSCD, such as with canine herpes virus-1 keratitis (Ledbetter et al 2013). Chemical damage to the cornea in dogs can lead to corneal changes that also share many similarities with LSCD in humans. Another disease that shares such similarities is symblepharon in cats caused by Feline Herpes Virus-1 and for which there is currently no treatment. Furthermore, it is possible that chronic irritation and/or immune mediated conditions such as canine keratoconjunctivitis sicca, lymphocytic–plasmacytic keratitis (aka chronic superficial keratitis or corneal pannus) and pigmentary keratitis (aka Pigmentary keratopathy) might develop into, or in part be caused by LSCD. Last but not least, naturally occurring aniridia has been described in a breed of dog, although it is considered a very rare disease, and it is not known whether or not the corneas of these dogs might be affected by LSCD as they are in humans with aniridia (Hunter et al 2007).

Recently, a dog with possible LSCD and conjunctivalization of the cornea caused by Canine Herpes Virus-1 suggested a diagnosis of neurotrophic keratitis (Ledbetter et al 2013). Interestingly, the authors postulated based on the studies of others (Cavanagh et al 1989; Ueno et al 2012), a potential negative effect of corneal sensory nerve depletion on the LESC leading to or aggravating the LSCD. This resonated with the findings in the recent study describing the presence of telocytes in stem cell niches of mice that also contained nerve endings (Luesma et al, 2013) and the well-known relationship between corneal epithelial health and a healthy corneal nerve supply (Yamada et al 2005). The dog cornea has approximately 10 corneal nerve trunks and the cat cornea approximately (Chang-Ling 1989; Barrett et al, 1991). Although generally speaking this makes the cat cornea more sensitive to that of dogs, sensitivity also depends on the shape of the skull. There are three basic skull shapes, dolicocephalics (long skulled dogs such as rough collies), mesaticephalic (medium sized skulled dogs and cats, such as Labradors and domestic short haired cats) and brachycephalic (short sized skull dogs and cats, such as Bulldogs and Persian cats). Brachycephalic dogs and cats have the lowest number of corneal nerve trunks and thus lower corneal sensitivity than the rest of the skull shapes (Blocker et al 2001). As mentioned earlier, indirect pathologic events that produce an abnormal microenvironment for LESCs are known to play a role in LSCD. Pathological events in the limbal stroma through exposure to sulfur mustard were postulated to cause delayed LESC death in rabbits through such a pathway (Kadar et al, 2011). It is possible that some of the spontaneous, severe, medial corneal pigment proliferation seen with Pigmentary Keratitis in Pugs, which is frequently accompanied by marked medial canthal entropion, could be worsened in part by a comparatively poor corneal sensation, and/or the effect of corneal nerve amount on the health on the LESC microenvironment. There is evidence to support the role of UVB induced damage to LESC niches in mice resulting in LSCD (Das et al, 2013). Once resolved, lymphocytic–plasmacytic infiltrate of the cornea in dogs (a.k.a. chronic superficial keratitis) can lead to chronic corneal scarring with long lasting pigmentation in breeds with heavily pigmented limbus, like German shepherds Interestingly, this condition is worsened by the effect of solar radiation although the use of UV-blocking contact lenses did not appear to have an effect on the progression of the disease in one study (Denk et al

2011). Dogs wore the lenses for approximately six months, the geographic location where the study took place (Munich, Germany) has median solar UV radiation that is predictably lower than in warmer latitudes or higher altitudes. A similar study in a location with a higher solar UV radiation might have led to different results. There are genetic factors that regulate LESC proliferation in the bovine cornea (Sun et al, 2006) and many cytokines that affect corneal wound healing and originate in the fluids bathing the cornea (Welge et al, 2001) as well as corneal keratocytes (West-Mays et al, 2006) and corneal epithelial cells (Rolando et al 2001). More recently, nerve growth factor was described as an essential support for stem cell renewal and, importantly, as a probable growth factor with critical regulatory functions in the LESC niche of the human limbus (Qi et al 2008).These findings have started to shed some light on the potential auto-regulatory roles of LESCs.

In the last decade, several tissue engineering approaches was developed to replace the gold standard fibrin matrix. Of these, many are scaffolds that have been tested on animal models in order to evaluate the *in vivo* manteinance of reconstructed epithelia.

In recent years, numerous papers on this subject have been published. To date, the most commonly used method, alternative to fibrin matrix, is the use of denuded amniotic membrane as a scaffold. For example, Bin et al in 2012 tested the biological functions of tissue-engineered human corneal epithelia reconstructed with LESCs and denuded amniotic membrane by transplantation in limbal stem cell deficiency (LSCD) rabbit models. They showed that this treatment could reconstruct a multilayered corneal epithelium with normal functions in restoring corneal transparency and thickness of LSCD rabbits after transplantation. Similarly, Pang et al were able to transplant post-primary explant outgrowths that retained the capacity for LSCD recovery found in primary explants. Finally, Selver et al and Tananuvat et al in 2016, applied the same procedure using both LESCs and OMESCs and obtaining well-layered and transparent epithelial sheets that were maintained *in vivo* on rabbits ocular surface.

3 Aim

Limbal stem cells deficiency (LSCD) is characterized by conjunctival epithelial ingrowth, neovascularization, recurrent corneal erosion and persistent ulcers, as well as corneal scarring and ultimately leads to visual impairment and blindness. When the cornea is entirely covered with a fibro-vascular tissue, the chances of success of a traditional penetrating keratoplasty are virtually absent, due to the lack of epithelial stem cells responsible of maintainance and renewal of the transplanted tissue.

We aimed to identify new approaches for the treatment of this pathology, thus my work focused on three main issues:

- In order to better understand the potentiality of epithelial stem cells in this work primary cultures derived from four different tissues: limbus, oral mucosa, conjunctiva and skin were analyzed. To better investigate the exhaustion of clonogenic potential and the self-renewal of epithelial stem cells we added to the survey p63-defective oral mucosa primary cell lines obtained from three patients affected by EEC syndrome, already known to cause an acceleration in epithelial aging (Barbaro et al, 2016). Once characterized the *in vitro* aging of the primary cultures obtained from these epithelia a possible approach to exploit the potentiality of somatic stem cells was to try to delay this aging and, given the key role of Notch in mediating the differentiation of adult epithelial stem cells, we decided to act on this pathway. We performed the administration of DAPT, a γ-secretase inhibitor, with the aim to inhibit or slow down differentiation processes in epithelial stem cell cultures derived from Holoclones, Meroclones and Paraclones of H-LESCs.
- My research group was also able to identify a unique homozygous-heterozygous mosaicism of EEC Syndrome, demonstrating that epithelial stem cells have an intrinsic potential for regenerative medicine that can be exploited with a deeper characterization. Our ultimate goal is to reconstruct the ocular surface of this patient and demonstrate a proof-of-principle approach, based only on stem cell strategy, that allows us to bypass gene therapy approaches.

- Transplantation of autologous limbal epithelial stem cells (LESCs) or oral mucosa epithelial stem cells (OMESCs) cultured on fibrin glue has shown to be, currently, the most advanced approach for surgical treatment of severe corneal opacity, such as, unilateral or bilateral LSCD, respectively. Fibrin gels don't alter the proliferative potential/stemness and don't induce clonal variations and loss of stem cells (Rama et al. 2001). It acts as an inert material, with the only function of carrier to allow the transfer of stem cells from the culture dish to the eye of the patient, and, then, to be naturally and completely absorbed after a few days. Fibrin is not, however, a scaffold that can repair or replace damaged corneal stroma. In addition, cell proliferation can lead to thinning of the fibrin layer, making the sheet difficult to manipulate during the surgical application. The fibrin gel is not a porous material and any blood accumulation below the graft may lead to an impaired reabsorption of the scaffold and, therefore, to a higher probability of failure. Finally, this matrix is not able to maintain the stem cells culture without the use of murine feeder layers with the effects related to the use of components of animal origin. Thus, we characterized a tissue engineered product obtained expanding LESCs or OMESCs *in vitro* on stromal scaffolds (human keratoplasty lenticules). HKLs are a system that appear to be a particularly attractive, animal-free (feeder-free) and full-thickness scaffolds for corneal/oral mucosa stem cells and stromal reconstruction. This applies to patients with moderate or severe depletion of limbal cells associated to impairment of stromal tissue, as a result of chemical, thermal or infective damage and without existing therapeutic alternatives (penetrating or lamellar keratoplasty). The use of HKLs could also provide an interesting organotypic culture system for evaluation of the growth, proliferation, and differentiation processes of corneal stem cells and the development of new pharmaceutical drugs (e.g., eye drops, medicinal products), as they might represent a valid *in vitro*-based alternative method for assessing toxicity and safety. The final aim of the present study is to move to the use of these scaffolds *in vivo* (animal models), as an essential step for the achievement of clinical applications.

4 Methods

4.1 Cell cultures

Human and Canine keratinocytes were obtained from ocular biopsies taken from whole eye cadaver donors. Biopsies were minced and trypsinized (0,05% trypsin/0,01% EDTA; Gibco®) at 37°C for 2 hours. Once isolated, cells were plated onto lethally irradiated 3T3-J2 cells ($2.4\times10^4/cm^2$) and cultured in 5% CO_2, using a mixture of DMEM and Ham's F12 media (2:1; Gibco®) containing Fetal Calf Serum (FCS 10%; Euroclone, Milan, Italy), penicillin-streptomycin (1%; Gibco®), glutamine (2%; Euroclone, Milan, Italy), insulin (5 μg/ml; Euroclone, Milan, Italy), adenine (0,18 mM; Euroclone, Milan, Italy), hydrocortisone (0,4 μg/ml; Euroclone, Milan, Italy), cholera toxin (0,1 nM; Euroclone, Milan, Italy), triiodothyronine (2 nM; Euroclone, Milan, Italy), and epidermal growth factor (10 ng/ml; Euroclone, Milan, Italy). Subconfluent primary cultures were passaged and serially propagated until exhaustion. In DAPT-treated primary cell lines the same medium was used with DAPT (20μM; Sigma-Aldrich, Milan, Italy) in addition.

4.2 Colony Forming Efficiency (CFE) assay

1000 cells for each passage were plated in 100-mm dishes, cultured at low density for 12 days and stained with Crystal Violet (Sigma-Aldrich, Milan, Italy). Colony-Forming-Efficiency (CFE) assays (number of colonies generated by seeded cells) and evaluation of the number of clonogenic cells were used to assess the presence of epithelial stem cells.

4.3 Human keratoplasty lenticules and preparation of hemicorneas *in vitro*

Corneoscleral rims were preserved at 4°C and used within 1–2 days from their excision. Each specimen was firmly placed in an artificial chamber and the epithelium manually removed after bathing the surface of the cornea with an isotonic solution containing 5 mg/ml of trypsin and 2 mg/ml of EDTA (Sigma-Aldrich, Milan, Italy). HKLs were

obtained by microkeratome resection of epithelium-free corneas. Limbal keratinocytes were plated onto HKLs at a concentration of 5×104 cells/cm2. Hemicorneas were cultured under submerged conditions for 7 days and air lifted for 14 further days.

4.4 Histology

Hemicorneas were fixed in 4% paraformaldehyde overnight at 4°C (PFA; Sigma-Aldrich, Milan, Italy), embedded in Optimal Cutting Temperature (OCT; Sigma-Aldrich, Milan, Italy) compound, frozen, and cryostat sectioned (5-7 μm).

4.5 Impression Cytology (IC)

To perform the impression cytology (IC) (Barbaro et al. 2010), subjects were anaesthetized topically before a sterile membrane (Millicell CM 0,4 mm, Millipore, Bedford, MA) was gently pressed onto the ocular surfaces for a few seconds. To increase the number of cells collected, the ocular surface was slightly dried up by keeping the eye open before sampling. With this procedure, approximately 50-70% of the epithelial cells of the ocular surface were collected onto the membranes. Membranes were labeled to match the presence of specific markers with the sector of the ocular surface analyzed. Cells were fixed with Kito-Fix (Kaltek, Padua, Italy). Membranes were cut with a blade, laid down into wells of a multiwell plate, mounted and analyzed by indirect immunofluorescence.

4.6 Immunofluorescence, and Imaging

Samples were then blocked in PBS-BSA 1% and incubated with antibodies against p63, involucrin, laminin-β4, laminin-β3, ΔNp63α, keratin 3, keratin 12 and mucin 1, for 1h at 37°C.

Fluorescein isothiocyanate (FITC) conjugated secondary antibodies (1:100; Santa Cruz Biotechnology; 1:500; Sigma-Aldrich, Milan, Italy) or rhodamine, tetramethylrhodamine (TRITC) conjugated secondary antibodies (1:100; Santa Cruz Biotechnology; 1:500; Sigma-Aldrich, Milan, Italy) were incubated for 1h at room temperature. Nuclei were stained with far-red fluorescent DNA dye (DRAQ5®, 1:2000, Cell Signaling Technology, Boston, MA) for 10 min at room temperature. Specimens

were analyzed with Nikon confocal laser scan microscopy (Nikon Corporation, Minato, Tokio) and image analysis was performed using the NIS-Elements Advanced Research softwere (Nikon Corporation, Minato, Tokio).

Table 2. List of primary antibodies, source, working dilution and company.

Antibody	Source	Dilution	Company
p63	rabbit polyclonal	1:100	Primmbiotech, Milan, Italy
ΔNp63α	rabbit polyclonal	1:100	Primmbiotech, Milan, Italy
Involucrine	goat polyclonal	1:200	Santa Cruz Biotechnology, Santa Cruz, CA
laminin-β4	goat polyclonal	1:200	Santa Cruz Biotechnology, Santa Cruz, CA
laminin-β3	goat polyclonal	1:200	Santa Cruz Biotechnology, Santa Cruz, CA
keratin 3	Mouse monoclonal (AE5 clone)	1:100	MP Biomedicals, Solon, OH
keratin 12	goat polyclonal	1:100	Santa Cruz Biotechnology, Santa Cruz, CA
mucin 1	rabbit polyclonal	1:100	Santa Cruz Biotechnology, Santa Cruz, CA

4.7 Purification of mRNA and reverse transcription

Total RNAs from primary keratinocytes were extracted and purified using the RNeasy Micro kit (Qiagen, Hilden, Germany). The purity of the RNA preparation was verified by measuring its absorbance ratio at 260/280. 500 ng of RNA was used to synthesize the cDNA with random hexanucleotide primers and MoMULV reverse transcriptase (Applied Biosystem, Foster City, CA) at 42°C for 1h.

4.8 real-time PCR

50 ng of cDNA was amplified in an AB7900 real-time PCR detection system (Applied Biosystem, Foster City, CA) using PowerUp SYBR™ Green Master Mix (Applied Biosystem, Foster City, CA) or TaqMan™ Universal Master Mix II (Applied Biosystem, Foster City, CA), in a total volume of 20 µl. For the absolute target gene quantification (Ab-qPCR), standard curves were created with amplicons cloned into a TOPO plasmid vector. The level of expression of the target gene was normalized to GAPDH.

For the relative gene expression analysis (Rel-qPCR), the difference in relative target gene expression was performed using the $2^{-\Delta\Delta Ct}$ method. GAPDH was used as internal control gene. The efficiency of the target amplification and the efficiency of the

reference amplification (GAPDH) was opportunely measured and resulted approximately equal.

4.9 PCR of the Exon 8 of the Tp63 Gene

DNA was extracted directly from oral mucosal biopsy or from the primary culture by using the DNeasy Blood & Tissue Kit (Qiagen, Hilden, Germany), following the manufacturer's instructions and procedures. Polymerase chain reaction (PCR) was performed on the genomic DNA extracted from tissue or cells, using forward and reverse primers designed to amplify exons 8 (Table 2; 61.6°C; amplicon length: 351 base pairs).

4.10 Sanger Sequencing

PCR products (6 ml) were submitted to a phase of the BigDye Terminator kit (Thermo Fisher Scientific, San Diego, CA). BigDye mix contained 2 ml of buffer, 2 ml of terminators, and 5 ml of primer mix (1 mM). The sequencing program was as follows: a first step of 96°C for 39, continued with 30 cycles of 96°C for 109, 50°C for 59, and 60°C for 49. After the BigDye treatment, sequencing was performed according to the Sanger method.

Table 3. List of primers and probes used in Ab-qPCR, Rel-qPCR, PCR and Sanger sequencing.

Gene	Sequence
ΔNp63α (human)	Fw: 5'-GCATTGTCAGTTTCTTAGCGAG-3' Rev: 5'-CCATGGAGTAATGCTCAATCTG-3' Probe: 5'-[6FAM]GGACTATTTCACGACCCAGG[BHQ1]-3'
GAPDH (human)	Fw: 5'-CCACTCCTCCACCTTTGACG-3' Fw: Rev: 5'-CATGAGGTCCACCACCCTGT-3' Probe: 5'-[TET]TTGCCCTCAACGACCACTTT[TAM]-3'
p63 (human; exon8)	Fw: 5'-GGTAGATCTTCAGGGGACTTTC-3' Rev: Rev: 5'-TTCTCACTGGCTCTGAGGG-3'
p63 (human; seq)	Fw: 5'-GTAGCAACCCTCTATTGTGTG-3' Rev: Rev: 5'-GCCGTTGGATGGGAAGTTC-3'
p63 (dog)	Fw: 5'-CGGAAGGCGGATACAGCATCA-3' Rev: 5'-AAGGCGCTTCGTACCGTCACCG-3'
ABCG2 (dog)	Fw: 5'-CAGGGCTGTTGGTAAATCTCA-3' Rev: 5'-TACTGCAAAGCCGCATAACC-3'
GAPDH (dog)	Fw: 5'-TGACACCCACTCTTCCACCTTC-3' Rev: 5'-CGGTTGCTGTAGCCAAATTCA-3'

4.11 Luciferase Reporter Assay

For the luciferase assay, HEK293T cells were plated at density of $2X10^5$ cells per well in a 24-well plate and transfected 24 hours later. Lipofectamine 2000™ (Thermo Fisher Scientific, San Diego, CA) was used as transfecting agent. A plasmid containing the luciferase gene under the control of the K14 promoter and expression vectors encoding for WT-, R311K-, R311G-, R304Q-, and R279H-ΔNp63α were used. When needed, the pcDNA empty vector (Thermo Fisher Scientific, San Diego, CA) was added to reach the total amount of DNA (500 ng) used in each transfection. In all cases, 10 ng of Renilla luciferase vector (pRL-CMV; Promega, Madison, WI) was cotransfected as a control of the transfection efficiency. Cells were transfected at 80%-90% confluence and incubated at 37°C for 6 hours before medium change. Luciferase activities of cellular extracts were measured by using a dual luciferase reporter assay system (Promega, Madison, WI) and light emission was measured over 1 and 5 seconds using a Modulus Microplate Reader luminometer (Promega, Madison, WI). All experiments were performed in triplicate.

4.12 Molecular Cytogenetics

Bacterial artificial chromosome (BAC) genomic clones were obtained from Source BioScience (Berlin, Germany) and labeled by random priming (BioPrime DNA labeling system; Thermo Fisher Scientific, San Diego, CA) with Biotin-14-dCTP (Thermo Fisher Scientific, San Diego, CA) or digoxigenin-11-dUTP. Molecular combing analysis was performed as previously described (Palumbo et al. 2010). Briefly, R311K keratinocytes were harvested and immobilized in agarose plugs. High-molecular-weight DNA obtained after β-agarase I digestion (3 U per 1–2 plugs; EuroClone, Milan, Italy) in 0,1 M MES, pH 6,5, was combed on silanized surfaces, according to a standard procedure (Palumbo et al. 2010). A range of 250–300 ng of each labeled probe was hybridized per each slide in the presence of 13X Cot-1 DNA (Thermo Fisher Scientific, San Diego, CA) and 10 μg of salmon sperm DNA (Thermo Fisher Scientific, San Diego, CA). To detect the biotin-labeled probes, 594 Alexa Fluor-conjugated streptavidin (1:50; Thermo Fisher Scientific, San Diego, CA) and biotinilated antistreptavidin antibodies (1:50; Rockland, Limerick, PA) were used. The digoxigenin-labeled probe was detected by a

monoclonal anti-digoxigenin antibody (1:25; Roche, South San Francisco, CA) and a 488 Alexa Fluor-conjugated anti-mouse IgG (1:50; Thermo Fisher Scientific, San Diego, CA).

Combed DNA was scored under a 40X oil immersion objective (numerical aperture [NA]: 1,30) by using a motorized fluorescence microscope (Zeiss Axio Imager.M1; Zeiss International, Oberkochen, Germany) equipped with a charge-coupled device (CCD) camera (Coolsnap HQ^2; Photometrics, Tucson, AZ). Single wavelength images were merged and adjacent fields were aligned using Adobe Photoshop CS2 (Adobe Systems, San Jose, CA). Measurements of fluorescent signals were done using Metavue software (Molecular Devices, Sunnyvale, CA) according to the molecular combing calibration factor (1 μm = 2 kb) and the magnification features of the objective and the CCD camera (1 pixel = 0,16125 μm = 0,3225 kb).

For interphase fluorescence *in situ* hybridization (FISH), cells were layered onto microscope slides by using the Cytospin III (Thermo Fisher Scientific, San Diego, CA). Chromosome spreads were obtained by standard procedures. FISH was carried out with a cocktail of three BAC probes directly labeled with Cy5-AP3-dUTP (GE Healthcare, Little Chalfont, UK), or indirectly labeled with Biotin-16-dUTP or digoxigenin-11-dUTP (Roche Biochemicals, Basilea, Switzerland). Biotin- and digoxigenin-labeled probes were acquired in red and green fluorescences, respectively. Slides were analyzed under a 40X or a 100X oil immersion objectives with a NA of 1,30. Images were captured and merged as previously described (Palumbo et al. 2010).

4.13 Multiphoton microscopy

Multiphoton or 2-photon optical microscopy is based on the collection of signals that derive from the nonlinear excitation of self-fluorescent molecules and/or molecules that generate secondary or tertiary harmonic signals. The laser beam emits, at high frequencies (femtoseconds), a series of photons interacting at the focal plane with the molecules under examination. The molecules, absorbing two or more photons of length λ in the infrared range, move to an excited state and return to the normal state emitting a photon of wavelength $\lambda/2$ (second harmonic signal), $\lambda/3$ (third harmonic signal) or a fluorescence signal of length $\lambda < \lambda/2$. Fluorescence (TPEF), second

harmonic (SHG) and third harmonic (THG) signals can thus be recorded simultaneously using the same exciting source and various detectors present on the same optical path of the excited source or off the optical path (not descanned detector, NDD). In addition, signals emitted by excited molecules can be detected either in forward scattering or in backward scattering. TPEF, SHG, and THG signals are generated by nonlinear optical phenomena that are very interesting for non-invasive imaging of biological tissues.

In the corneal tissue context, TPEF signals are generated by self-fluorescent molecules, such as NADPH, enabling visualization of cellular structures such as mitochondria (and hence epithelial cells, stromal keratinocytes and endothelial cells). The NADPH excitation wavelength is 710 nm. TPEF signals of weaker intensity are also generated by collagen when the tissue is excited at wavelengths of 825 nm. The source of TPEF emission depends on cross-links between collagen molecules.

SHG signals are generated, on the other hand, only by non-centrosymmetric molecules, such as collagen, with the emission of a single high-energy photon with half the excitation wavelength. In the corneal tissue context, therefore, SHG signals can only be generated by the stroma. The SHG signals can be recorded both in forward and backward scatter. Collagen emits SHG signals when energized at wavelengths between 800 nm and 860 nm. The back-scattered SHG signals are weaker than the forward scattered signals. The signals collected in back scatter are more homogeneous and do not reflect the orientation of collagen fibers as forward scatter.

Finally, THG signals are generated by the corneal interface structures, such as, ground substance of the stroma present between the collagen lamellae. The THG signal is generated by the optical heterogeneities between structures with different refractive index, if their size is comparable to the section of the laser beam. The THG signals in the corneal stroma can be generated by excitation of a ≥1100 nm wavelength.

In summary, 2-photon microscopy allows to generate and analyze TPEF (self-fluorescence), SHG (second harmonic) and THG (third harmonic) signals by obtaining complementary information on the microstructure of both cellular and extracellular components of the tissue analyzed.

4.14 spectrophotometry

Spectrophotometry setup consists of two main components: (1) a light source and (2) a spectrophotometer.

1) An AvaLight-DH-S-BAL source was used, whose spectrum is derived from the combination of a deuterium and a halogen lamp. Electromagnetic radiation emitted by the lamp has a spectrum ranging from UV to IR (200-1100 nm). The emitted light is transmitted to the specimen via FC-UV600, FC-UV-600-2-SR (Avantes) optic fibers. FC-UV-600 and FC-UV-600-2-SR has a numerical aperture (NA) of 0,22. Connectors are SMA905 (Avantes). The lenses used to convert divergent beams in parallel beams have a diameter of 6 mm and a focal length of 8,7 mm. The beam diameter is about 2 mm.

2) The light transmitted by the tissue is collected from a lens and transmitted to an optic fiber (FC-UV-600-2-SR type). The optic fiber connects to an AvaSpec 2048L spectrophotometer, which is then connected to a computer with signal capture software (Avasoft).

5 Results

5.1 Keratinocytes characterization in vitro show differences and similarities between their tissues of origin

During the three years of PhD I had the opportunity to collect and review cellular biology data of four diverse types of primary epithelial cells, derived from four different epithelia (skin, oral mucosa, limbus/cornea and conjunctiva).

To better investigate the exhaustion of clonogenic potential and the self-renewal of epithelial stem cells we took in consideration also p63-defective oral mucosa primary cell lines obtained from three patients affected by EEC syndrome, already known to cause an acceleration in epithelial aging (Barbaro, Nasti, Del Vecchio, et al. 2016). All these epithelia have been studied in the last years for their potential in clinical applications from our research group.

Epithelial stem cells isolated from human biopsies were cultured *in vitro* and serially propagated until exhaustion of their proliferative ability. Colony forming efficiency assay (CFE; number of colonies generated by seeded cells × 100%) was performed to evaluate the number of clonogenic cells at every passage together with the number of abortive colonies. Cellular biology was also characterized in terms of number of final cells collected at the time of the passage, and number of days in culture for each passage. Epithelial stem cells reflect the physiology of their tissue as their function in maintaining them, consequently these populations have particular traits and single behaviors that *in vitro* allow to distinguish ones from another.

From comparative analysis of cell biology data we can appreciate how human limbal epithelial stem cells (H-LESCs) and conjunctiva epithelial stem cells (H-CESCs) lose their clonogenic ability after only 7 passages in culture, while human oral mucosa stem cells (H-OMESCs) can easily reach 11 passages and human skin epithelial stem cells (H-SESCs) 20 passages. Also OMESCs carrying the p63 mutations R279H, R304Q and R311K have no more colony-forming cells after only 6, 5 and 4 passages respectively (Figure 6, Figure 7F). Infact, the decrease of clonogenic cells number along the passages is more attenuated in H-SESCs and H-OMESCs, while it has a significantly

faster decrease in primary cells from the epithelia of the ocular surface and in p63-defective OMESCs. So, the ability to generate a colony by a cell, and therefore the ability to self-renew, is closely related to the life span of a primary culture. To this end, it has shown how long-lasting cultures maintain a high amount of clonogenic cells even at more advanced passages (Figure 7A). For example, at passage 6, when H-LESCs, H-CESCs and mutated OMESCs are almost exhausted, H-OMESCs retain 3840 clonogenic cells on average, and H-SESCs 11000. Even the number of final cells fits with the results described so far (Figure 7B). A peculiarity of epithelial cells is the enlargement of the cytoplasm with the increase in cell dimension during differentiation. It is well known how how the size of cells composing an epithelial primary culture vary from 6-10 µM of stem cells, to 10-18 µM of transient amplifying cells, up to 18-36 µM of terminally differentiated/post-mitotic cells (Barrandon and Green, 1987; Rochat et al., 1994; Pellegrini et al., 1999). Then, at confluence, the greater the percentage of undifferentiated cells, the smaller the space that each one occupies and, consequently, the greater the number of cells. Otherwise, abortive colonies follow an exact opposite trend and their number increases faster in primary cultures with a more reduced life span (H-LESCs, H-CESCs and R304Q, R279H- and R311K-OMESCs). In particular, figure 7C shows how H-SESCs and H-OMESCs pass the 50% of aborted colonies only after 13 and 6 passages, respectively, while all the other primary cultures reach this value already at the 4^{th}. We can, then, observe that H-LESCs, H-CESCs and mutated OMESCs have a shorter life span and can be maintained *in vitro* for less then 40 days (35 days on average for H-LESCs and H-CESCs, 36 for R279H-OMESCs, 34 for R304Q-OMESCs and 28 for R311K-OMESCs), compared to 62 days for H-OMESCs and 83 for H-SESCs (Figure 7D). This also applies to the days needed to reach confluence for each passage. Again, H-SESCs reach the last passage of the other primary cell lines in many less days (for example, they reach the 6^{th} passage in 21 days compared to 35 of H-LESCs and H-CESCs). Also the mean of cumulative cell doublings that these primary cell lines can sustain till exhaustion goes this way. Infact, H-SESCs can exceed 95-96 cell doublings and H-OMESCs can easily reach 54 cell doublings. On the contrary, H-LESCs end their life span with a mean of 36 and 39 cell doublings and R279H-, R304Q- and R311K-OMESCs with only 33, 29 and 17, respectively (Figure 7E). Finally, the expression of the epithelial stem cells marker ΔNp63α follows the same trend: a higher expression in H-

SESCs compared to the other primary cells analyzed, probably due to a higher percentage of stem cells in culture (Figure 8).

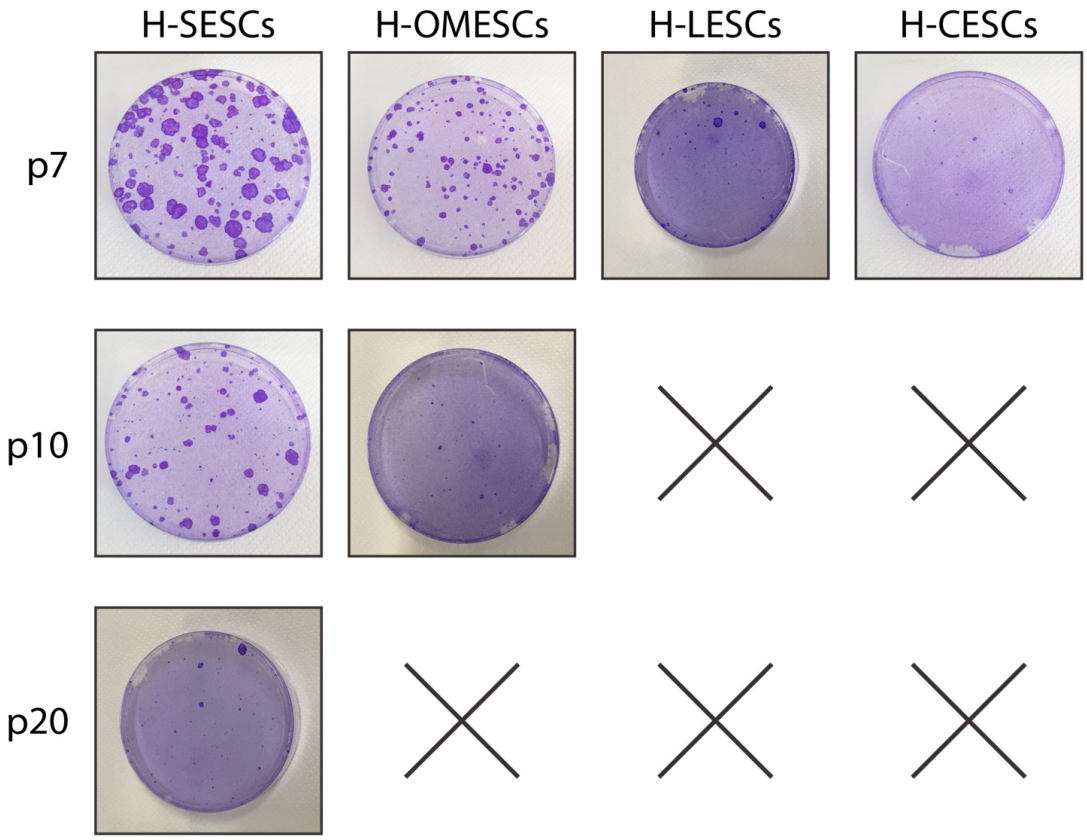

Figure 6. *Colony forming efficiency (CFE) of H-SESCs, H-OMESCs, H-LESCs and H-CESCs was evaluated at the last passage in culture of each primary cell line.*
Images are representative of data obtained from at least three independent experiments. Abbreviations: SESCs, skin epithelia stem cells; OMESCs, oral mucosa epithelial stem cells; LESCs, limbal epithelia stem cells; CESCs, conjunctival epithelial stem cells.

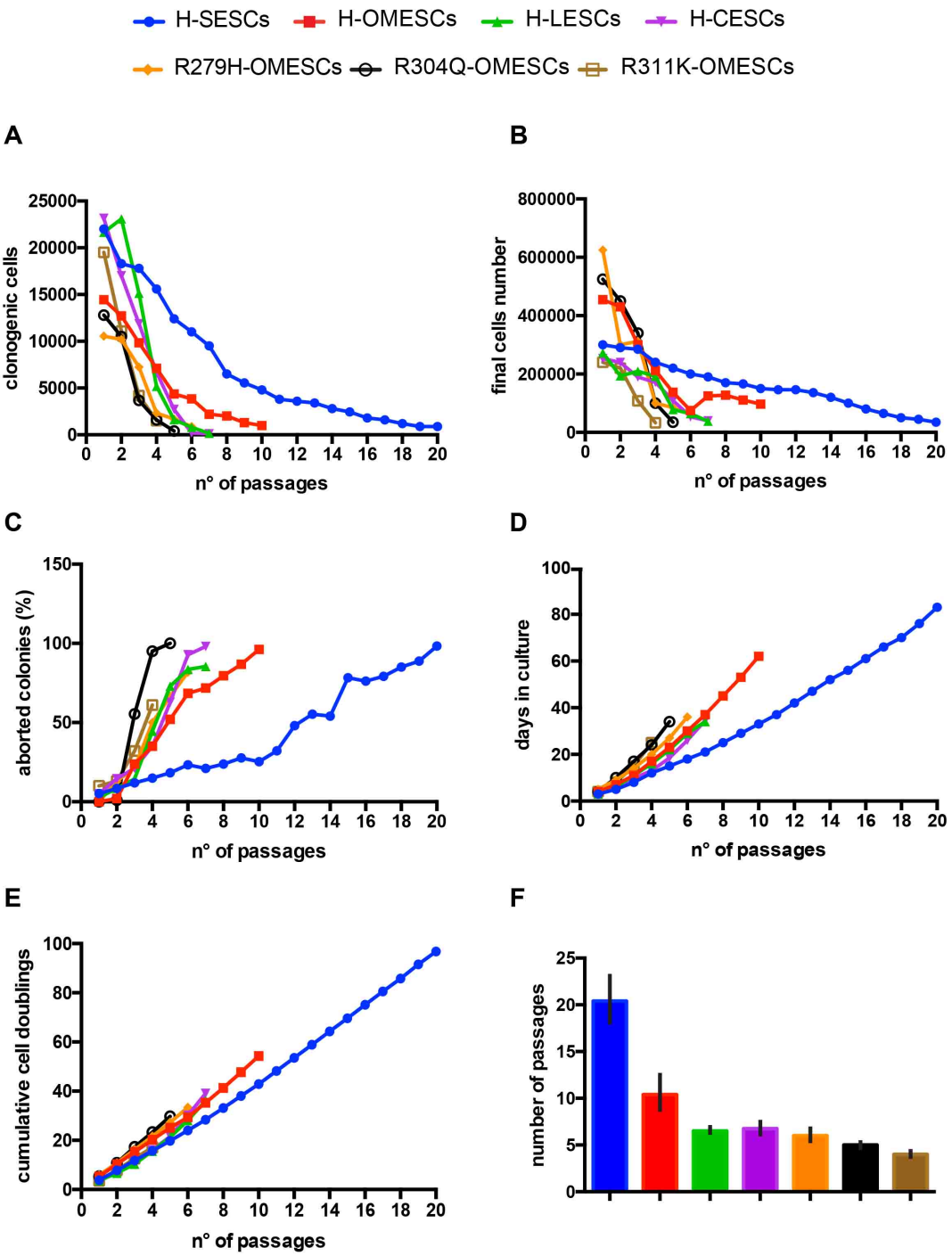

Figure 7. *Comparison of clonogenic ability and proliferative potential of human epithelial stem cells obtained from skin, oral mucosa, limbal and conjunctival biopsies. All data have been obtained from at least three unrelated normal subjects (n≥3 independent experiments). Quantification of (A) clonogenic cells number, (B) final cells number (C) percentage of aborted colonies, (D) days in culture, (E) cumulative cell doublings and (F) number of passages of H-SESCs (blue), H-OMESCs (red), H-LESCs (green), H-CESCs (purple), R279H-OMESCs (orange), R304Q-OMESCs (black), R311K-OMESCs (brown) is shown. All data have been obtainned from at least three unrelated normal subjects (n≥3 independent experiments). Abbreviations: SESCs, skin epithelial stem cells; OMESCs, oral mucosa epithelial stem cells; LESCs, limbal epithelial stem cells; CESCs, conjunctival epithelial stem cells.*

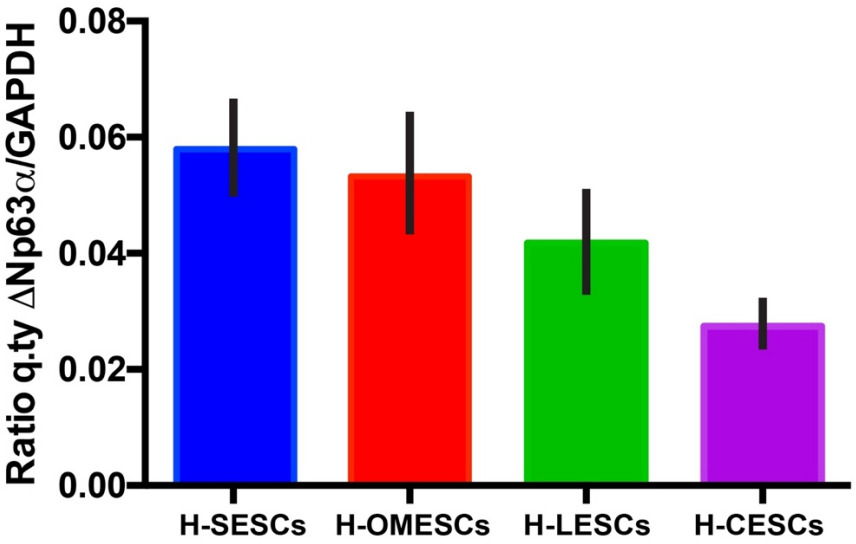

Figure 8. *ΔNp63α expression in primary cells (first passage) from healthy donors. Absolute quantitative PCR showing ΔNp63α copy number in total RNA from H-SESCs, H-OMESCs, H-LESCs and H-CESCs. Results are normalized against GAPDH. All data have been obtainned from at least three unrelated normal subjects (n≥3 independent experiments). Abbreviations: SESCs, skin epithelial stem cells; OMESCs, oral mucosa epithelial stem cells; LESCs, limbal epithelial stem cells; CESCs, conjunctival epithelial stem cells; GAPDH, glyceraldehyde-3-phosphate dehydrogenase.*

5.2 DAPT administration retards the aging of epithelial stem cells

Once characterized the *in vitro* aging of the primary cultures obtained from these four epithelia, the next step was to try to delay this aging and, given the key role of Notch in mediating the differentiation of adult epithelial stem cells, we decided to act on this pathway (Totaro et al. 2017). We performed the administration of DAPT with the aim to inhibit or slow down differentiation processes in epithelial stem cell cultures derived from Holoclones, Meroclones and Paraclones of H-LESCs.

The continuous administration of DAPT has allowed to obtain enriched cultures of epithelial stem cells, as confirmed by prolonged life-span (serial passages in culture), increased clonogenic capacity of the cells in culture, as determined following CFE (Colony Forming Efficiency) assays and therefore a reduced rate of stem cell ageing in vitro. In particular, figure 9 shows that the cell lines treated with DAPT after 3-5 passages (when they should be close to the end of their life span) have a recovery in clonogenic cells presence. Interestingly, the number of clonogenic and final cells of

DAPT-treated holoclones and meroclones, after an initial physiological decrease, go to an increasing phase and then back down till exhaustion. Specifically, DAPT treatment led the number of clonogenic cells to rise from 17700 to 30000 in 6 passages of holoclone-type cultures and from 9000 to 16900 for meroclones (Figure 10A-D). The number of final cells follows the same trend moving from 270000 to 416000 for the cultures derived from holoclones and from 112000 to 420000 for the one derived from meroclones (Figure 10B-E). These results were confirmed, again, by the expression of the epithelial stem cells marker ΔNp63α, which was assessed through q-PCR and showed a significant increase in cultures after treatment with DAPT (Figure 10C-F).

These data show the ability of DAPT to improve the quality and efficiency of stem cell cultures. The use of DAPT could therefore open interesting opportunities for epithelial stem cell-based therapies as it could (1) replace and hence eliminate the use of feeder layer; (2) reduce the size of the biopsy used to isolate the patient stem cells, thus allowing a less invasive surgery, which would benefit patients suffering from corneal disorders greatly; (3) delay the premature aging of the epithelial stem cells from patients with genetic defects, such as EEC syndrome or Epidermolysis Bullosa and finally (4) enrich the percentage of stem cells within a batch of cells, thus making gene therapy strategies with low efficiencies of correction/targeting, such as Gene Editing tools (i.e., CRISPR), more efficacious.

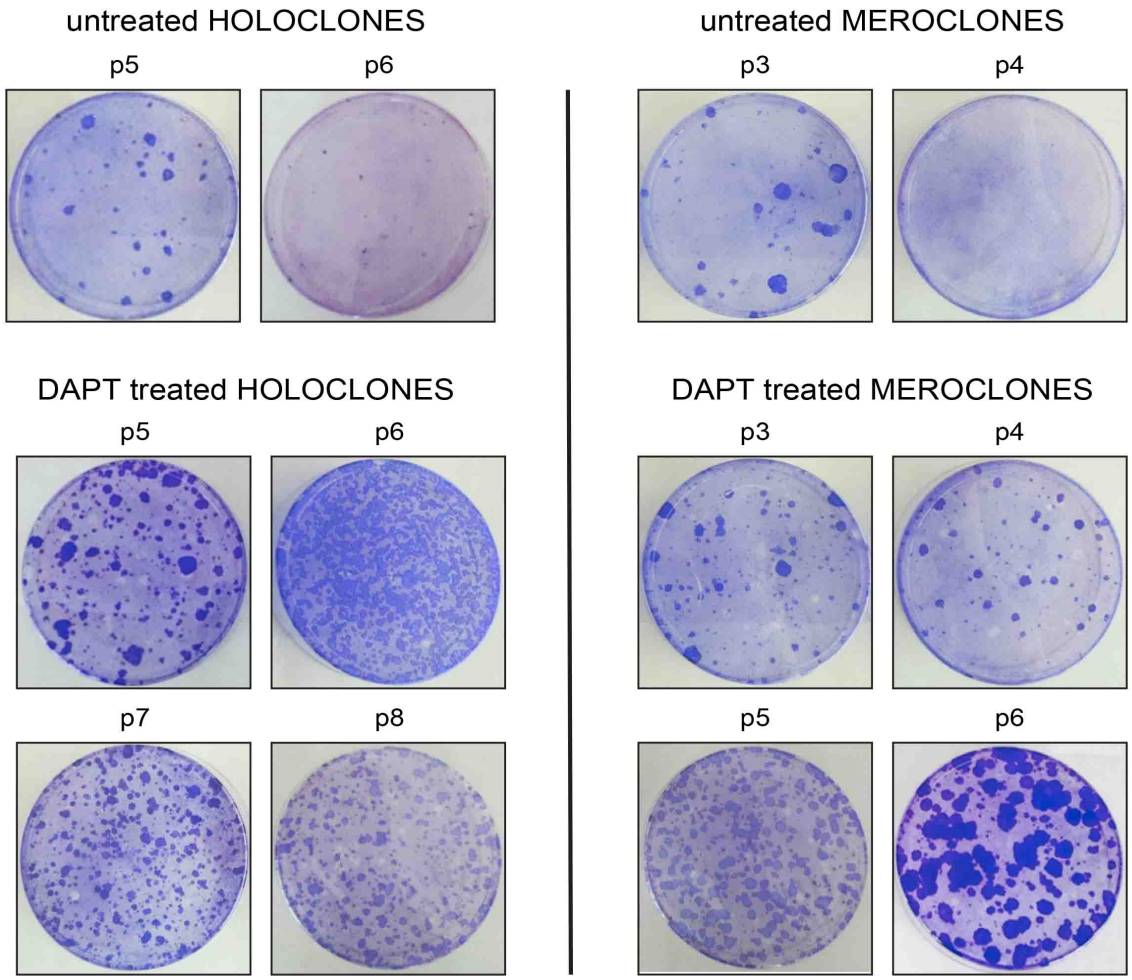

Figure 9. *Colony forming efficiency of Holoclones and Meroclones treated with DAPT was compared at the last two passages in culture of the untreated cell lines. Images are representative of data obtained from at least three independent experiments.*

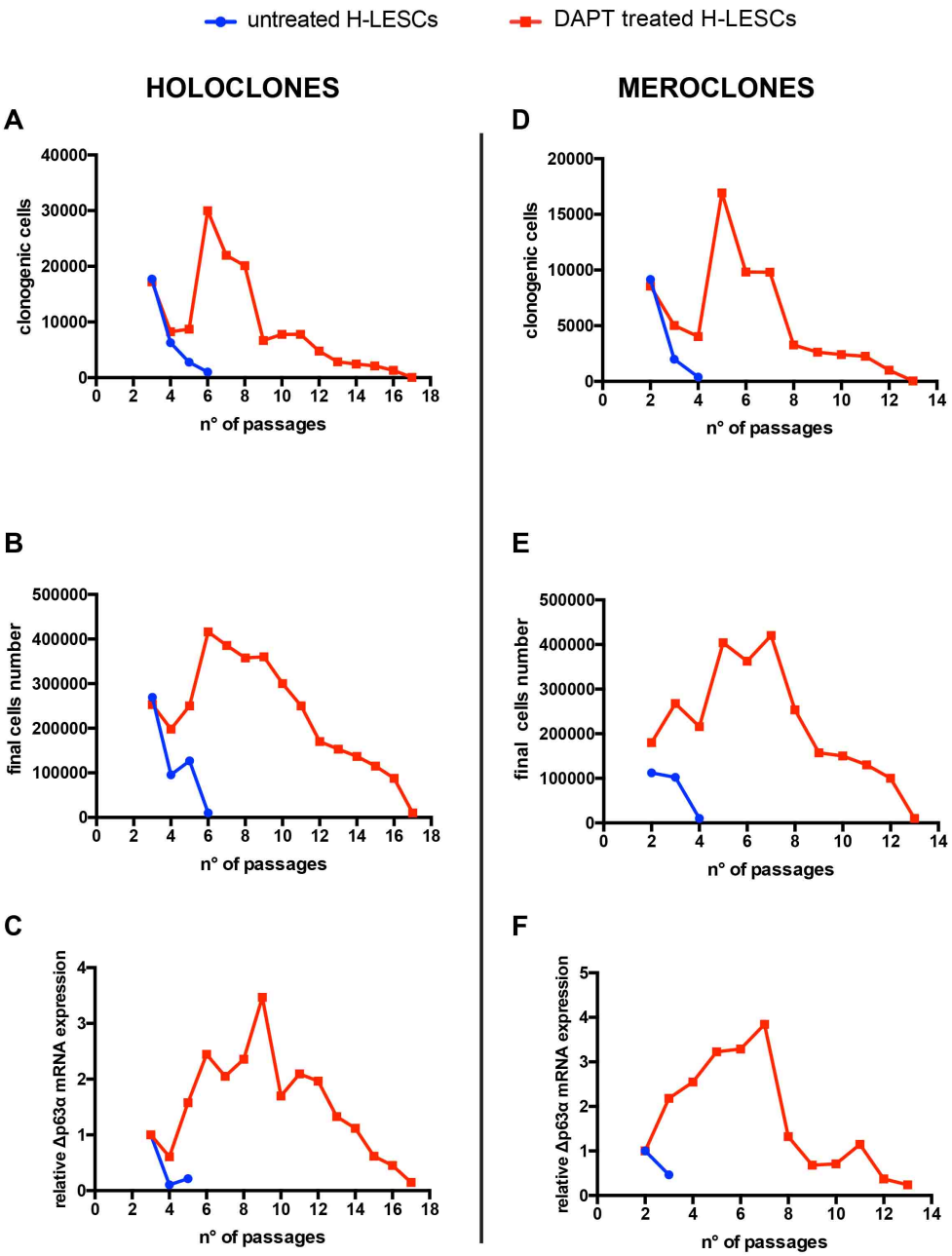

Figure 10. *Comparison of clonogenic ability and proliferative potential of untreated and DAPT-treated H-LESCs. Quantification of (A, D) clonogenic cells number, (B, E) final cells number and (C, F) relative quantitative PCR showing ΔNp63α mRNA relative expression in Holoclones and Meroclones at the cell passages indicated. Results are normalized against GAPDH. All data have been obtainned from at least three unrelated normal subjects (n≥3 independent experiments). Abbreviations: SESCs, skin epithelial stem cells; OMESCs, oral mucosa epithelial stem cells; LESCs, limbal epithelial stem cells; CESCs, conjunctival epithelial stem cells; GAPDH, glyceraldehyde-3-phosphate dehydrogenase.*

5.3 Personalized Stem Cell Therapy to Correct Corneal Defects Due to a Unique Homozygous-Heterozygous Mosaicism of EEC Syndrome

Demonstrating that epithelial stem cells have an intrinsic potential for regenerative medicine that can be exploited with a deeper characterization, we have been able to apply a cell therapy protocol to a patient affected by EEC syndrome in a rare form of mosaicism. It was a case of EEC syndrome associated with severe conjunctivalization of the cornea and symblepharon (Figure 11F-G). The loss of the corneal epithelium was confirmed through impression cytology analysis using antibodies against cytokeratin 12 (cK12) and mucin 1 (MUC1) (Figure 11H) (Barbaro et al. 2010) (Barbaro, Nasti, Raffa, et al. 2016).

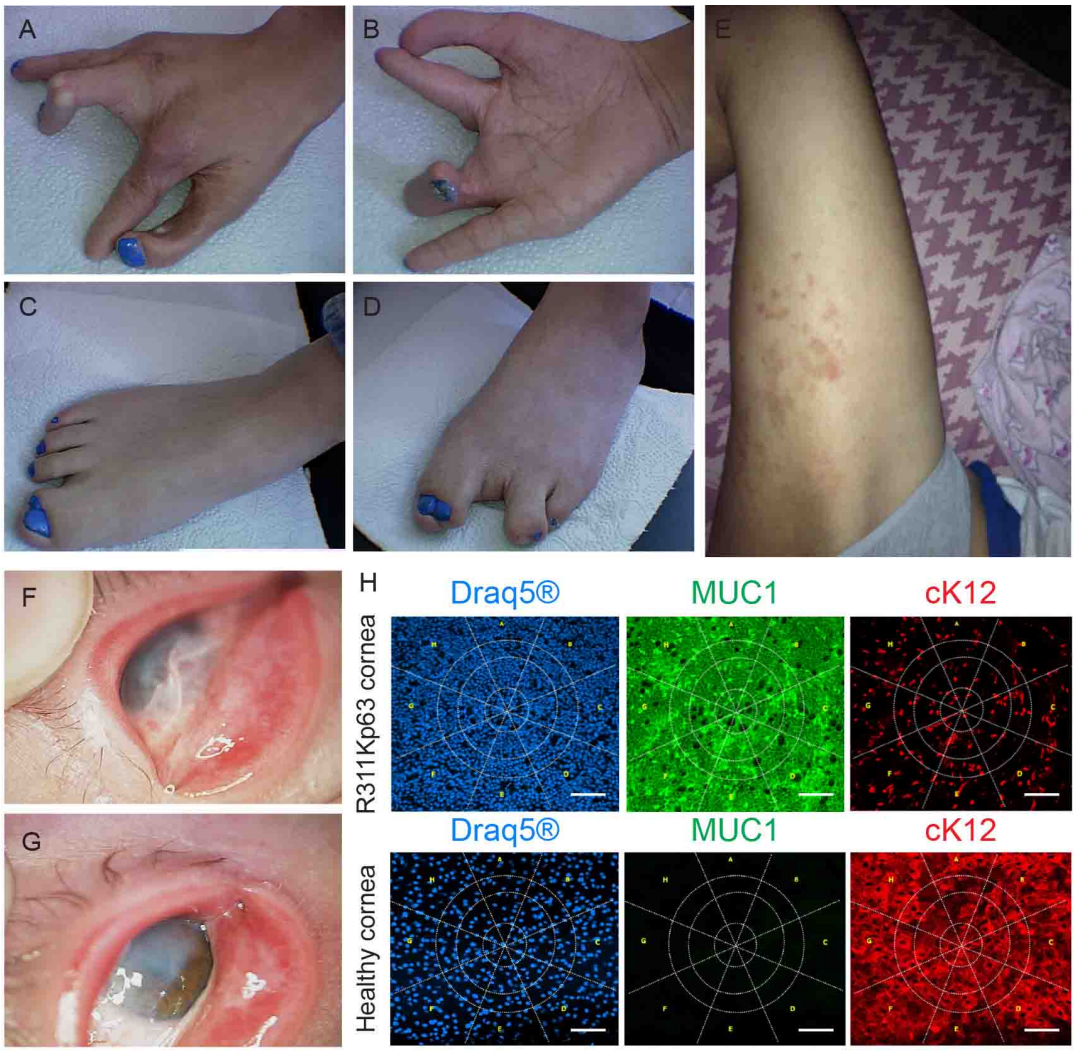

Figure 11. *Phenotypic features of R311K-p63 mutation.*
(A–G): Photographs showing the phenotypic tracts of ectrodactyly-ectodermal dysplasia-clefting (EEC) syndrome in the patient. Ectrodactyly and sindactily are visible in hands and feet

(A–D). Dermatitis often appears on the skin (E). The pannus, due to the conjunctivalization of the ocular surface, and the symblepharon are present in both eyes (F, G). (H): Analysis of impression cytology specimens from the patient and from a healthy subject. Specimens were stained with antibodies against the K12/MUC1 couple of markers and DRAQ5 (for DNA staining). Panel staining: DRAQ5 (blue); MUC1 (green), and cK12 (red). Immunostaining with MUC1 and cK12 shows a severe conjunctivalized cornea. Scale bar 100 μm.
Abbreviations: cK12, cytokeratin 12; MUC1, mucin 1.

The genetic analysis showed that the patient was unexpectedly homozygous for a novel and de novo missense mutation in the p63 gene, R311K. The homozygous mutation detected in this patient occurred in codon 311 at nucleotide 1049 and caused the conversion from arginine to lysine in exon 8 (R311K; AGA > AAA; c.1049G > A) (Figure 12A). Sequencing of the corresponding region in the DNAs obtained from the parents, brother, and paternal sperm (Figure 12A) confirmed that the mutation was *de novo*. The involved amino acid has a high degree of phylogenetic conservation (Figure 12B), and the mutation is located in the same position as another EEC causative mutation, p.R311G, which was previously described (willoughby et al, 2005). An in-depth analysis of the sequence chromatogram revealed a small G peak, corresponding to the wild-type sequence, below the A peak, corresponding to the mutant sequence (Figure 12A). The faint G peak was detectable in all the sequence chromatograms, probably because of a low level of mosaicism, both in leukocytes from the peripheral blood and in OMECs from biopsy specimens of buccal mucosa. To better explore and obtain an estimate of the degree of mosaicism, we cloned the PCR products from both leukocytes and OMECs. Sequence analysis of 100 clones showed that approximately 90% of the clones were derived from the mutant allele, whereas 10% of clones represented the normal allele (Figure 12A). This result suggested a somatic mosaicism in which 80% of the patient cells carry 2 mutant alleles and, thus, are homozygous, while approximately 20% of patients cells presents the mutation in an heterozygous form. Homozygous mutations in dominant disorders are frequently lethal in embryos and p63-null mice die soon after birth (Yang et al. 1999). Furthermore, no other mutation in the p63 gene has ever been found in a homozygous condition. Our idea is that when the mutation arises in heterozygosity a milder form of EEC syndrome is generated. *In silico* analysis (Figure 12C-E) supported this hypothesis and showed that R311K mutation was still able to bind the p63 site on the genomic DNA. Meanwhile,

the severe heterozygous EEC-causing mutation, such as R311G, lost this capacity. To determine the transactivation capacity of the mutated sequences (and, therefore, the severity of a specific p63 mutation), a luciferase assay was developed by transfecting cell lines with either wild-type or mutant p63 sequences together with a reporter construct containing the luciferase gene under the control of cK14 promoter. The luciferase assay showed a reduced R311K-p63 transcriptional activity, thus confirming its pathogenicity, but a milder effect in the heterozygous state (Figure 13) (Barbaro, Nasti, Raffa, et al. 2016).

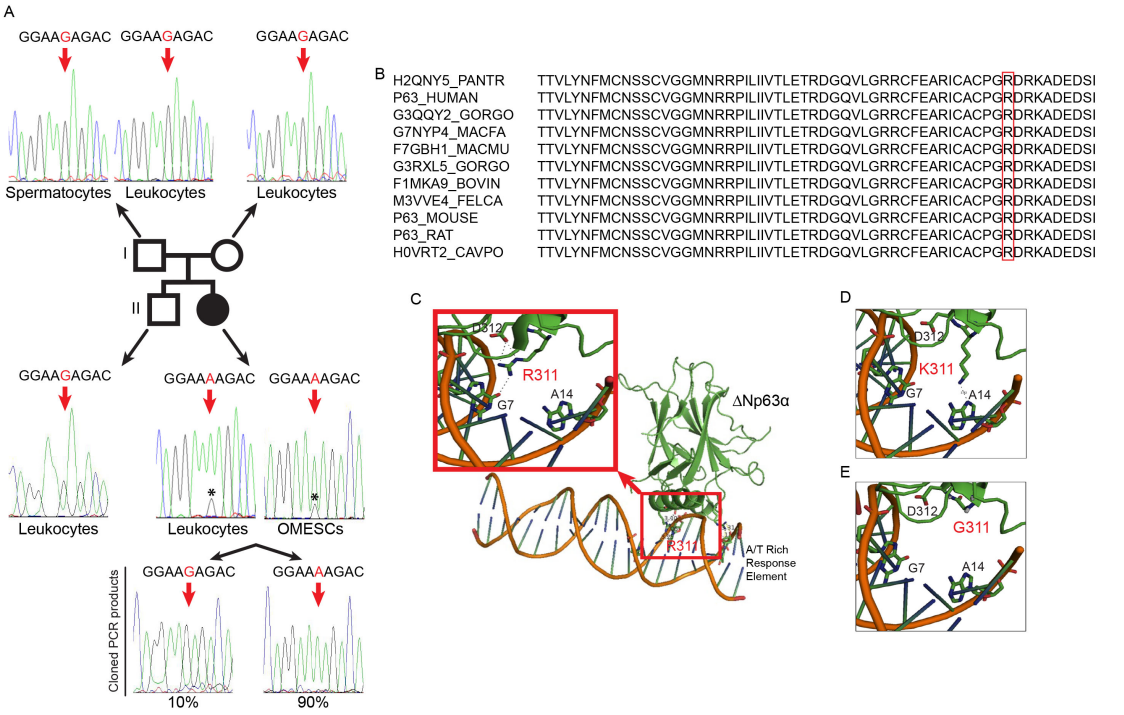

Figure 12. *Genotype and functional characterization of R311K-p63 mutation. (A): Schematic representation of R311K-p63 mutation in the patient's family. The chromatograms of exon 8 of the p63 gene in the father's spermatocytes and leukocytes and in the mother's leukocytes are shown at the top. The wild-type sequence is shown; the red arrows indicate the base involved in the point mutation. The chromatograms of exon 8 of the p63 gene in the brother's leukocytes and in the patient's leukocytes and OMESCs are shown in the lower part of this panel. The sequence from the brother's cells indicates the wild-type pattern; those of the patient with ectrodactyly-ectodermal dysplasia-clefting (EEC) show the G to A transition at nucleotide position 1049 (in red), resulting in the R311K codon. The low wild-type G peak (*) below the mutant A peak is indicative of a mosaicism condition. The sequencing of single molecules of exon 8 of the patient, amplified from leukocytes and OMESCs by PCR and cloned into a TOPO vector, shows the presence of 90% of mutated and 10% of wild-type PCR fragments. (B): Alignment of p63 protein sequence from different species. (C–E): Three-dimensional model of ΔNp63α protein. The arginine in the wild-type form of the p63 protein can bind DNA in G7 through 2 hydrogen bonds and the amino acid in D312 through a hydrogen bond (C). The glycine in the same position (311), clinically responsible for a severe EEC syndrome, leads to a complete loss of the ability to bind the DNA and flanking amino acid (E).*

Meanwhile, the lysine loses the 3 hydrogen bonds of the wild-type protein but still binds DNA, acquiring a hydrogen bond in A14 on the consensus DNA-binding site (D). Abbreviations: OMESCs, oral mucosal epithelial stem cells.

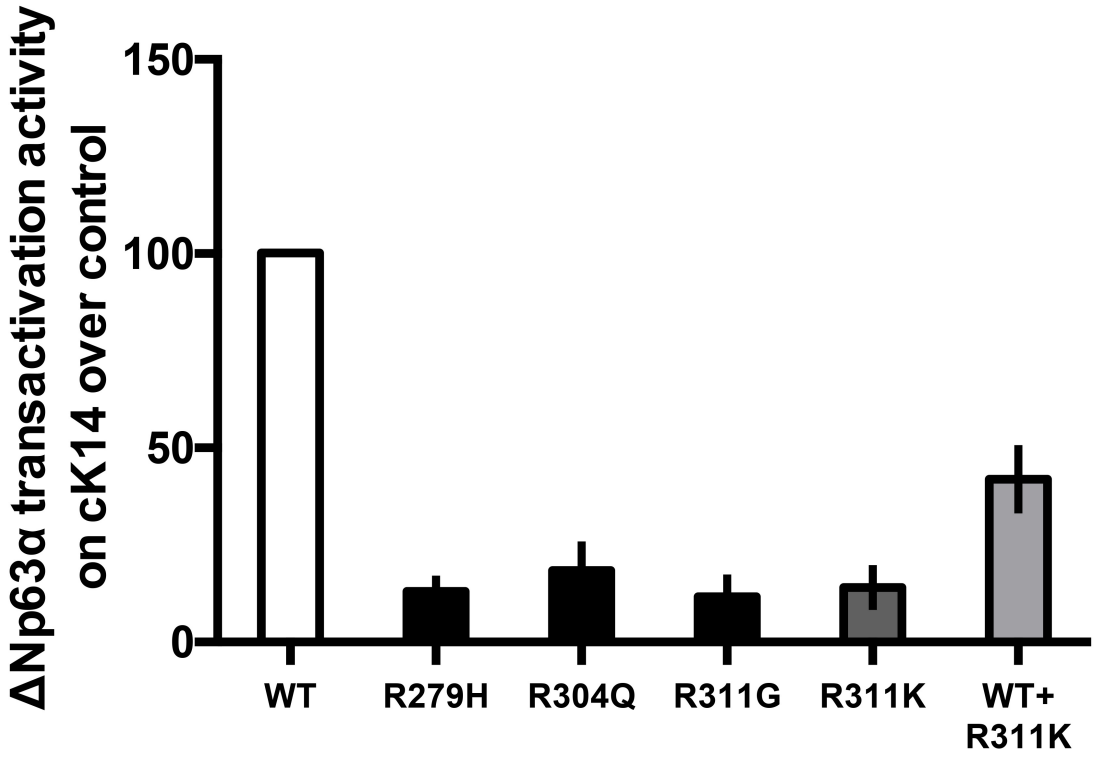

Figure 13. *Transactivation potential of ΔNp63α protein and of its EEC mutants determined by transient transfection into HEK293T cells. Keratin-14 promoter, cloned in the luciferase reporter vector, was cotransfected along with an empty expression vector (pcDNA 3.1) or the indicated ΔNp63α expressing plasmid: wild-type (WT), DNA-binding domain mutants (R279H; R311K; R311G; R304Q), and a 1:1 combination of WT and R311K mutant. Transfection efficiency was normalized with a Renilla reporter vector. The result is the mean of four independent experiments.*

To find a possible explanation, cytogenetic and molecular analyses were performed. By molecular cytogenetics (Figure 14A-C), we excluded the presence of large genomic rearrangements, deletions, or duplications in R311K-OMESCs. The resolution of the analysis on DNA extended fibers (molecular combing; Figure 14A-B) is 5 kb. Interphase FISH with 2 BAC clones closely mapping at p63 and a distal probe mapping in the short arm of chromosome 3 had a resolution of 100 kb (Figure 14A-C). The presence of genomic rearrangements, deletions, or duplications within the p63 gene was excluded by quantitative p63-specific real-time PCR analysis Figure 14D). Our overall hypothesis is, therefore, that a likely mechanism explaining the homozygous status of the patient

could be tracked back to a de novo mutation followed by an allelic gene conversion of the wild-type allele by the de novo mutant allele in the p63 gene (Figure 14E) (Barbaro, Nasti, Raffa, et al. 2016).

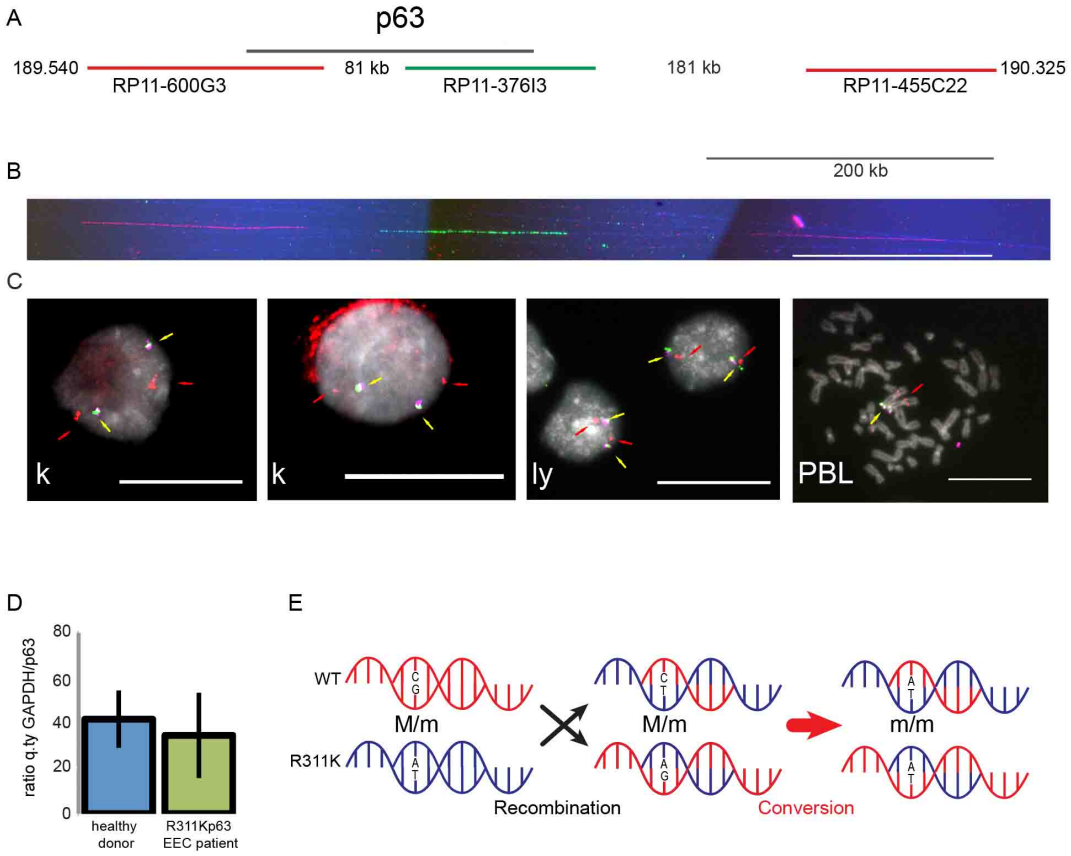

Figure 14. *Cytogenetic and molecular analyses suggest an allelic-conversion hypothesis. (A): Schematic representation of the p63 genomic region at 3q27, indicating the distance from the centromere (Mb). The black line identifies the p63 gene; the red and green lines represent the genomic clones (bacterial artificial chromosome [BAC]) used as probes in molecular combing analysis. Probes are differentially spaced and allowed to orientate the molecule in the centromere-telomere direction. Their identity is revealed through red and green fluorescence. (B): An example of fluorescent in situ hybridization (FISH) on DNA extended molecules of R311K keratinocytes prepared through the molecular combing assay. In red and green are visible three probes that hybridize as the expected pattern represented in (A). To verify the integrity of the molecules, DNA was counterstained with an anti-ssDNA antibody (blue fluorescence). Only the expected pattern was observed in mutated keratinocytes (a normal human cell line was used as positive control). Calibration bar = 200 kb. (C): Representative images from interphase FISH analysis of R311K keratinocytes. A human normal lymphoblastoid cell line and human PBLs were used as controls. Yellow arrows indicate the overlapping hybridization signals from two BAC clones closely mapping at p63 (RP11-373I6: magenta fluorescence; RP11-600G3: green fluorescence; see [A]). Because of the proximity of the probes, the hybridization signals are merging in a yellow fluorescence. Red arrows indicate the position of a third probe (RP11-468L11: red fluorescence) mapping in the short arm of chromosome 3 at 3p14.2, and used to monitor the chromosome integrity. In all cell types, the hybridization signals are consistent with a normal chromosome set. The location of the same probes is also shown in a metaphase spread from human PBLs. Calibration bars = 20 mm. (D): Comparative real-time quantitative*

PCR analysis of genomic DNA extracted from healthy donors (n = 5) and from the patient with R311K-p63 mutation EEC (three different sample preparations) excluded large and small rearrangements, deletions, or duplications in the p63 gene. (E): Schematic representation of the allelic gene conversion event that occurred after the de novo R311K-p63 mutation, causing the generation of the homozygous mutation in the patient with EEC. Abbreviations: EEC, ectrodactyly-ectodermal dysplasia-clefting; GAPDH, glyceraldehyde-3-phosphate dihydrogenase; ly, lymphoblastoid cell line; k, keratinocyte; PBL, peripheral blood lymphocyte; q.ty, quantity.

R311K-OMESCs were characterized, ex vivo expanded, and analyzed by clonal analysis (Figure 15A). CFE assay showed that only 24 of approximately 400 clones had a high clonogenic ability and proliferative potential in vitro; in addition, at least 6 of these resulted holoclones. Results from sequencing analysis demonstrated that all the 24 clones were heterozygous (Figure 15B), thus suggesting a selective growth advantage of the heterozygous stem cells compared with the homozygous ones. Stem cell content evaluated by quantifying DNp63α expression through real-time qPCR was comparable to that observed in cultured autologous limbal epithelial cells sheets (CA-LECSs) successfully transplanted in patients with LSCD caused by traumatic events (Figure 15C). Finally, to test the regenerative ability of the selected R311K-OMESCs carrying the hypomorphic allele, we set up organotypic cultures derived by pooling all R311K-p63 heterozygous holoclones (R311K-HHs) grown on a HKL model (Figure 15D). Compared with OMESCs from healthy donors (H-OMESCs; n = 3) and patients with EEC syndrome (EEC-OMESCs; n = 2, with p.R279H and p.R304Q p63 mutations), epithelia generated by p.R311K-HHs were more similar to H-OMESCs and well organized into basal column-shaped cells expressing DNp63α suprabasal cuboid wing cells, expressing cK3; and flat, squamous, superficial terminally differentiated cells, as indicated by the expression of involucrin. The basal cuboidal cell layer was firmly attached to the underlying extracellular matrix and to the basement membrane through laminin β3. In sharp contrast, tissues generated from R279H- and R304Q-p63 OMESCs showed defects in both stratification and differentiation, thus resulting in severe tissue hypoplasia and lack of proper tissue polarity (Figure 15D). Collectively, these results strongly support the potential clinical use of p.R311K-HHs for the development of CA-OMESCs, to reconstruct the ocular surface of this unique case of EEC syndrome. In this study, we report the first and only case, to our knowledge, of an EEC patient with a

homozygous mutation in the p63 gene. To our knowledge, this patient shows the most severe ocular phenotype. The fact that the patient survived despite having a homozygous mutation in the p63 gene is intriguing, thus predicting a milder severity of this mutation when in the heterozygous state. Arginine and lysine are both positively charged amino acids, thus suggesting that, in particular cases, their exchange could be well tolerated (Barbaro, Nasti, Raffa, et al. 2016).

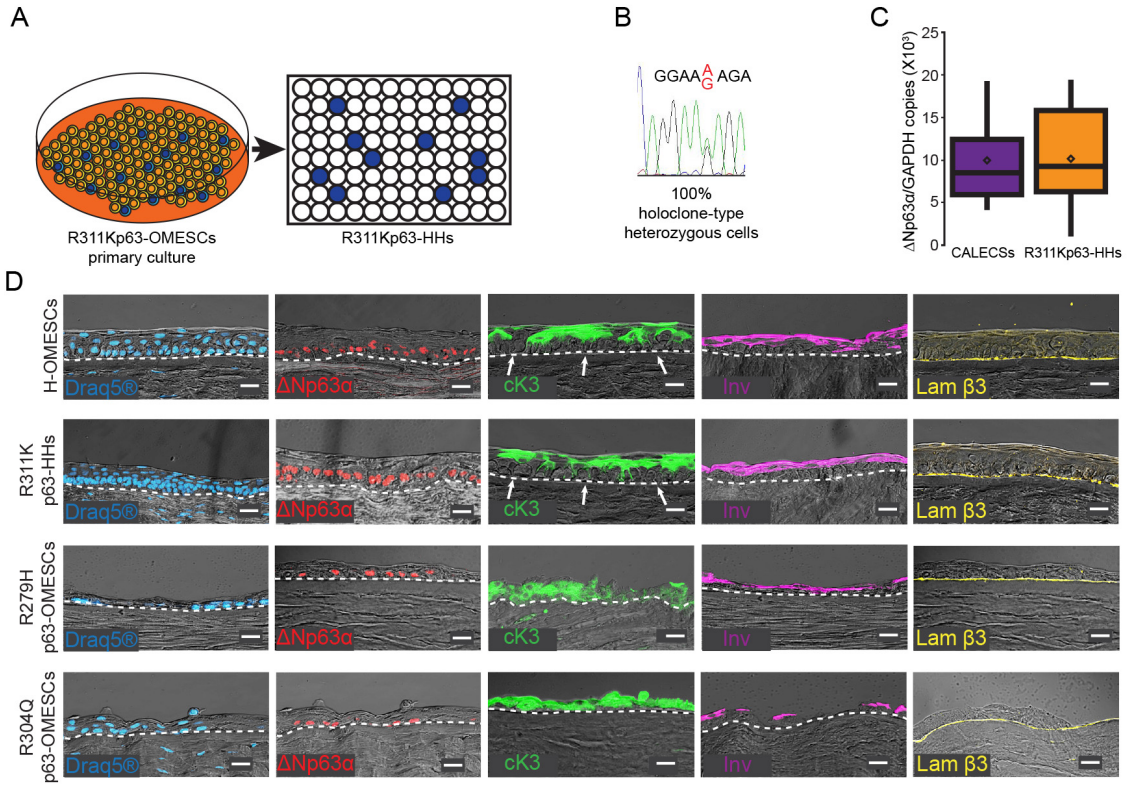

Figure 15. *Isolation of R311K-p63 heterozygous holoclones and expression of epithelial cell markers in reconstructed hemicorneas.*
(A): Cultivation of primary mosaic R311K-OMESCs and isolation of 400 heterozygous R311K-p63 clones through clonal analyses. (B): A representative chromatogram of the sequence around the R311K mutation site of the p63 gene obtained from all the 24 holoclones, previously selected through colony-forming efficiency assay after single-cell clonal amplification. (C): Real-time quantitative analysis of ΔNp63α expression found in CA-LECSs (n = 19) successfully transplanted in patients with limbal stem cell deficiency, and in R311K-HHs (n = 24). A comparable stem cell content is observed. (D): DRAQ5 staining and expression of epithelial cell markers in reconstructed hemicorneas generated by growing (a) healthy OMESCs, (b) R311K-HHs, (c) R279H-OMESCs, and (d) R304Q-OMESCs onto human keratoplasty lenticules. Cryosections were analyzed through immunofluorescence using ΔNp63α (red), cK3 (green), Inv (violet), and Lam β3 (yellow) antibodies (n = 3) Scale bars 20 μm. Note that the R311K-p63 HHs' resulting epithelium was well organized and stratified into four to five cell layers, with basal cuboidal cells differentiating upward to winged cells. The strong expression of the stem cell marker ΔNp63α confirms the maintenance of basal and undifferentiated

progenitor cells, which are also negative for cK3 (white arrows). Abbreviations: CA-LECS, cultured, autologous limbal epithelial cells sheet; cK, cytokeratin; HHs, heterozygous holoclones; Inv, involucrin; Lam β3, laminin β3; OMESCs, oral mucosal epithelial stem cell sheet.

5.4 Human keratoplasty lenticules (HKLs): an organotypic culture system for the treatment of total limbal stem cells deficiency

To summarize the reasons that lead us to the choice of human keratoplasty lenticules (HKLs), natural scaffolds obtained removing the corneal epithelium from central cornea biopsies (from deceased donors), we can say that the advantages of these scaffolds are multiple:

• They allow *in vitro* reconstruction of well structured epithelia, with the correct thickness and expressing the normal differentiation markers detectable in the epithelia of origin (see later).

• The thickness of the stroma facilitate the handling of the sheet (this is useful for the graft of the scaffold and for manipulation by surgeons).

• Stem cells can be cultivate directly on the scaffolds, with no need to add murine feeder layer, maintaining their classical features and well-ordered differentiating, forming an epithelial structure of 4-6 layers (very similar to the original epithelium). Avoiding the use of murine cells can be very beneficial and increase the safety degree of the graft.

• Using these scaffolds it's possible to reconstruct *in vitro* a much more ample portion of the cornea: the stroma, provided by the same scaffold, and the epithelium, rebuilt starting from the collection of stem cells (this is a necessary condition for deeper lesions of the cornea, which are not involving only the epithelium).

• This scaffold, replacing also the connective tissue of the receiver, should not be absorbed or eliminated, avoiding the complications that result from this additional, but essential step for the fibrin matrix. (Barbaro et al. 2009).

5.5 Human limbal epithelial stem cells (H-LESCs) and oral mucosa epithelial stem cells (H-OMESCs) cultured onto HKLs can form well-organized epithelial sheets

Preliminary data, from which I started to develop my work, collected by the research team of Eye Bank Foundation of Veneto (FBOV) and Department of Molecular Medicine of University of Padua in 2009-2016, were obtained through the use of human stem cells (H-LESCs and H-OMESCs). Limbal stem cells (H-LESCs) expanded onto HKLs gave rise to a keratinized stratified squamous epithelium morphologically similar to that of normal corneas. The resulting corneal epithelium was characterized by correct expression of several markers in each cell layer (keratin 14, α6, β1, and β4 integrins, p63 and ΔNp63α in basal layers, 14-3-3σ, keratin 3, and keratin 12 in the upper one). In the stroma of HKLs, keratocytes maintained the biosynthetic and phenotypic appearances typical of resting/quiescent cells and expressed keratan sulfate, CD-34, and ALDH3A1. Fibroblastic transformation was observed with the appearance of VSX1 and α-SMA. HKLs did not alter the clonogenic/proliferative capacity of limbal stem cells. No differences were seen when HKL was compared to fibrin glue (Barbaro et al. 2009). Also stem cells of the oral mucosa (H-OMESCs) have shown the ability to form epithelia with the same characteristics, except for the number of layers, slightly greater (5-6 layers on average, against 3-4 layers of the epithelia formed by LESCs) (Barbaro et al. 2009).

5.6 Analysis by two-photon and confocal microscopy and spectrophotometry confirm the quality of HKLs over fibrin matrix

In order to consolidate the advantages summarized above we performed analysis with two different techniques: two-photon microscopy to evaluate the structure of the scaffolds and the distribution of the epithelial cells on them and spectrophotometry to evaluate the transparency of the reconstructed tissues. Two-photon microscopy and spectrophotometry experiments were performed in laboratories of IRCCS “G. B. Bietti” Foundation as part of a collaborative project.

The characteristics of hemicorneas prepared by microkeratome were similar among the various samples analyzed. The epithelium was layered in 3-5 planes, from basal cells layer to terminally differentiated cells on the surface. These epithelia appeared less thick than normal corneal tissue. In at least 50% of the samples, structures similar to "Vogt palisades" have been observed (data not shown). The stroma of Hemicorneas has a structure comparable to that of normal corneal tissue, with greater density of keratocytes in the frontal stroma and the typical anisotropy of collagen organization. Stacks of 4-10 µm were obtained from the surface of all the sample to a depth of 250 µm. Both the epithelial and stromal components of the hemicornea have been clearly identified. The stroma (figure 16A) has a normal structure and we have been able to appreciate collagen fibers and syncytia of keratocytes. Epithelial cells were homogeneously distributed upon the total surface and well attached to the scaffold as we can deduce from the stretched shape (Figure 16B). The characteristics of fibrin specimens cultivated with corneal limbal stem cells was similar among the various samples analyzed. The epithelium stratifies in 3-7 planes, from basal cells layer to terminally differentiated cells on the surface. The architecture of the epithelium is more chaotic than the one observed in hemicorneas. The cells of the basal layer were not fully adhered to each other and stratification is very heterogeneous between different areas of the samples (Figure 16C). Structures similar to "Vogt palisades" were not found. The fibrin gel is an inert and acellular support whose structure does not emit TPEF or SHG signals. The main differences between regenerated epithelium on fibrin support and on hemicorneas therefore appear to be within the capacity of hemicorneas to provide an active support for optimal differentiation and stratification to limbal epithelial stem cells. When the stroma of the reconstructed hemicorneas was analyzed, the expression pattern of specific markers was found to be similar to that of normal human corneas. DRAQ5-stained keratocytes (Figure 16D) were surrounded by abundant ECM and expressed CD-34 (Figure 16E). As expected, we also found keratocytes undergoing fibroblastic transformation, as they expressed F-actin stress fibers containing α-SMA protein (Figure 16F).

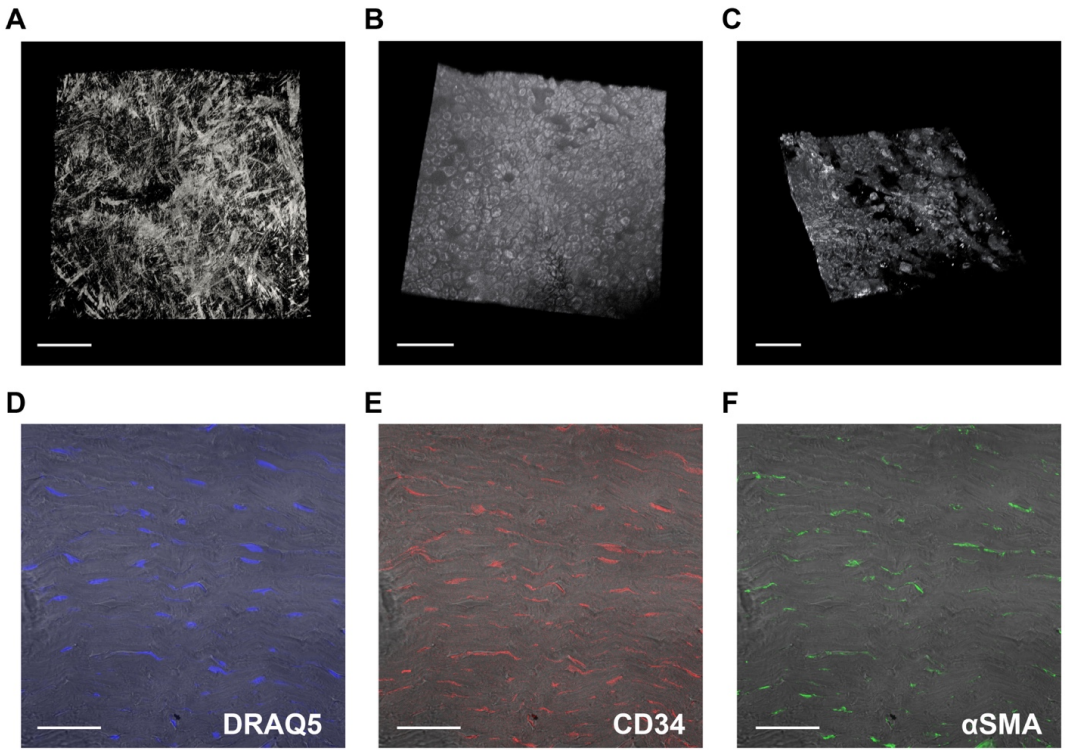

Figure 16. *(A,B,C) Two-photon microscopy of HKLs and H-LESCs plated on these scaffolds. (A) Collagen fibers of the frontal stroma are well defined. (B) H-LESCs plated on HKLs show they are well distributed and joined to each other, as in the normal human cornea. (C) On the countrary, in epithelia reconstructed upon fibrin-based scaffolds the basal layer consists of non-adherent cells with rounded morphology. (D) Keratocytes in the stromal part of the hemicornea stained with DRAQ5™. Expression of specific markers of the corneal stroma: (E) CD-34, a specific marker of keratocytes, (F) α-SMA, a muscle protein of F-actin stress fibers, typically found in myofibroblasts. Images are representative of data obtained from at least three independent experiments. Scale bar 100 μm. Abbreviations: HKLs, human kertoplasty lenticules; LESCs, limbal epithelial stem cells.*

We also verified that HKLs maintained a good transparency with and without epithelial cells on them. We found that in the wavelength range of visible light, the transmittance (T) of hemicorneas in the central tissue positions was on average 15% lower than the stromal lenticules, while in the paracentral position (2 mm), the T of hemicorneas was 10% lower. The measurements in the UV-A and UV-B wavelength range confirm this trend ranging between 12% and 15% lower transmittance in central hemicorneas and between 6% and 8% in paracentral. Finally, in the infrared wavelength range (IR), the T of hemicorneas in the central positions was 17% to 23% lower than keratoplasty lenticules in central regions and 10% to 15% in paracentral. The average T values of all samples are shown in figure 17. Overall, the relative

reduction of hemicorneal light transmittance compared to stromal lenticules was consistent with the state of the knowledge on biophysics of corneal light-tissue interaction.

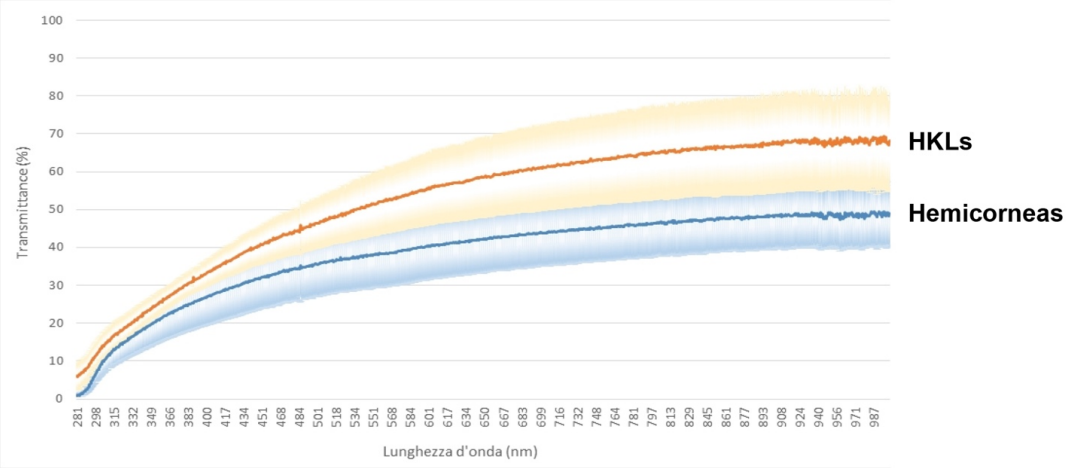

Figure 17. *Average transmittance curves in the wavelength range of 280-1000 nm of reconstructed hemicorneas (blue curve) and HKLs (red curve). The presence of epithelium reduces tissue transmission by 15-20% on average in each measuring position. These differences are in accordance with knowledge about absorbance properties of corneal epithelium. Abbreviations: HKLs, human kertoplasty lenticules.*

5.7 Synthetic scaffolds are not able to sustain epithelial stem cells differentiation and stratification

In the context of a collaboration between different european laboratories we had the chance to test several synthetic scaffolds capable of mimic the structure of corneal stroma. The precise formulation of these scaffolds has not been provided, but these are foam-based and polyester structures or cross-linked collagen fibers. The results however were unsatisfactory as we had several problems such as the ingrowth of epithelial cells inside the scaffolds and the formation of abnormal clusters and abnormal stratification. Markers such as ΔNp63α and cK3 were stained with immunofluorescence assays to evaluate the orientation of reconstituted epithelia (figure 18). All tested synthetic scaffolds were unable to support the formation of well organized epithelial sheets.

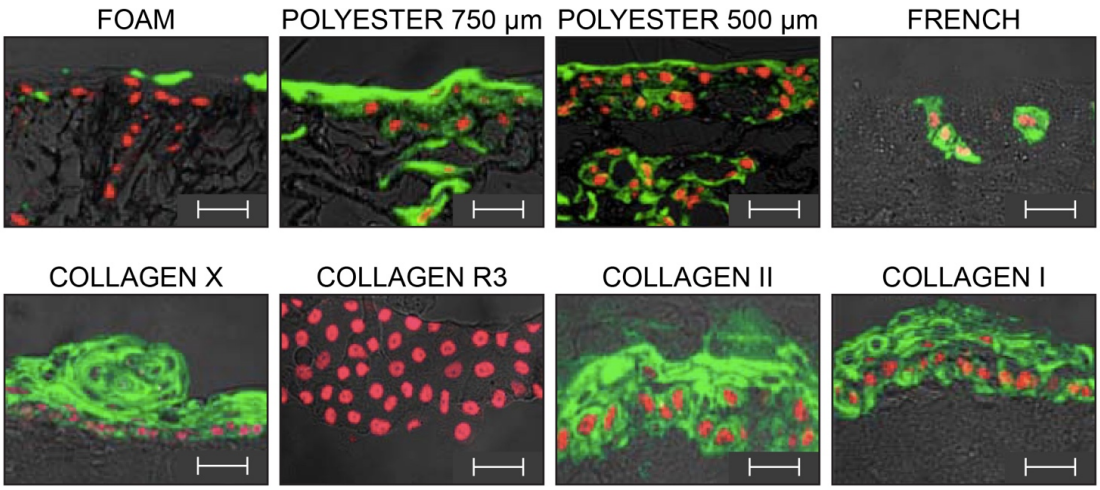

Figure 18. *Immunofluorescence staining of ΔNp63α (red) and cK3 (green) of reconstructed epithelia originated from H-LESCs plated on the different scaffolds tested. Images show epithelial cells ingrowth, abnormal differentiation clusters and abnormal stratification and are representative of data obtained from at least three independent experiments. Scale bars 100 µm. Abbreviations: LESCs, limbal epithelial stem cells.*

5.8 Setting of the cohort of animal patients

Based on data obtained with human stem cells, next step was to move to an animal model in order to assess, *in vivo*, the transplantability and functionality of these epithelioid structures.

Based on that, we started a collaboration with the veterinary department to understand what could be the most useful model for our purpose and to assess the existence, in the clinic, of injuries or alterations comparable to LSCD. The proposal of veterinarians was to focus on one animal species, considering dogs as useful models for our purpose. Indeed, there are several features that make these species ideal for our purposes. First of all, dogs are common animals and make up the largest percentage of patients referring to the veterinary clinic. Also, diseases presenting clouding and conjunctivalization of corneal surface are not uncommon in these animals (physical damages from scratches and bites, chemical damage from environmental and domestic factors, progressed infectious and not infectious keratitis) and these lesions are often profound, involving the stromal tissue. For this reason, the use of these models is favored by the possibility of work on not induced pathologies. Furthermore, they have an eye anatomy very similar to human and corneal stem cells reside in the

outer ring of the cornea that is organized in niches just like the human limbus (GÜL SANCAK et al, 2014). Finally, the life span of these animals is quite long (10-13 years on average) allowing the implementation of longer and more detailed follow up analysis able to provide data about long term self renewal and maintenance of the implanted tissue.

5.9 Canine corneal epithelial stem cells (C-LESCs) and canine oral mucosa epithelial stem cells (C-OMESCs) characterization

As a first step, we started the characterization of cell lines obtained from biopsies of the cornea (C-LESCs) and oral mucosa (C-OMESCs) of canine origin. Biopsies were taken from cadavers at the time of euthanasia, in the Department of Veterinary and transported in DMEM s/f + penicillin/streptomycin 5%. We collected biopsies from four different dogs, taken from different points of the limbus and from oral mucosa. All the material collected was plated in culture, allowing us to obtain, from each subject, two primary lines of corneal cells and two lines of oral mucosal cells. After plating on 3T3-J2 feeder layer, the primary lines were serially propagated until exhaustion. This allowed us to get data of life span to compare the behavior of these cells with H-LESCs. In addition, for each passage, we performed colony forming efficiency assays (CFE) to estimate the proportion of clonogenic cells present in the culture. The data obtained from these assays showed a trend of canine cell line comparable to that of human limbal cells, showing a similar decrease of colony forming efficiency (CFE) and clonogenic cell number and a similar percentage of aborted colonies during serial cultivation (figure 19-20). In particular, the slope of clonogenic cells is less pronounced in C-LESCs and C-OMESCs, suggesting the possibility that these cells retain a greater proportion of clonogenic cells, in more advanced passages, with particular regard to the C-OMESCs (figure 20). Also replicative senescence, as suggested by the number of passages in culture, is comparable to human cell lines. Finally, transcript expression analysis of p63 and ABCG2 (two stem/progenitor epithelial cells marker) showed a progressive decrease during passages (figure 21).

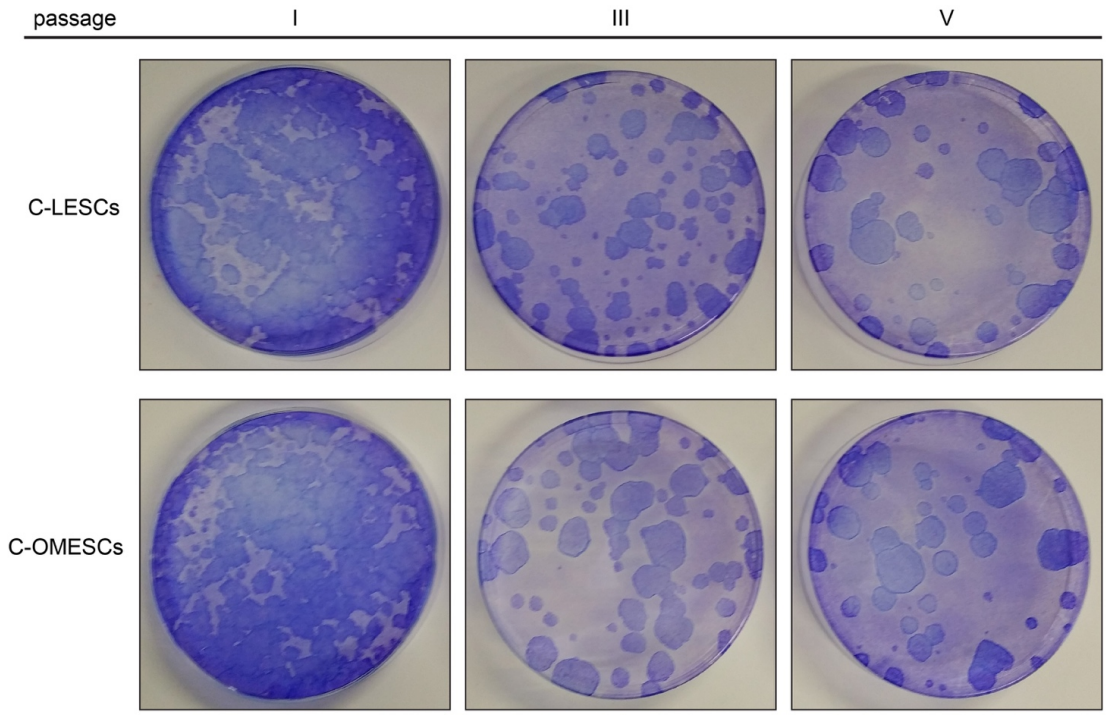

Figure 19. *Colony forming efficiency (CFE) of C-LESCs and C-OMESCs was evaluated at three different passages in culture. Images are representative of data obtained from at least three independent experiments. Abbreviations: LESCs, limbal epithelia stem cells; OMESCs, oral mucosa epithelial stem cells.*

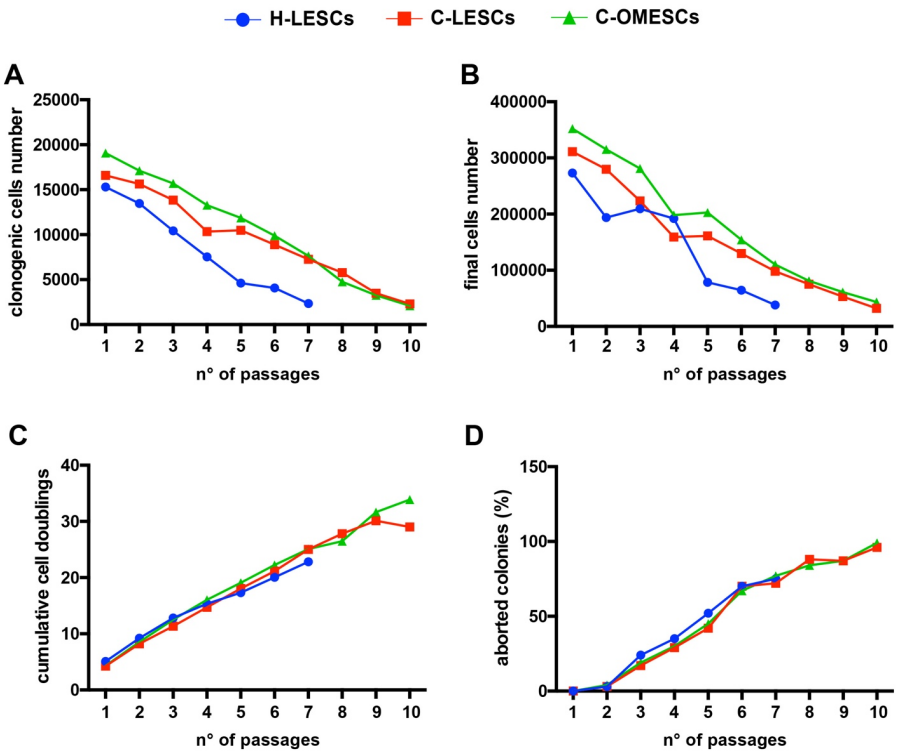

Figure 20. *Comparison of clonogenic ability and proliferative potential of human and canine epithelial stem cells obtained from limbal and oral mucosa biopsies. All data have been obtained from four unrelated normal subjects (n≥3 independent experiments). Quantification of (A) clonogenic cells number, (B) final cells number (C) cumulative cell doublings, (D) percentage of aborted colonies of H-LESCs (blue), C-LESCs (red) and C-OMESCs (green) is shown. Abbreviations: LESCs, limbal epithelial stem cells; OMESCs, oral mucosa epithelial stem cells.*

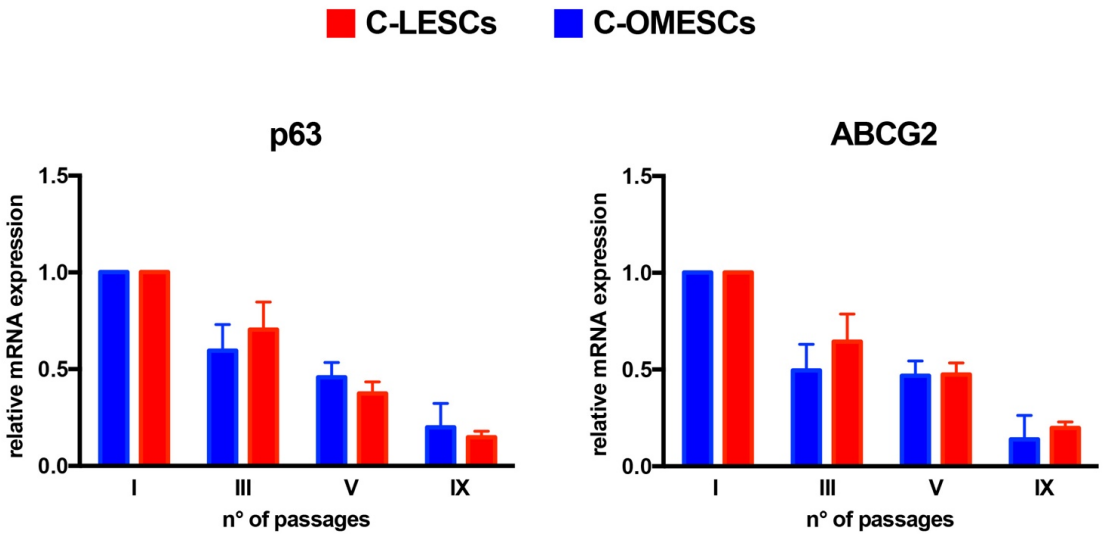

Figure 21. *p63 and ABCG2 expression during passages in culture of canine primary cell lines. Relative quantitative PCR showing p63 and ABCG2 copy number in total RNA from C-LESCs and C-OMESCs. Results are normalized against GAPDH. Abbreviations: LESCs, limbal epithelial stem cells; OMESCs, oral mucosa epithelial stem cells; GAPDH, glyceraldehyde-3-phosphate dehydrogenase.*

5.10 Reconstructed canine keratoplasty lenticules

Human keratoplasty lenticules (HKLs) are naturally derived matrices obtained from human corneas that we evaluated for their ability to mimic the local environment of human corneal epithelial stem cells and provide a template for cell growth and extra cellular matrix (ECM) production. Primary human and canine epithelial stem cells were seeded onto HKLs and allowed to grow for 7 days. It is known that keratinocytes cultured at the air–liquid interface give rise to a multilayered epithelium, thus mimicking the naturally occurring conditions of corneal epithelia. Human and canine epithelial cells seeded onto HKLs were therefore cultured in submerged conditions for 7 days and, once confluent, air lifted at the air–liquid interface for 14 further days. The resulting epithelia was well organized and stratified into four to five cell layers, as

shown by the staining with the far-red fluorescent DNA dye DRAQ5® (Figure 22-23), with basal cuboidal cells differentiating upward to winged cells. The layer of basal cuboidal cells was firmly attached to the underlying ECM and to the basement membrane through integrinβ4 (Figure 22). Maintenance of stemness potential and differentiation pathways are both important factors for the development of healthy corneal epithelia. For this reason, specific markers of stemness and differentiation were evaluated. Both human and canine basal epithelial cells expressed p63, an epithelial stem/progenitor cell marker (Figure 22). Differentiation pathways were not altered, as indicated by the expression of involucrin (Figure 23), a terminal differentiation marker for stratified epithelia. We also observed the presence of a basement membrane underneath the epithelial cell layers and preservation of the Bowman's membrane (data not shown). Importantly, expression of the different markers resembled that observed in normal epithelia, thus suggesting that HKLs are able to support the growth and maintain the differentiation pathways of epithelial stem cells.

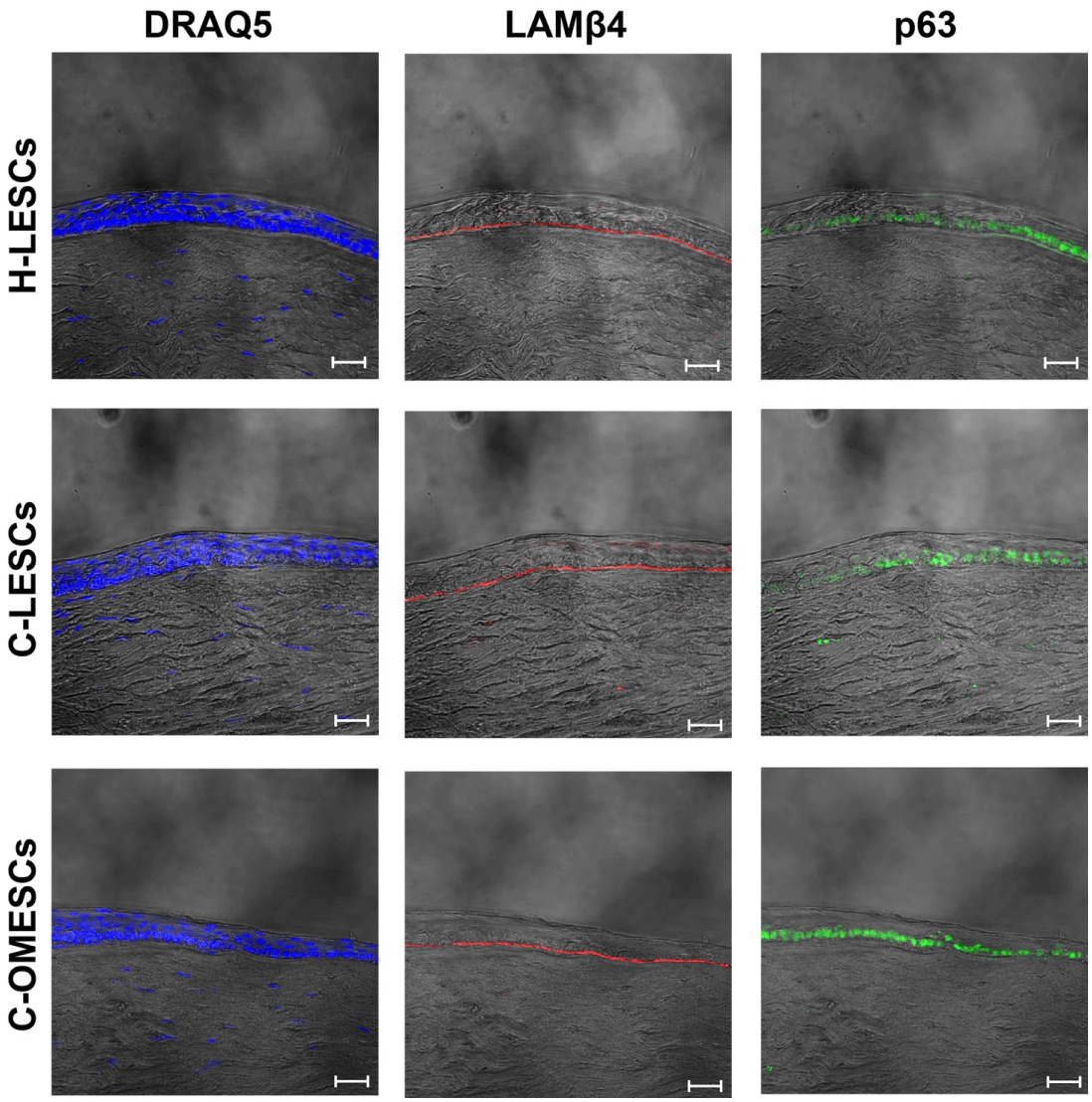

Figure 22. *DRAQ5 staining and expression of epithelial stem cells markers in reconstructed hemicorneas generated by growing H-LESCs, C-LESCs and C-OMESCs onto human keratoplasty lenticules (HKLs). Cryosections were analyzed through immunofluorescence using p63 (green) and Lamβ4 (red) antibodies (n= 3) Scale bars 20 μm. Note that all epithelia were well organized and stratified into four to five cell layers, with basal cuboidal cells differentiating upward to winged cells. The strong expression of the stem cell marker p63 confirms the maintenance of basal and undifferentiated progenitor cells. Abbreviations: LESCs, limbal epithelial stem cells; OMESCs, oral mucosa epithelial stem cells.*

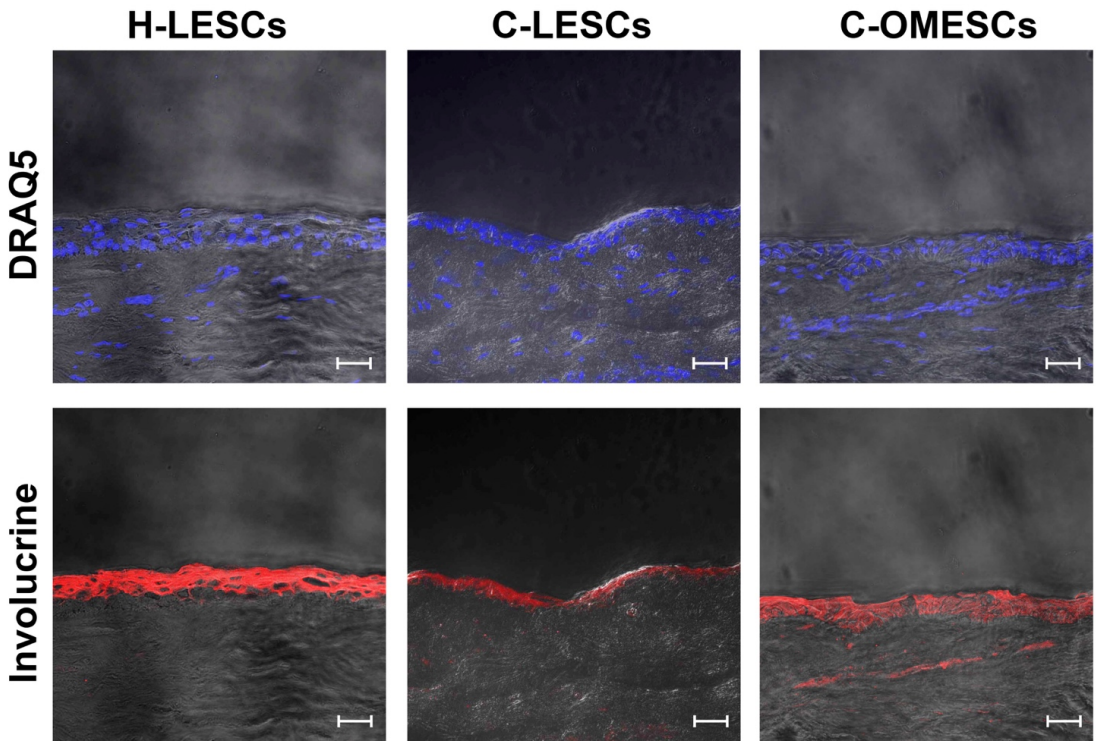

Figure 23. *DRAQ5 staining and expression of epithelial differentiated cells markers in reconstructed hemicorneas generated by growing H-LESCs, C-LESCs and C-OMESCs onto human keratoplasty lenticules (HKLs). Cryosections were analyzed through immunofluorescence using Involucrine (red) antibodies (n = 3) Scale bars 20 μm. Abbreviations: LESCs, limbal epithelial stem cells; OMESCs, oral mucosa epithelial stem cells.*

6 Discussion and conclusions

In the last decade, stem cells have proved to represent a valid therapeutic approach to many untreated pathologies, thanks to their ability to regenerate and replace damaged tissues. Thus, adult or somatic stem cells immediately gained a pivotal role, with many advantages compared to embryonic stem cells or iPSCs that are connected to many adverse effects. Therefore, stem cells have become very useful in clinical application as a valuable tool for translational medicine. Among them, epithelial stem cells, have achieved a first-rate position from the very beginning because of the variety of pathologies associated with this cell type. Moreover, the accessibility of epithelial tissue allows us the epithelial stem cells isolation, maintenance and culture to deeply study their *in vitro* behavior, both in physiological and pathological conditions. In this work, we have focused on comparative features of somatic stem cells from four different epithelia *in vitro* and *in vivo* and on the possible advantages from such comparisons. *In vivo* behavior of the different epithelia (table 1) reflects the physiological role of the tissue. The necessity to protect the internal organs require a highly organized structure. For this reason, the epidermis is composed of 5 different cells layers to generate a functional barrier for the external environment. The incessant exposition to thermal shocks, pathogens and chemical agents submit skin epithelium to a continuous replacement of cells, known as homeostasis, processes of proliferation and differentiation that culminate in the desquamations of keratinized flakes (cytomorphosis). The homeostasis is guaranteed by keratinocytes located in niches spatially harboured in the throughout layer, like in the interfollicular epidermis (IFE), in a turnover of 28 days [Blanpain et al. 2014]. Oral mucosa is linked to a similar function, that is to protect the oral cavity against pathogens and mechanical stress during mastication. It is possible to distinguish different areas by differences in keratinization of the mucosa. The gingivae and hard palate are keratinized, while the lower part of the mouth, the area near the lips and the surface under the tongue are not keratinized. The oral mucosa has higher number of cell layers and proliferation rate compared to epidermis (Figure 1) [Rowat et al, 1996; Gibbs et al, 2000; Andl et al, 2016]. Quiescent cells are located in the basal layer, while the proliferation is restricted to the parabasal and adjacent suprabasal layers [Kotelnikov et al, 1996; Dwivedi et al,

2013; Prince et al, 2007; Liu et al, 1998; Bosch et al, 1993; Hsu et al, 2013; Okumura et al, 2014; Andl et al, 2016]. Under homeostasis conditions the turnover of this epithelium is from 14 days to 24 days for hard palate. The anterior acular surface represents a very unique case from the point of view of the epithelia that cover it: the cornea, centrally, and the sclera peripherally. The main feature that makes the cornea a particular epithelium is the transparency that allows it to play its role in focusing and transmitting light without scatter through the lens and onto the retina, ensuring the vision [Bukowiecki et al. 2017]. Its easily accessibility and avascularisation make the cornea an intriguing site for gene and cell therapies. Because of its location in the outermost part of the eye, it is vulnerable to damage caused by burns, abrasions, contact lens problems, alteration in tear production, infections and other diseases [Saghizadeh, et al. 2017]. Corneal epithelium consists of a single basal layer and in stratified squamous epithelial cells, constantly renewed in corneal homeostasis, essential to guarantee the structural uniformity and the transparency of the tissue. During corneal homeostasis LESCs proliferate and generate transient amplifying cells (TA) that divide, differentiate and migrate to the centre of the cornea (traced by keratine 14 expression), to regenerate the epithelium (Saghizadeh, et al. 2017). LESCs are present in basal layer of the limbus, corneoscleral junction responsible for the drainage of water humor and for the protection of limbal epithelial stem cells, in specific niches called Palisades of Vogt (Figure 1) [Davanger et al. 1971]. Described for the first time by Streiff in 1914, with the name of “radial stripes”, Palisades of Vogt have an undulated appearance, due to radially oriented fibrovascular ridges, projected into the deeper layers of the limbus. These invaginations are called limbal crypts and furnish the right environment for limbal stem cells (Zhang et al), that have been identified and localized based on the colony-forming ability, proliferative potential, slow cycling nature (BrdU or EdU label-retaining cells), expression of specific antigens and markers (ΔNp63α) [Saghizadeh et al, 2017]. Whilst it is commonly known that the stem cells of corneal epithelium reside in the limbal area, the location of conjunctival stem cells is controversial: possible sites proposed in last years are fornix region, limbus, bulbar conjunctiva, palpebral conjunctiva and at the mucocutaneous junction on the eyelid margin. Previous studies suggest that CESCs are uniformly distributed throughout the whole surface [Nagasaki et al, 2005; Pellegrini et al, 1999], but recent

further studies demonstrated that CESCs are located in the fornix and/or in the bulbar conjunctiva. In fact, the fornix may provide greater physical protection, intraepithelial mucous crypts, vasculature, and immune cells, typical features of stem cells niches (Stewart et al, 2015). So, the integrity of the anterior ocular surface is also guaranteed by the conjunctival homeostasis, in a two-stage process described by Potten et al, to renew the stratified conjunctival epithelium. The small population of CESCs, that divided infrequently, generate daughter cells that in turn produce transient amplifying cells, an actively proliferating cells population. These one migrate and differentiate toward the fornix to replace the mature cells continuously lost [Potten et al.]. To better understand their reflected behavior *in vivo* and permit to apply their strengths in regenerative medicine *in vitro* characterization of primary epithelia cell lines is essential. Pioneering studies by H. Green in the 1970s allowed to set sophisticated protocols for the *in vitro* maintenance of primary cells focusing on the clinical application of the tissues regenerated by these cells. Green himself immediately proposed the potential of stratified *in* vitro epithelial sheets for the treatment of all the cases, such as burns, where the lack of the epithelial stem cells compartment results in a failure of a self-maintaining epithelium reconstruction (Rheinwald and Green, 1975; Barrandon and Green, 1987). Thanks to advancement of technology, discovery of epithelial stem cell marker that allow to identify and quantify the presence of stem cells within primary cultures, such as ΔNp63α (Di Iorio et al, 2005) and innovative scaffolds employment, such as fibrin matrices (Pellegrini et al., 1999), amniotic membrane (Meller et al, 2002), or human keratoplasty lenticules (HKL; Barbaro et al, 2009), it was possible to produce epithelial sheets easier to transplant and more suitable to long-term engraftment. Expanding, differentiation and layering abilities of epithelial stem cells (actually regenerating an ex vivo working tissue) also provided a useful tool to gene therapy approaches for a number of pathologies characterized by mutations that affect an epithelium homeostasis (Mavilio et al, 2006; Barbaro et al, 2016). *In vitro* behavior of epithelial stem cells reflect their *in vivo* physiological trend. Thus, as the renewal of the epidermidis after an injury require around three weeks, *in vitro* proliferation of H-SESCs proceeds for 20 days. Similar considerations could be applicable to all the stem cells of those tissues. The proliferation ability and the stem cells potential could notably increase thanks to the

DAPT subministration. This molecule, by inhibiting the Notch signaling, can enrich the stem cells population obtained from a biopsy and delay their premature aging. DAPT treatment could widen the therapeutic window in various pathologies, such as the EEC syndrome, where it is very narrow. The stem cells enrichment in primary cultures could provide a cell population on which gene therapy approaches, such as gene editing, can be effective. Diseases like limbal stem cells deficiency (LSCD) can be overcome using epithelial stem cells of other body regions which, even though having distinctive characteristics, maintain the same pattern and are applicable to effective cell therapy. Nishida et al. study of epithelia cells, in 2004, permits to successfully transplant oral mucosal cell sheets on the ocular surface obtaining a new transparent epithelium. As well as, my group in 2016 have been able to isolate the cell population with a mild phenotype from a patient affected by Ectrodactyly-Ectodermal dysplasia-Clefting (EEC) syndrome with a rare mosaicism, enriching these primary cells *in vitro* and producing well-organized and stratified epithelial sheets. The novelty and the importance of this study are related to the ability to isolate and recover stem cells heterozygous for p63, which appear to have an extraordinary regenerative capacity comparable to that of healthy cells, thus representing a valuable source for starting a customized cell therapy approach for this unique case of EEC syndrome, based solely on epithelial stem cell manipulation. This part of my work highlights and emphasizes the potential of regenerative and personalized medicine, obtained through the development of CA-OMESCs, to reconstruct the ocular surface of this unique case of EEC syndrome, and demonstrates a proof-of-principle approach, based only on stem cell strategy, that bypassing gene therapy approaches provides evidence of the feasibility of an innovative strategy to correct a severe corneal pathology.

The replacement of diseased tissues and organs by means of tissue engineering approaches is rapidly becoming a reality and the possibility to obtain bioengineered corneal replacements recently demonstrated (Nishida et al. 2004) (Pellegrini et al. 1997) (Barbaro et al. 2009). Successful tissue engineering depends on the availability of suitable scaffolds during the initial stages of reconstruction. The choice of an appropriate matrix is, therefore, of crucial importance. The ideal scaffold should fulfill several requirements, including biocompatibility and the possibility to be repopulated

with autologous recipient cells. Various types of matrices, such as polymers, amniotic membrane, or fibrin gel, have been investigated for ocular surface reconstruction. However, none of them is completely devoid of problems. Compared to these matrices, HKLs appear to be particularly attractive because of their anatomic similarity to the human cornea, with the stroma acting as a physiologically functional tissue substitute and not simply as a scaffold for limbal stem cells propagation (Barbaro et al. 2009). Our model might, therefore, be considered as a step forward toward the development of a tissue-engineered hemicornea in which corneal epithelial stem cells proliferate, establish contacts with the keratocytes of the underlying stroma, and renew the epithelium by producing transiently amplifying cells and differentiated cell layers. The possibility of cultivate limbal epithelial stem cells onto HKLs *in vitro* and of obtain a physiologically functional tissue with proliferating keratinocytes and keratocytes is an important feature that make HKL a potential and interesting scaffold for the treatment of LSCD (Barbaro et al. 2009). In addition, HKLs have some further advantages that are worth discussing in depth. Firstly, the use of HKL could overcome some of the problems associated with the use of fibrin gel and improve fibrin-cultured limbal stem cell transplantation. Occasionally, in fact, corneal stem cell proliferation causes a progressive thinning of the fibrin glue, thus making manipulation of stem cell grafts by surgeons extremely difficult. In addition, as the fibrin glue is not a porous material, this might cause stagnation of blood residues underneath the fibrin-cultured stem cells in vivo, thus not allowing optimal reabsorption of the fibrin and interaction of keratinocytes with the underlying corneal stroma (Barbaro et al. 2009). Another potential advantage of HKLs is their ability to sustain corneal stem cell proliferation even in the absence of lethally irradiated 3T3-J2 feeder layers. Murine feeder layers are essential for the maintenance of the stemness and proliferative potential of epithelial stem cells cultured in vitro. However the development of feeder-free culture conditions for corneal epithelial stem cells would be of great interest. In fact, although lethally irradiated and therefore unable to replicate, murine 3T3-J2 fibroblasts are still present in grafts suitable for transplantation with percentages of approximately 5% (Barbaro et al, 2009). Limbal stem cell transplantation, as it is currently carried out, might therefore induce inflammatory responses against the xenogeneic component of the graft (the murine fibroblasts), thus potentially reducing the possibilities of

successful outcomes. In addition, it is very likely that, in the near future, guidelines regulating the clinical applications of stem cells will require the development of animal-free culture systems (no murine feeder layers or culturing media with animal-derived proteins/growth factors) (Barbaro et al, 2009). HKL could therefore be an advantageous scaffold for limbal stem cells. Another interesting feature of HKLs is the possibility to be freeze dried, thus eliminating viable, and potentially immunogenic, keratocytes. Recently, various decellularization procedures have been used to eliminate cells and create a cell-free matrix, which can be repopulated with recipient cells after implantation. Advantages would not only be limited to the lower antigenicity of freeze-dried HKLs (Barbaro et al, 2009). Stability, safety, and sterility are all properties that would make HKLs more suitable than other carriers in the strictly regulated Good Manufacturing Practice (GMP) settings that are now required for production/manufacture of cell-therapy products for human use. In the future, the possibility of culturing and expanding limbal stem cells onto HKLs might open-up new and intriguing perspectives for the surgical treatment of LSCD associated to deep stromal damages. The management of these cases of LSCD is currently carried out using a multistaged approach. The ocular surface is firstly stabilized through pannus resection and transplantation of autologous cultured limbal stem cells. Visual rehabilitation is normally gained through a second stage involving penetrating keratoplasty. Improvements in microsurgical techniques and introduction of new devices have recently led to increasing numbers of lamellar keratoplasty procedures being performed. This appears to be true both for the anterior lamellar keratoplasty (ALK), replacing the anterior stroma, and for the posterior lamellar keratoplasty (PLK), which involves the replacement of deep stromal and endothelial layers. Lenticules for both ALK and PLK are prepared by surgeons just before surgery or, very often, provided by eye banks. In cases of LSCD patients with eyes having milder and superficial stromal scarring, transplantation of autologous limbal stem cells cultured onto HKLs might, therefore, be performed using ALK surgical procedures. In these cases the multistaged approach described earlier would be replaced by just one step in which grafts of HKL with limbal stem cells would replace the damaged stroma of the recipient at once. This technique would also provide tectonic tissue support to LSCD

corneas, which are normally thinner and have higher risks of perforations than healthy ones (Barbaro et al, 2009).

For all these reasons, moving to the use of these scaffolds *in vivo*, in animal models, will be an essential step for the achievement of clinical applications. The data obtained so far on the primary cultures of dog showed a behavior of stem cells comparable to those of humans. Reconstructed hemicorneas of canine origin have proved to be able to organize, stratify and bind to the stroma, expressing the correct differentiation and stem cell markers. With the data we collect on HKLs from C-CESCs and C-OMESCs we will transfer the technology on animal patients. Moreover, expanding the animal patients cohort, including cats and rabbits (Selver et al, 2015; GÜL SANCAK et al, 2014), we can get a pool of subjects large enough to allow us to carry out all the necessary *in vivo* studies. Future findings will also lead to obtain a complete corneal equivalent by plating limbal/corneal keratinocytes onto lenticules normally used for PLK, i.e., complete with Descemet's membrane and endothelium. Finally, the use of HKLs could provide an interesting *in vitro* organotypic culture system for evaluation of the growth, proliferation, and differentiation processes of corneal stem cells from patients with disorders/pathologies that make propagation of cells onto commonly used plastic Petri dishes difficult and the development of new pharmaceutical drugs (e.g., eye drops, medicinal products), as they might represent a valid *in vitro*-based alternative method for assessing toxicity and safety.

To summarize and conclude my discussion, primary epithelial cells have unique characteristics with an inimitable potential that makes them a malleable tool, able to adapt to different necessities. And so on, although these data are intriguing, further investigation could provide more and more useful data for their clinical application in regenerative medicine. As a proof-of-principle that epithelial stem cells have an intrinsic potential for regenerative medicine that can be exploited with a deeper characterization, my group have been able to apply, *in vitro*, a cell therapy protocol to a patient affected by a rare mosaic form of EEC syndrome.

HKLs appear to be particularly attractive, animal-free (feeder-free) and full-thickness scaffolds for corneal reconstruction. We have already started with the last step, that is the recruitment of canine patients to assess the transplantability and functionality of

these organotypic structures. We are contacting a research group from the Department of Surgery, Faculty of Veterinary Medicine, Turkish Republic of Northern Cyprus that published a case report of LSCD in a dog [Özgencil et al, 2017] with the aim of creating a small cohort on which to start with first transplantation trials.

7 References

Allen EH, Atkinson SD, Liao H, Moore JE, Leslie Pedrioli DM, Smith FJ, McLean WH, Moore CB: Allele-specific siRNA silencing for the common keratin 12 founder mutation in Meesmann epithelial corneal dystrophy. Invest Ophthalmol Vis Sci 2013; 54(1): 494-502

Andersen, Peter, Hideki Uosaki, Lincoln T. Shenje, and Chulan Kwon. 2012. "Non-Canonical Notch Signaling: Emerging Role and Mechanism." Trends in Cell Biology 22 (5):257–65.

Andl C D, Le Bras G F, Loomans H, Kim A S, Zhou L, Zhang Y, Andl T: Association of TGFβ signaling with the maintenance of a quiescent stem cell niche in human oral mucosa. Histochem Cell Biol. 2016; 146(5):539-555.

Ang, Marcus, Ryan Man, Eva Fenwick, Ecosse Lamoureux, and Mark Wilkins. 2017. "Impact of Type I Boston Keratoprosthesis Implantation on Vision-Related Quality of Life." The British Journal of Ophthalmology, September.

Aravena, Carolina, Fei Yu, and Anthony J. Aldave. 2017. "Long-Term Visual Outcomes, Complications, and Retention of the Boston Type I Keratoprosthesis." Cornea, October.

Artavanis-Tsakonas, S., M. D. Rand, and R. J. Lake. 1999. "Notch Signaling: Cell Fate Control and Signal Integration in Development." Science (New York, N.Y.) 284 (5415):770–76.

Augustin M, Bamberger C, Paul D, Schmale H: Cloning and chromosomal mapping of the human p53-related KET gene to chromosome 3q27 and its murine homolog Ket to mouse chromosome 16. Mamm Genome 1998; 9(11): 899-902.

Barbaro V, Confalonieri L, Vallini I, Ferrari S, Ponzin D, Mantero G, Willoughby CE, Parekh M, Di Iorio E: Development of an allele- specific real-time PCR assay for discrimination and quantification of p63 R279H mutation in EEC syndrome. J Mol Diagn 2012; 14(1): 38- 45.

Barbaro V, Nasti AA, Del Vecchio C, Ferrari S, Migliorati A, Raffa P, Lariccia V, Nespeca P, Biasolo M, Willoughby CE, Ponzin D, Palù G, Parolin C, Di Iorio E. 2016. "Correction of Mutant P63 in EEC Syndrome Using SiRNA Mediated Allele-Specific Silencing Restores Defective Stem Cell Function." Stem Cells 34 (6):1588–1600.

Barbaro V, Nasti AA, Raffa P, Migliorati A, Nespeca P, Ferrari S, Palumbo E, Bertolin M, Breda C, Miceli F, Russo A, Caenazzo L, Ponzin D, Palù G, Parolin C, Di Iorio E. 2016. “Personalized Stem Cell Therapy to Correct Corneal Defects Due to a Unique Homozygous-Heterozygous Mosaicism of Ectrodactyly-Ectodermal Dysplasia-Clefting Syndrome.” Stem Cells Translational Medicine 5 (8):1098–1105.

Barbaro V, Ferrari S, Fasolo A, Ponzin D, Di Iorio E. 2009. “Reconstruction of a Human Hemicornea through Natural Scaffolds Compatible with the Growth of Corneal Epithelial Stem Cells and Stromal Keratocytes.” Molecular Vision 15 (October):2084–93.

Barbaro V, Ferrari S, Fasolo A, Pedrotti E, Marchini G, Sbabo A, Nettis N, Ponzin D, Di Iorio E. 2010. “Evaluation of Ocular Surface Disorders: A New Diagnostic Tool Based on Impression Cytology and Confocal Laser Scanning Microscopy.” The British Journal of Ophthalmology 94 (7):926–32.

Barrandon Y, Green H: Three clonal types of keratinocyte with different capacities for multiplication. Proc Natl Acad Sci USA 1987; 84(8): 2302-2306.

Barrett P M, Scagliotti R H, Merideth R E, Jackson P A: Absolute corneal sensitivity and corneal trigeminal nerve anatomy in normal dogs. Prog Vet Comp Ophthalmol 1991; 1:245–54.

Blanpain, C. and Fuchs, E. 2014. Plasticity of epithelial stem cells in tissue regeneration. Science; 344(6189), pp.1242281-1242281.

Blanpain C. and Fuchs E. 2006. “Epidermal Stem Cells of the Skin.” Annual Review of Cell and Developmental Biology 22:339–73.

Blanpain C, Horsley V, Fuchs E. 2007. “Epithelial Stem Cells: Turning over New Leaves.” Cell 128 (3):445–58.

Blanpain C, Lowry WE, Geoghegan A, Polak L, Fuchs E. 2004. “Self-Renewal, Multipotency, and the Existence of Two Cell Populations within an Epithelial Stem Cell Niche.” Cell 118 (5):635–48.

Blocker T, Van Der Woerdt A: A comparison of corneal sensitivity between brachycephalic and Domestic Short- haired cats. Vet Ophthalmol 2001; 4:127–130.

Bonthagarala, Brahmaiah, Ch.Dileep, and K.Manasa. 2013. “STEM CELL: PAST, PRESENT AND FUTURE- A REVIEW ARTICLE.” International Journal of Experimental Pharmacology, March.

Brennan NA. n.d. “Beyond Flux: Total Corneal Oxygen Consumption as an Index of Corneal Oxygenation during Contact Lens Wear.” Optometry and Vision Science : Official Publication of the American Academy of Optometry 82 (6):467–72.

Bukowiecki A, Hos D, Cursiefen C, Eming S. 2017. Wound-Healing Studies in Cornea and Skin: Parallels, Differences and Opportunities. International Journal of Molecular Sciences; 18(6), p.1257.

Buono KD, Robinson GW, Martin C, Shi S, Stanley P, Tanigaki K, Honjo T, Hennighausen L. 2006. “The Canonical Notch/RBP-J Signaling Pathway Controls the Balance of Cell Lineages in Mammary Epithelium during Pregnancy.” Developmental Biology 293 (2):565–80.

Buss PW, Hughes HE, Clarke A. 1995. Twenty-four cases of the EEC syndrome: clinical presentation and management. J Med Genet; 32 (9):716-723.

Carroll DK, Carroll JS, Leong CO, Cheng F, Brown M, Mills AA, Brugge JS, Ellisen LW. 2006 p63 regulates an adhesion programme and cell survival in epithelial cells. Nat Cell Biol; 8(6): 551-561.

Cavanagh HD, Colley AM. 1989. The molecular basis of neurotrophic keratitis. Acta Ophthalmol Suppl; 192: 115–134.

Celli J, Duijf P, Hamel BC,Bamshad M,Kramer B,Smits AP, Newbury-Ecob R, Hennekam RC, Van Buggenhout G, van Haeringen A, Woods CG, van Essen AJ, de Waal R, Vriend G, Haber DA, Yang A, McKeon F, Brunner HG, van Bokhoven H. 1999. Heterozygous germline mutations in the p53 homolog p63 are the cause of EEC syndrome. Cell; 99(2): 143-153.

Chan-Ling T. 1989. Sensitivity and neural organization of the cat cornea. Invest Ophthalmol Vis Sci; 30:1075–1082.

Chen C, Gorlatova N, Kelman Z, Herzberg O. 2011. Structures of p63 DNA binding domain in complexes with half-site and with spacer- containing full response elements. Proc Natl Acad Sci USA; 108(16): 6456-6461.

Cotsarelis G, Cheng SZ, Dong G, Sun TT, Lavker RM. 1989. Existence of slow-cycling limbal epithelial basal cells that can be preferentially stimulated to proliferate: implications on epithelial stem cells. Cell; 57(2): 201-209.

Das P, Pereira J A, Chaklader M, Law A, Bagchi K, Bhaduri G. 2013. Phenotypic alteration of limbal niche-associated limbal epithelial stem cell deficiency by ultraviolet-B exposure-induced phototoxicity in mice. Biochem Cell Biol; 91:165–175.

Davanger, M., Evensen, A. 1971. Role of the pericorneal papillary structure in renewal of corneal epithelium. Nature; 229: 560-1.

Davison TS, Vagner C, Kaghad M, Ayed A, Caput D, Arrowsmith CH. 1999. p73 and p63 are homotetramers capable of weak heterotypic interactions with each other but not with p53. J Biol Chem; 274(26): 18709-18714.

Denk N, Sandmeyer L S, Lim C C, Bauer B S, Grahn B H. 2011. A retrospective study of the clinical, histological, and immunohistochemical manifestations of 5 dogs originally diagnosed histologically as necrotizing scleritis. Vet Ophthalmol; 15:102–109.

Di Iorio E, Barbaro V, Ferrari S, Ortolani C, De Luca M, Pellegrini G. 2006. Q-FIHC: quantification of fluorescence immunohistochemistry to analyse p63 isoforms and cell cycle phases in human limbal stem cells. Microsc Res Tech; 69(12): 983-991.

Di Iorio E, Barbaro V, Ruzza A, Ponzin D, Pellegrini G, De Luca M. 2005. Isoforms of DeltaNp63 and the migration of ocular limbal cells in human corneal regeneration. Proc Natl Acad Sci USA; 102(27): 9523-9528.

Di Iorio E, Ferrari S, Fasolo A, Böhm E, Ponzin D, Barbaro V. 2010. Techniques for culture and assessment of limbal stem cell grafts. Ocul Surf; 8(3): 146-153.

Di Iorio E, Kaye SB, Ponzin D, Barbaro V, Ferrari S, Böhm E, Nardiello P, Castaldo G, McGrath JA, Willoughby CE. 2012. Limbal stem cell deficiency and ocular phenotype in ectrodactyly-ectodermal dysplasia-clefting syndrome caused by p63 mutations. Ophthalmology; 119(1): 74-83.

Dötsch V, Bernassola F, Coutandin D, Candi E, Melino G. 2010. p63 and p73, the ancestors of p53. Cold Spring Harb Perspect Biol; 2(9): a004887.

Dua HS, Joseph A, Shanmuganathan VA, Jones RE. 2003. Stem cell differentiation and the effects of deficiency. Eye (London); 17:877–885.

Dua, HS. 1998. “The Conjunctiva in Corneal Epithelial Wound Healing.” The British Journal of Ophthalmology 82 (12):1407–11.

Dua, HS, Saini JS, Azuara-Blanco A, Gupta P. 2000. “Limbal Stem Cell Deficiency: Concept, Aetiology, Clinical Presentation, Diagnosis and Management.” Indian Journal of Ophthalmology 48 (2):83–92.

Dua HS, Harminder S, Faraj LA, Said GD, Gray T, Lowe J. 2013. “Human Corneal Anatomy Redefined: A Novel Pre-Descemet’s Layer (Dua’s Layer).” Ophthalmology 120 (9):1778–85.

Elmén J, Thonberg H, Ljungberg K, Frieden M, Westergaard M, Xu Y, Wahren B, Liang Z, Ørum H, Koch T, Wahlestedt C. 2005. Locked nucleic acid (LNA) mediated improvements in siRNA stability and functionality. Nucleic Acids Res; 33(1): 439-447.

Ferrari S, Barbaro V, Di Iorio E, Fasolo A, Ponzin D. 2009. “Advances in Corneal Surgery and Cell Therapy: Challenges and Perspectives for Eye Banks.” Expert Review of Ophthalmology 4 (3):317–29.

Fuchs E, Raghavan S. 2002. Getting under the skin of epidermal morphogenesis. Nat Rev Genet; 3(3): 199-209.

Fuchs E, Chen T. 2013. A matter of life and death: self-renewal in stem cells. EMBO; 14(1):39-48.

Gambardella L, Barrandon Y. 2003. The multifaceted adult epidermal stem cell. Curr Opin Cell Biol; 15(6): 771-777.

Gibbs S, Ponec M. 2000. Intrinsic regulation of differentiation markers in human epidermis, hard palate and buccal mucosa. Archives of Oral Biology 2000; 45(2), pp.149-158.

Gonzalez-Alegre P, Miller VM, Davidson BL, Paulson HL. 2003. Toward therapy for DYT1 dystonia: allele-specific silencing of mutant TorsinA. Ann Neurol; 53(6): 781-787.

Gül Sancak R, Özen A, Pinarli F A, TiRyaki M, Ceylan A, Acar U, DeliBaşI T. 2014. Limbal Stem Cells in Dogs and Cats Their Identification Culture and Di erentiation into Keratinocytes. Kafkas Univ Vet Fak Derg; 20(6): 909-914.

Hamada T, Chan I, Willoughby C, Goudie DR, McGrath JA. 2002. Common mutations in Arg304 of the p63 gene in ectrodactyly, ectodermal dysplasia, clefting syndrome: lack of genotype-phenotype correlation and implications for mutation detection strategies. J Invest Dermatol; 119(5): 1202-1203.

Hayashi S, Osawa T, Tohyama K. 2002. “Comparative Observations on Corneas, with Special Reference to Bowman’s Layer and Descemet’s Membrane in Mammals and Amphibians.” Journal of Morphology 254 (3):247–58. https://doi.org/10.1002/jmor.10030.

He L, Hannon GJ. 2004. MicroRNAs: small RNAs with a big role in gene regulation. Nat Rev Genet; 5(7): 522-531.

Hickerson RP, Smith FJ, Reeves RE, Contag CH, Leake D, Leachman SA, Milstone LM, McLean WH, Kaspar RL. 2008. Single-nucleotide- specific siRNA targeting in a dominant-negative skin model. J Invest Dermatol; 128(3): 594-605.

Hu C, Diévart A, Lupien M, Calvo E, Tremblay G, Golicoeur P. 2006. "Overexpression of Activated Murine Notch1 and Notch3 in Transgenic Mice Blocks Mammary Gland Development and Induces Mammary Tumors." The American Journal of Pathology 168 (3):973–90.

Hunter LS, Sidjanin DJ, Hijar MV, Johnson JL, Kirkness E, Acland GM. 2007. Cloning and characterization of canine PAX6 and evaluation as a candidate gene in a canine model of aniridia. Mol Vis; 13:431–442.

Iso T, Kedes L, Hamamori Y. 2003. "HES and HERP Families: Multiple Effectors of the Notch Signaling Pathway." Journal of Cellular Physiology 194 (3):237–55.

Jacobs WB, Govoni G, Ho D, Atwal JK, Barnabe-Heider F, Keyes WM, Mills AA, Miller FD, Kaplan DR. 2005. p63 is an essential proapoptotic protein during neural development. Neuron; 48(5): 743-756.

Jost CA, Marin MC, Kaelin WG. 1997. p73 is a simian [correction of human] p53-related protein that can induce apoptosis. Nature; 389(6647): 191-194.

Kadar T, Horwitz V, Sahar R, Cohen M, Cohen L, Gez R. 2011. Delayed loss of corneal epithelial stem cells in a chemical injury model associated with limbal stem cell deficiency in rabbits. Curr Eye Res; 36:1098–1107.

Käsmann B, Ruprecht KW. 1997. Ocular manifestations in a father and son with EEC syndrome. Graefes Arch Clin Exp Ophthalmol; 235(8): 512-516.

Kaur P, Li A, Redvers R, Bertoncello I. 2004. Keratinocyte stem cell assays: an evolving science 2004. J Invest Dermatol Symp Proc; 9(3): 238-247.

Kenyon KR, Tseng SC. 1989. Limbal autograft transplantation for ocular surface disorders. Ophthalmology; 96(5): 709-722.

Koster MI, Kim S, Mills AA, DeMajo FJ, Roop DR. 2004. p63 is the molecular switch for initiation of an epithelial stratification program. Genes Dev; 18(2): 126-131.

Kotelnikov VM, Coon JS, Taylor S, Hutchinson J, Panje, W, Caldareill DD, LaFollette S, Preisler HD. 1996. Proliferation of epithelia of noninvolved mucosa in patients with head and neck cancer. Head Neck; 18(6):522-8.

Ledbetter EC, Marfurt CF, Dubielzig RR. 2013. Metaherpetic corneal disease in a dog associated with partial limbal stem cell deficiency and neurotrophic keratitis. Vet Ophthalmol; 16:282–288.

Lee HO, Lee JH, Choi E, Seol JY, Yun Y, Lee H. 2006. A dominant negative form of p63 inhibits apoptosis in a p53-independent manner. Biochem Biophys Res Commun; 344(1): 166-72.

Lehrer MS, Sun TT, Lavker RM. 1998. Strategies of epithelial repair: modulation of stem cell and transit amplifying cell proliferation. J Cell Sci; 111(Pt 19): 2867-2875.

Lin Z, He H, Zhou T, Liu X, Wang Y, He H, Wu H, Liu Z. 2013. A mouse model of limbal stem cell deficiency induced by topical medication with the preservative benzalkonium chloride. Invest Ophthalmol Vis Sci; 54:6314–6325.

Luesma MJ, Gherghiceanu M, Popescu LM. 2013. Telocytes and stem cells in limbus and uvea of mouse eye. J Cell Mol Med; 17:1016–1024.

Merindano MD, Costa J, Canals M, Potau JM, Ruano D. 2017. “A Comparative Study of Bowman’s Layer in Some Mammals: Relationships with Other Constituent Corneal Structures.” European Journal of Anatomy 6 (3):133–39.

Mangiulli M, Valletti A, Caratozzolo MF, Tullo A, Sbisa E, Pesole G, D'Erchia AM. 2009. Identification and functional characterization of two new transcriptional variants of the human p63 gene. Nucleic Acids Res; 37(18): 6092-6104.

Maurice DM. 1957. “The Structure and Transparency of the Cornea.” The Journal of Physiology 136 (2):263–286.1.

Mavilio F, Pellegrini G, Ferrari S, Di Nunzio F, Di Iorio E, Recchia A, Maruggi G, Ferrari G, Provasi E, Bonini C, Capurro S, Conti A, Magnoni C, Giannetti A, De Luca M. 2006. Correction of junctional epidermolysis bullosa by transplantation of genetically modified epidermal stem cells. Nat Med; 12(12): 1397-1402.

Mavilio F, Ferrari S, Di Nunzio F, Maruggi G, Bonini C, Capurro S, Conti A, Giannetti A, Pellegrini G, De Luca M. 2006. Correction of Laminin-5-Deficient Junctional Epidermolysis Bullosa by Transplantation of Genetically Modified Epidermal Stem Cells. A Phase-I Clinical Trial. Molecular Therapy 2006; 13 p.S280.

Meller D, Dabul V, Tseng S. 2002. Expansion of Conjunctival Epithelial Progenitor Cells on Amniotic Membrane. Experimental Eye Research; 74(4):537-545.

Miller VM, Xia H, Marrs GL, Gouvion CM, Lee G, Davidson BL, Paulson HL. 2003. Allele-specific silencing of dominant disease genes. Proc Natl Acad Sci USA; 100(12): 7195-7200.

Mills AA, Zheng B, Wang XJ, Vogel H, Roop DR, Bradley A. 1999. p63 is a p53 homologue required for limb and epidermal morphogenesis. Nature; 398(6729): 708-713.

Mills AA. 2006. p63: oncogene or tumor suppressor? Curr Opin Genet Dev; 16(1): 38-44.

Moll UM, Slade N. 2004. p63 and p73: roles in development and tumor formation. Mol Cancer Res; 2(7): 371-386.

Nagasaki T, Zhao J. 2005. Uniform distribution of epithelial stem cells in the bulbar conjunctiva. Investigative Ophthalmology and Visual Science; 46(1):126–132.

Nam E, Fujita N, Morita M, Tsuzuki K, Yi Lin H, Shu Chung C, Nakagawa T, Nishimura R. 2015. Comparison of the canine corneal epithelial cell sheets cultivated from limbal stem cells on canine amniotic membrane, atelocollagen gel, and temperature-responsive culture dish. Veterinary Ophthalmology; 18(4): 317–325.

Nardi AC, Ferreira U, Netto Júnior NR, Magna LA, Rodini ES, Richieri-Costa A. 1992. Urinary tract involvement in EEC syndrome: a clinical study in 25 Brazilian patients. Am J Med Genet; 44(6): 803-806.

Natan E, Joerger AC. 2012. Structure and kinetic stability of the p63 tetramerization domain. J Mol Biol; 415(3): 503-513.

Nicolas M, Wolfer A, Raj K, Kummer JA, Mill P, van Noort M, Hui CC, Clevers H, Dotto GP, Radtke F. 2003. “Notch1 Functions as a Tumor Suppressor in Mouse Skin.” Nature Genetics 33 (3):416–21.

Nishida K, Yamato M, Hayashida Y, Watanabe K, Yamamoto K, Adachi E, Nagai S, Kikuchi A, Maeda N, Watanabe H, Okano T, Tano Y. 2004. “Corneal Reconstruction with Tissue-Engineered Cell Sheets Composed of Autologous Oral Mucosal Epithelium.” The New England Journal of Medicine 351 (12):1187–96.

Nylander K, Vojtesek B, Nenutil R, Lindgren B, Roos G, Zhanxiang W, Sjöström B, Dahlqvist A, Coates PJ. 2002. Differential expression of p63 isoforms in normal tissues and neoplastic cells. J Pathol; 198(4): 417-427.

O'Callaghan AR, Daniels JT. 2011. Concise review: limbal epithelial stem cell therapy: controversies and challenges. Stem Cells; 29:1923–1932.

Özgencil FE, Gülmez N, Gültekin C, Sayiner S. 2017. Corneal Impression Cytology for the Diagnosis of Limbal Stem Cell Deficiency in a Dog. Kafkas Univ Vet Fak Derg.

Palumbo E, Matricardi L, Tosoni E, Bensimon A, Russo A. 2010. "Replication Dynamics at Common Fragile Site FRA6E." Chromosoma 119 (6):575–87.

Pan Y, Lin MH, Tian X, Cheng HT, Gridley T, Shen J, Kopan R. 2004. "Gamma-Secretase Functions through Notch Signaling to Maintain Skin Appendages but Is Not Required for Their Patterning or Initial Morphogenesis." Developmental Cell 7 (5):731–43.

Pang K, Du L, Zhang K, Dai C, Ju C, Zhu J, Wu X. 2016. Three-Dimensional Construction of a Rabbit Anterior Corneal Replacement for Lamellar Keratoplasty. PLoS ONE; 11(12): e0168084.

Parsa R, Yang A, McKeon F, Green H. 1999. Association of p63 with proliferative potential in normal and neoplastic human keratinocytes. J Invest Dermatol; 113(6): 1099-1105.

Pellegrini G, Dellambra E, Golisano O, Martinelli E, Fantozzi I, Bondanza S, Ponzin D, McKeon F, De Luca M. 2001. p63 identifies keratinocyte stem cells. Proc Natl Acad Sci USA; 98(6): 3156- 3161.

Pellegrini G, Golisano O, Paterna P, Lambiase A, Bonini S, Rama P, De Luca M. 1999. Location and clonal analysis of stem cells and their differentiated progeny in the human ocular surface. J Cell Biol; 145(4): 769-782.

Pellegrini G, Traverso CE, Franzi AT, Zingirian M, Cancedda R, De Luca M. 1997. Long-term restoration of damaged corneal surfaces with autologous cultivated corneal epithelium. Lancet; 349(9057): 990-993.

Plattner K, Goldblum D, Halter J, Kunz C, Koeppl R, Gerber-Hollbach N. 2017. "Osteo-Odonto-Keratoprosthesis in Severe Ocular Graft versus Host Disease." Klinische Monatsblatter Fur Augenheilkunde 234 (4):455–56.

Potten CS. 2004. Keratinocyte stem cells, label-retaining cells and possible genome protection mechanisms. J Invest Dermatol Symp Proc; 9(3): 183-195.

Potten CS. 2008. Epidermal cell production rates. J Invest Dernatol 1975; 65:488-500.

Qi H, Li DQ, Shine HD, Chen Z, Yoon K-C, Jones DB: Nerve growth factor and its receptor TrkA serve as potential markers for human corneal epithelial progenitor cells. Exp Eye Res; 86:34–40.

Rama P, Bonini S, Lambiase A, Golisano O, Paterna P, De Luca M, Pellegrini G. 2001. Autologous fibrin-cultured limbal stem cells permanently restore the corneal surface of patients with total limbal stem cell deficiency. Transplantation; 72(9): 1478-1485.

Rangarajan A, Talora C, Okuyama R, Nicolas M, Mammucari C, Oh H, Aster JC, Krishna S, Metzger D, Chambon P, Miele L, Aguet M, Radtke F, Dotto GP. 2001. “Notch Signaling Is a Direct Determinant of Keratinocyte Growth Arrest and Entry into Differentiation.” The EMBO Journal 20 (13):3427–36.

Rheinwald JG, Green H. 1975. Serial cultivation of strains of human epidermal keratinocytes: the formation of keratinizing colonies from single cells. Cell; 6(3):331-43.

Rinne T, Brunner HG, van Bokhoven H. 2007. p63-associated disorders. Cell Cycle; 6(3): 262-268.

Rochat A, Kobayashi K, Barrandon Y. 1994. Location of stem cells of human hair follicles by clonal analysis. Cell; 76(6): 1063-1073.

Roelfsema NM, Cobben JM. 1996. The EEC syndrome: a literature study. Clin Dysmorphol; 5(2):115-127.

Rolando M, Zierhut M. 2001. The ocular surface and tear film and their dysfunction in dry eye disease. Surv Ophthalmol; 45:S203–S210.

Romano RA, Ortt K, Birkaya B, Smalley K, Sinha S. 2009. An active role of the DeltaN isoform of p63 in regulating basal keratin genes K5 and K14 and directing epidermal cell fate. PLoS One; 4(5): e5623.

Sherwood RA, Parsons TS. 1977. The Vertebrate Body. Saunders.

Saghizadeh M, Kramerov A, Svendsen C, Ljubimov A. 2017. Concise Review: Stem Cells for Corneal Wound Healing. Stem Cells; 35(10):2105-2114.

Salvalaio G, Fasolo A, Bruni A, Frigo AC, Favaro E, Ponzin D. 2003. “Improved Preparation and Preservation of Human Keratoplasty Lenticules.” Ophthalmic Research 35 (6):313–18.

Sanchez RF, Daniels JT. 2016. Mini-Review: Limbal Stem Cells Deficiency in Companion Animals: Time to Give Something Back? Current Eye Research; 41(4):425-432.

Schermer A, Galvin S, Sun TT. 1986. Differentiation-related expression of a major 64K corneal keratin in vivo and in culture suggests limbal location of corneal epithelial stem cells. J Cell Biol; 103(1): 49- 62.

Schwarz DS, Ding H, Kennington L, Moore JT, Schelter J, Burchard J, Linsley PS, Aronin N, Xu Z, Zamore PD. 2006. Designing siRNA that distinguish between genes that differ by a single nucleotide. PLoS Genet; 2(9): e140.

Selver OB, Durak I, Gürdal M, Baysal K, Ates H, Ozbek Z, Wang Z, Wu A, Wolosin JM. 2015. Corneal recovery in a rabbit limbal stem cell de ciency model by autologous grafts of tertiary outgrowths from cultivated limbal biopsy explants. Molecular Vision; 22:138-149.

Stewart RM, Sheridan CM, Hiscott PS, Czanner G, Kaye SB. 2015. Human Conjunctival Stem Cells are Predominantly Located in the Medial Canthal and Inferior Forniceal Areas. Invest Ophthalmol Vis Sci; 56(3):2021-30.

Sun L, Ryan DG, Zhou M, Sun TT, Lavker RM. 2006. EEDA: a protein associated with an early stage of stratified epithelial differentiation. J Cell Physiol; 206:103–111.

Sun TT, Lavker RM. 2004. Corneal epithelial stem cells: past, present, and future. J Invest Dermatol Symp Proc; 9(3): 202-207.

Tananuvat N, Bumroongkit K, Tocharusa C, Mevatee U, Kongkaew A, Ausayakhun S. 2016. Limbal stem cell and oral mucosal epithelial transplantation from ex vivo cultivation in LSCD-induced rabbits: histology and immunologic study of the transplant epithelial sheet. Int Ophtalmol.

Thurfjell N, Coates PJ, Uusitalo T, Mahani D, Dabelsteen E, Dahlqvist A, Sjöström B, Roos G, Nylander K. 2004. Complex p63 mRNA isoform expression patterns in squamous cell carcinoma of the head and neck. Int J Oncol; 25(1): 27-35.

Totaro A, Castellan M, Battilana G, Zanconato F, Azzolin L, Giulitti S, Cordenonsi M, Piccolo S. 2017. “YAP/TAZ Link Cell Mechanics to Notch Signalling to Control Epidermal Stem Cell Fate.” Nature Communications 8 (May).

Truong AB, Kretz M, Ridky TW, Kimmel R, Khavari PA. 2006. p63 regulates proliferation and differentiation of developmentally mature keratinocytes. Genes Dev; 20(22): 3185-3197.

Tsai RJ, Li LM, Chen JK. 2000. Reconstruction of damaged corneas by transplantation of autologous limbal epithelial cells. N Engl J Med; 343(2): 86-93.

Ueno H, Ferrari G, Hattori T, Saban DR, Katikireddy KR, Chauhan SK. 2012. Dependence of corneal stem/progenitor cells on ocular surface innervation. Invest Ophthalmol Vis Sci; 53:867–872.

van Bokhoven H, Brunner HG. 2002. Splitting p63. Am J Hum Genet; 71(1): 1-13.

van Bokhoven H, Hamel BC, Bamshad M, Sangiorgi E, Gurrieri F, Duijf PH, Vanmolkot KR, van Beusekom E, van Beersum SE, Celli J, Merkx GF, Tenconi R, Fryns JP, Verloes A, Newbury-Ecob RA, Raas-Rotschild A, Majewski F, Beemer FA, Janecke A, Chitayat D, Crisponi G, Kayserili H, Yates JR, Neri G, Brunner HG. 2001. p63 gene mutations in EEC syndrome, limb-mammary syndrome, and isolated split hand-split foot malformation suggest a genotype-phenotype correlation. Am J Hum Genet; 69 (3): 481-492.

Vauclair S, Nicolas M, Barrandon Y, Radtke F. 2005. “Notch1 Is Essential for Postnatal Hair Follicle Development and Homeostasis.” Developmental Biology 284 (1):184–93.

Watt FM. 2001. Stem cell fate and patterning in mammalian epidermis. Curr Opin Genet Dev; 11(4): 410-417.

Welge-Lu¨en U, May CA, Neubauer AS, Priglinger S. 2001. Role of tissue growth factors in aqueous humor homeostasis. Curr Opin Ophthalmol; 12:94.

West-Mays JA, Dwivedi DJ. 2006. The keratocyte: corneal stromal cell with variable repair phenotypes. Int J Biochem Cell B; 38:1625–1631.

Willoughby CE, Chen I, Ellis I, McGrath JA, Kaye S. 2005. Mutations in p63 Gene in Ectrodactyly-Ectodermal dysplasia-Clefting (EEC) syndrome and their relevance to the ocular phenotype. Invest Ophthalmol Vis Sci; 46: E-Abstract 1833.

Xu B, Fan TJ, Zhao J, Sun A, Wang RX, Hu XZ, Yu HZ, Fan XY, Xu XH. 2012. Transplantation of tissue-engineered human corneal epithelium in limbal stem cell deficiency rabbit models. Int J Ophtalmol; 5(4):424-429.

Yamada N, Yanai R, Inui M, Nishida T. 2005. Sensitizing effect of substance P on corneal epithelial migration induced by IGF-1, fibronectin, or interleukin-6. Invest Ophthalmol Vis Sci; 46:833–839.

Yamamoto N, Tanigaki K, Han H, Hiai H, Honjo T. 2003. “Notch/RBP-J Signaling Regulates Epidermis/Hair Fate Determination of Hair Follicular Stem Cells.” Current Biology: CB 13 (4):333–38.

Yang A, Kaghad M, Caput D, McKeon F. 2002. On the shoulders of giants: p63, p73 and the rise of p53. Trends Genet; 18(2): 90-95.

Yang A, Kaghad M, Wang Y, Gillett E, Fleming MD, Dotsch V, Andrews NC, Caput D, McKeon F. 1998. p63, a p53 homolog at 3q27-29, encodes multiple products with transactivating death-inducing and dominant negative activities. Mol Cell; 2(3): 305-316.

Yang A, Schweitzer R, Sun D, Kaghad M, Walker N, Bronson RT, Tabin C, Sharpe A, Caput D, Crum C, McKeon F. 1999. p63 is essential for regenerative proliferation in limb, craniofacial and epithelial development. Nature; 398(6729): 714-718.

Zhang Y, Sun H, Liu Y, Chen S, Cai S, Zhu Y, Guo P. 2016. The Limbal Epithelial Progenitors in the Limbal Niche Environment. Int J Med Sci; 13(11):835-840.